1991

Mechanism and Enhancement of Phase Segregation in Drilling Fluids.

John Marvin Griffin
Louisiana State University and Agricultural & Mechanical College

Order Number 9200065

Mechanism and enhancement of phase segregation in drilling fluids

Griffin, John Marvin, Ph.D.

The Louisiana State University and Agricultural and Mechanical Col., 1991

U·M·I
300 N. Zeeb Rd.
Ann Arbor, MI 48106

Mechanism and Enhancement of Phase Segregation in Drilling Fluids

A Dissertation

Submitted to the Graduate Faculty of the
Louisiana State University and
Agricultural and Mechanical College
in partial fulfillment of the
requirements for the degree of
Doctor of Philosophy

in

The Department of Petroleum Engineering

by
John M. Griffin
B.S., Emory University, 1975
M.S., University of Alabama, 1979
May 1991

Acknowledgements

The author wishes to express his appreciation to his major professor, Dr. Andrew K. Wojtanowicz, for his example and guidance throughout this research. The valuable assistance of the Dissertation Committee is gratefully acknowledged.

Financial support was provided by the Louisiana Department of Natural Resources and an Amoco Foundation fellowship. These funds were supplemented by the author's wife and parents and the Atchafalaya Presbyterian Church of Bayou Current, Louisiana.

The author acknowledges his father for his encouragement in mathematics and science at an early age and the loving support of his mother through the years.

Table of Contents

Table of Contents (cont.)

Table of Contents (cont.)

List of Tables

Tables (cont.)

List of Figures

Figures (cont.)

Figures (cont.)

Figures (cont.)

Figures (cont.)

Abstract

Dewaterability of a compressible suspension can be characterized by two fundamental properties of viscoelastic networks: permeability and bulk modulus of elasticity. Time required for dewatering can be obtained from the former, while the latter can furnish the data required for predicting ultimate compaction. A method has been derived and an apparatus constructed for measurement of these two properties in a centrifugal field. The method was applied to a variety of drilling fluids and mineral suspensions. A floor-mounted laboratory centrifuge was used in this investigation. The methods developed have merit for evaluating pre-treatments prior to centrifugal dewatering.

A method for quantifying the density distribution from top to bottom of a sedimented cake less than 2 cm in height is reported. In one experiment, this density variation was less than 13%.

The feasibility of replacing chemical pre-treatments by applying an alternating current electric field (electrocoagulation) was investigated. Several fluids were electrically treated before centrifuging. Upon centrifuging, only certain suspensions exhibited a cake while others did not. In those instances where a cake could be collected, its moisture content was measured. In the most effective electrical treatment, a salt/polymer drilling fluid containing 6% by

weight solids (94% moisture) before treatment and centrifuging yielded a cake with a moisture content of 91%. This compares with a moisture content of 65% if the suspension had been chemically pre-treated. This meant that in the most optimum treatment, an unacceptably high moisture content was obtained. Thus, in view of this study, electrical treatments are unable to replace chemical pre-treatments to enhance centrifugal solid/liquid separation.

Two mechanisms of electrocoagulation, ionization and electrostriction, are presented. The consistent increase in conductivity is more easily explained by the ionization mechanism. Thus, it is the favored mechanism to explain electrocoagulation.

Introduction

In many cases, drilling waste must be disposed off-site. Economics have dictated these wastes be minimized prior to transporting them to approved disposal facilities. Centrifugal dewatering has been applied to effect this minimization. However, certain difficulties in its application have motivated this investigation. These difficulties include inability of field personnel to properly select and adjust chemicals which destabilize the fluid prior to centrifuging. Over-treatment can result and more importantly, sedimented cake is discharged with high moisture content.

The research can be divided into two parts. The first part investigates the fundamental properties which affect dewatering; that is, the compression and removal of free water from a chemically destabilized suspension. Enhancement is achieved through more efficient destabilization of the suspension to be dewatered, as well as more efficient densification of the suspension in a centrifugal field. From a better understanding and quantification of permeability (Chapter II) and bulk modulus (Chapter III), a foundation is laid from which both optimum chemical, centrifugal pre-treatment and application of centrifugal forces can be selected.

The second part evaluates electrical treatment as a means to replace chemical pre-treatments. Finally, the two

parts are combined when the permeability and modulus of an electrically destabilized suspension is measured.

Chapter I reviews relevant experimental and theoretical studies related to dewatering of mineral suspensions.

Chapter II describes the apparatus developed and the equations derived for measurement of permeability of viscoelastic networks. The effect of consolidating stress on expression of free water from a flocculated mineral network is addressed. For numerous fluid systems, the response to consolidating stress is compared. In place of the compression-permeability (C-P) cell which deformed viscoelastic networks in a manner not representative of a centrifuge, a centrifugal permeameter was constructed. Previously, drilling fluid dewatering had been evaluated only with regard to compression; permeability was not simultaneously measured. In order to measure permeability using this apparatus, a derivation of permeability was developed from Darcy's law for linear flow. Two obstacles in permeability measurement were successfully addressed. One, the obstacle for determining base-line pressure was overcome by a series of experiments and comparison with a constructed, static, permeameter capable of measuring unconsolidated, compressible networks. Two, the declining flow rate as the experiment proceeded meant there was no simple relation with pressure. A method was developed that found a linear relation between the logarithmic value of observed data and time.

A doser was made for introducing a drilling fluid while the centrifuge rotated at full speed. This allowed for rate of sedimentation to be observed. These observations, which occurred too rapidly for observation with the unaided eye, were made possible using a video camera.

Difficulties have been reported in the field in dewatering certain drilling fluid types. These difficulties are explained in terms of fundamental properties. Permeability and bulk modulus are proposed as being the fundamental properties which adequately characterize the dewatering of a viscoelastic network.

The derivation of bulk modulus of elasticity for measurement in a centrifugal field is presented in Chapter III. Using the identical fluid systems from Chapter II, data for calculating bulk modulus were simultaneously obtained. The response to various drilling fluids and mineral suspension to consolidating stress is reported.

A method for measuring density variations along the cake height is reported. This method requires oven drying the cake following centrifugation.

In addition, it is shown how the consolidation data obtained in the centrifuge can be used to compute two commonly measured geotechnical parameters, namely, coefficient of compressibility and compressibility index.

The effect of alternating current on destabilizing drilling fluids is presented in Chapter IV. Arguments for

accepting the ionization mechanism over the electrostriction mechanism are presented in light of experimental data. Routinely measured mud properties before and after electrical treatment are augmented with Capillary Suction Time, zeta potential, and centrifugal separation.

Permeability and bulk modulus of elasticity of a sedimented cake are obtained following an electric field treatment. These measurements are compared with those made on chemically pre-treated suspensions as described in Chapters II and III.

Conclusions and recommendations are presented in Chapter V.

Chapter I

Literature Review of Dewatering Models

This chapter reviews relevant experimental and theoretical models which describe the dewatering of viscoelastic networks. The term, viscoelasticity, includes time in its stress-strain relation. While the research of this dissertation is concerned only with centrifugal dewatering, other types of filtration are useful and, therefore, included. The researcher of filtration must identify those properties by which the dewaterability of a sludge may be better understood, modeled, and, therefore, predicted. The objectives include:

1. Review models of fluid flow through porous media to determine which are applicable to dewatering of viscoelastic networks.
2. Review analytical methods needed to define model parameters and propose alternate methods as required.

The heterogeneous nature of industrial sludges suggests the need for highly complex models to describe properly their behavior under centrifugal forces. However, the numerous parameters included therein exceed the limits of readily and simply practiced measurements. This points out a shortfall in the literature. Fundamental properties are grouped into factors and left unexplained when unknown or

not understood.

1.1 Experimental models of compressible cake filtration

Beginning with the Poiseuille Law (Poiseuille, 1840) in 1840, flow of an incompressible fluid flow was modeled most simply as flow in a single capillary. Later, Darcy (1856) described flow in a system of multiple capillaries, i.e, a porous medium.

Later developments added the ability to incorporate both increased complexity and variety. The trend was toward incorporating fewer simplifying assumptions.

For flow in a cross-section containing equal length channels, Kozeny (Kozeny, 1927) solved the Navier-Stokes Equations using two inherent assumptions are:

1. fluid velocity is in the direction of flow, and
2. the flow path length is equal to the depth of the medium.

However, when experimental investigators sought to apply the Kozeny model, experimentally observed departure was observed. Scheidegger (1974) and Happel et al. (1965) criticized the Kozeny model for its inability to incorporate extremely complex geometries as those found in compressible slurries. Shortcomings of the Kozeny model motivated efforts to include channel tortuosity (Carman, 1937), particle aggregation (Happel and Brenner, 1965), and directional porosity (Tiller, 1975).

Efforts to incorporate the complexity of a compressible slurry included a monumental work by Grace (1953) who modeled filtration and included a "cake compressibility factor". This "factor" is an exponent to the applied pressure term which quantifies compression force in the compression-permeability (C-P) cell, and is a dimensionless constant for each suspension. This factor is identical to "compressibility index" as described in an investigation by Lockyear and White (1980). This value appears to be one of convenience, and groups fundamental parameters.

Grace attempted to model cake compressibility based on physical properties of clay-size (< 20 microns) particulate solids, but was unsuccessful. He was only able to conclude that this factor varied with filtration pressure. Other investigators following Grace's model included compressibility factor as an exponent to filtration pressure (Coackely and Jones, 1956; and Carman, 1958).

As this research is concerned with the measurement of permeability on compressible networks, the various factors affecting permeability were of interest. In examining the literature, several references to specific resistance were noted. These are useful due to the relation between specific resistance and permeability. Specific resistance is inversely proportional to permeability as described in the equation (Outmans, 1963; and Gregory and DeMoor, 1984),

$$\alpha_p = \frac{1}{k_s \rho_s (1 - \phi)} \quad [m/g] \qquad 1\text{-}1$$

where α_p specific resistance to filtration, m/g
k_s permeability, m^2
ρ_s solids density, g/m^3
ϕ porosity, void fraction

Coackely and Jones (1956) observed the effect of dilution upon specific resistance. They noted a significant decrease in specific resistance as a result of dilution. They were unable to account for this unexpected change. In seeking to account for this change, Ball (p. 22, 1978) postulated the mixing concurrent with dilution was causative. Mixing can also be expected to change particle size, surface area, and porosity.

In evaluating the multitude of investigations deriving filtration data from the C-P cell tests, Wakeman (1978, p. 265) stated

> "acceptance of C-P cells by previous workers has concealed the pressure and feed solids concentration effects on the compression coefficient when basic filtration data was subsequently analyzed."

Using a knowledge of pore space structure, Tierny and Chiang (1986) sought to develop models that could be used to predict rate of filtration and dewatering and final moisture content.

From a knowledge of particle size distribution, Gaudin and Fuerstenau (1962) made accurate predictions of sedimentation on flocculated kaolin slurries. The predictions were

based on estimating the number and size of pores for given conditions. The study demonstrated that a network model could be applied to filtration rate predictions.

De Yong (1974) modeled permeability in a fibrous matrix of paper pulp. The model includes a dependence of permeability on compressibility. As a result, theoretical predictions of experimental results was improved.

Several investigators have used centrifugal filtration studies to predict sludge behavior in a gravity thickener process (Visilind, 1977; Lockyear and White, 1980; and Bingeman and Coates, 1960). Lockyear and White (1980) determined the compressibility of a sludge by the effect the sludge blanket depth has on thickening. In a simple test, the sludge is centrifuged at different centrifugal accelerations, and the ultimate concentration noted in each case. A simple logarithmic plot of ultimate concentration versus centrifugal acceleration results in a straight line if a coefficient is included that is distinct for the particular sludge studied. Generally, the authors found that with coagulant additions, the rate of thickening increased and ultimate concentration declined. The procedure enabled optimum coagulant dosage to be found.

Bingeman and Coates (1960) offered some factors to improve upon the application of Darcy's law for centrifugal filtration. However, a difference between their study and this one is that the fluid they investigated was composed of

spherical, incompressible beads.

Alemi et al. (1976) used a laboratory set-up in which the hydraulic conductivity of a soil core was measured. The apparatus was similar to Svarovsky's (1981, p. 382) beaker experiment and the centrifugal permeameter presented in Chapter II. The fluid distribution following centrifugation in the unsaturated core was measured by an analytical balance. By measuring the filtrate collected during centrifugation and knowing the initial and final soil-water content, permeability was calculated. The method required an equilibrium cake thickness to be achieved before a permeability measurement was made, and is similar to the approach described in Chapter II.

From a practical standpoint, cake dewaterability can be evaluated in terms of effluent clarity and cake moisture (Wojtanowicz, 1988). Further, residual moisture content can be evaluated by the various parameters on which it is dependent: pressure, surface tension, particle size distribution, surface properties, presence of additives, and flocculants (Hermia, 1979). Hermia introduced a dimensionless "centrifugal drainage" number, and reported agreement with experimental data. The number is useful in evaluation of centrifugal equipment.

Hinds et al. (1986) suggested "centrifuge factor" for making comparisons between flocculant additives. The method compares cake and supernatant heights in a test tube follow-

ing centrifugation.

Wakeman (1978) modeled porosity distribution throughout the depth of a compressible filter cake. Liquid pressure was measured using pilot probes, and porosity measured using a resistivity technique. Shirato, Kato, et al., (1970), Shirato, Murase, et al., (1970), and Shirato et al., (1987) used the same method of pilot probes at successive depths to measure pressure in a gravity thickener. These investigators were the first to actually measure a pressure distribution in a gravity sedimented cake; previous models assumed a linear pressure distribution.

In other thickening studies, Visilind (1977) modified Stoke's law to obtain a sludge-dependent term, "settling coefficient." Here, settling refers to movement of particles without contact. Sequential to settling is compression which particles come into contact and deform one another. Visilind sought to use laboratory centrifugal compression of a sludge to predict behavior of a full-scale gravity thickener. The advantage is that time could be saved in evaluating treatments. For a specified solids concentration, a "sludge settling coefficient" is determined using a laboratory centrifuge. This coefficient is $v/(\omega^2 r)$

where

v = particle settling velocity, cm/sec
ω = angular velocity of the centrifuge rotor, radians/sec
r = radians from the center of rotation to the particle, cm

The utility of Visilind's work was to simplify evaluation of

equipment to permit more competitive bidding on contracts describing industrial separation services.

1.2 Theoretical models without experimental verification

In the literature, several models were not accompanied by experimentation. Some are especially applicable to centrifugal filtration. Foremost among these was one by Bear et al. (1984). These investigators have aptly noted that a lack of uniform methodology in solving centrifugal filtration problems has forced the use of pilot-scale evaluation procedures. The nature of previous investigations has resulted in applications only for specific cases. These authors

> "show how the theory of fluid flow through a deformable porous medium, in the presence of a centrifugal force, serves as a basis for construction of a rather general model of centrifugal filtration."

A complication of the filtration model necessarily arises from the flow occurring in a deformable medium. Consequently, permeability varies with compressibility of the cake medium. An analysis of

> "such a problem requires the simultaneous solution of both flow and the deformation equations."

When compressibility is considered, solid particle rearrangement during filtration and consequent compaction can be represented.

The authors proceed to develop equations for

1. internal pore pressure,
2. water saturation,
3. permeability, and
4. cake compaction in the radial direction.

Each parameter is a function of both radial distance and time. A system of non-linear equations are then developed. These equations are solved by an implicit, finite difference scheme.

Incorporating Hooke's law, two partial differential expressions were derived for volume strain with respect to radial distance (in one dimension) and for permeability. It was recognized that both porosity and permeability must be represented in terms of pressure and porosity respectively. The authors solved these two partial differential equations and illustrated their theoretical solution with a numerical example. The results characterized a sludge in a short period of time using only a one liter sample. The finite difference grid used distance nodes at 0.5 cm spacing with time nodes at 1 sec intervals. The numerically generated example had a rotational velocity of 40 sec^{-1} (240 rpm).

Manins and Roberts (1975) solved a system of governing partial differential equations for a fluid-filled Hookean elasto-porous medium with non-constant permeability. The authors solved the equations numerically, and showed that neglecting the varying value of permeability introduces

errors on the order of one hundred percent.

A model developed by Gray (1968) showed permeability to be based on flow velocity. The velocity term is included in the Reynold's number.

This literature review has been unable to identify a flow model which incorporates complexities associated with compressible slurries, and can be simply applied. Slight variations due to dilution, compression, surface area, porosity, and particle size cannot be accounted for by these models.

In this research, the measurement of permeability was accomplished using a newly constructed laboratory apparatus. For description of flow, Darcy's law was used as it was adequate for measurements made on compressed cores provided one condition was met, namely, the network had achieved an equilibrium thickness when compressed. To describe compression, bulk modulus of elasticity was measured simultaneously with a permeability measurement.

In one experiment, a variable density measurement was performed. This increase in the level of sophistication has the potential to improve theoretical predictions of network permeability at a specified level of compression.

Chapter II

Flow Properties of Dewatering Sediments

This chapter describes the measurement and analysis of permeability for several viscoelastic networks. These networks were compacted in a centrifugal field with a resultant decrease in permeability.

2.1 Experimental design and measurements

The experimental investigation is based on the application of Darcy's law for the linear flow case. A discussion of simplifying assumptions follows:

1. For a sedimented cake, when and an equilibrium cake thickness has been obtained, the cake is considered to have homogeneous density and permeability.

This assumption greatly simplifies the permeability computation. While some error is introduced with this assumption, conclusions between differences in slurry response at various rotary speeds can still be made. Later, in sub-chapter 3.1.3 (page 55) this assumption will be re-examined with regard to some experimental data.

2. Pressure is solely based upon hydrostatics of fluid above the point of interest. Viscous effects are neglected.

The permeability at increasing levels of consolidating

stress was measured. Typically, five levels of stress were applied and the resulting permeability was measured at each stress level. In each case, the cake height was observed.

Several types of stresses are referred to throughout this discussion, and some definitions are in order. Neutral stress or hydraulic stress is due to the water medium surrounding the solid particles. Total stress is the stress which results from the combined mass of the solid/liquid mixture. Effective stress is the difference between total stress and neutral stress, and quantifies the inter-particle forces. The term effective consolidation stress is equivalent to effective stress.

According to a rearrangement of Darcy's law,

$$k = \frac{q\ \mu\ dL}{A\ dP} \qquad 2\text{-}1$$

For these experiments, viscosity (μ) was 1.0 cp for fresh (tap) water at room temperature. The unit of permeability used was (k) darcies. Area (A) was the cross-sectional area of the permeameter (5.94 cm^2) and dL (cm) was the equilibrium cake thickness, later referred to as "H_e." H_e is also in centimeters.

Hydraulic pressure (P) across the cake can be expressed as (see Appendix A for its derivation),

$$P = 1/2\ \rho_w\ \omega^2\ (R_b^2 - R_L^2) \qquad 2\text{-}2$$

in consistent units, or as

$$P = 5.585 * 10^{-9} * N^2 * (R_b^2 - R_L^2),\ \text{atm} \qquad 2\text{-}3$$

for use in Darcy's law where N is rpm.

The pressure calculated is dependent upon the selected value of R_c in the equation

$$P = 5.584 \times 10^{-9} \times N^2 (R_c^2 - R_L^2), \text{ atm} \qquad 2\text{-}4$$

where R_c is the distance from the axis of rotation to some point of interest in the cake. In this work, the radius to the cake bottom R_b (cm) is arbitrarily substituted for R_c (cm).

Figure 2-1 illustrates the non-linear relation between flow rate and pressure. A means for computing permeability in this "falling head" experiment will be described. Flow through the constructed permeameter is illustrated schematically in Fig. 2-2.

2.1.1 Instrumentation

The laboratory centrifuge used in this research was a floor mounted Damon/IEC Size 2, Model EXD. The unit was equipped with a 3/4 hp electric motor capable of a relative centrifugal force of 4275 x g, and could reach a rotational velocity of 2500 rpm. The various suspensions were placed in tubes suspended during rotation on the centrifuge rotor. The centrifuge was then accelerated to various levels. At each level, an equilibrium cake thickness was obtained and its permeability measured.

In order to retain the sludge above a perforated base, loose sand was placed at the outer radius. Retaining screens were placed on either side of the sand (Fig. 2-3).

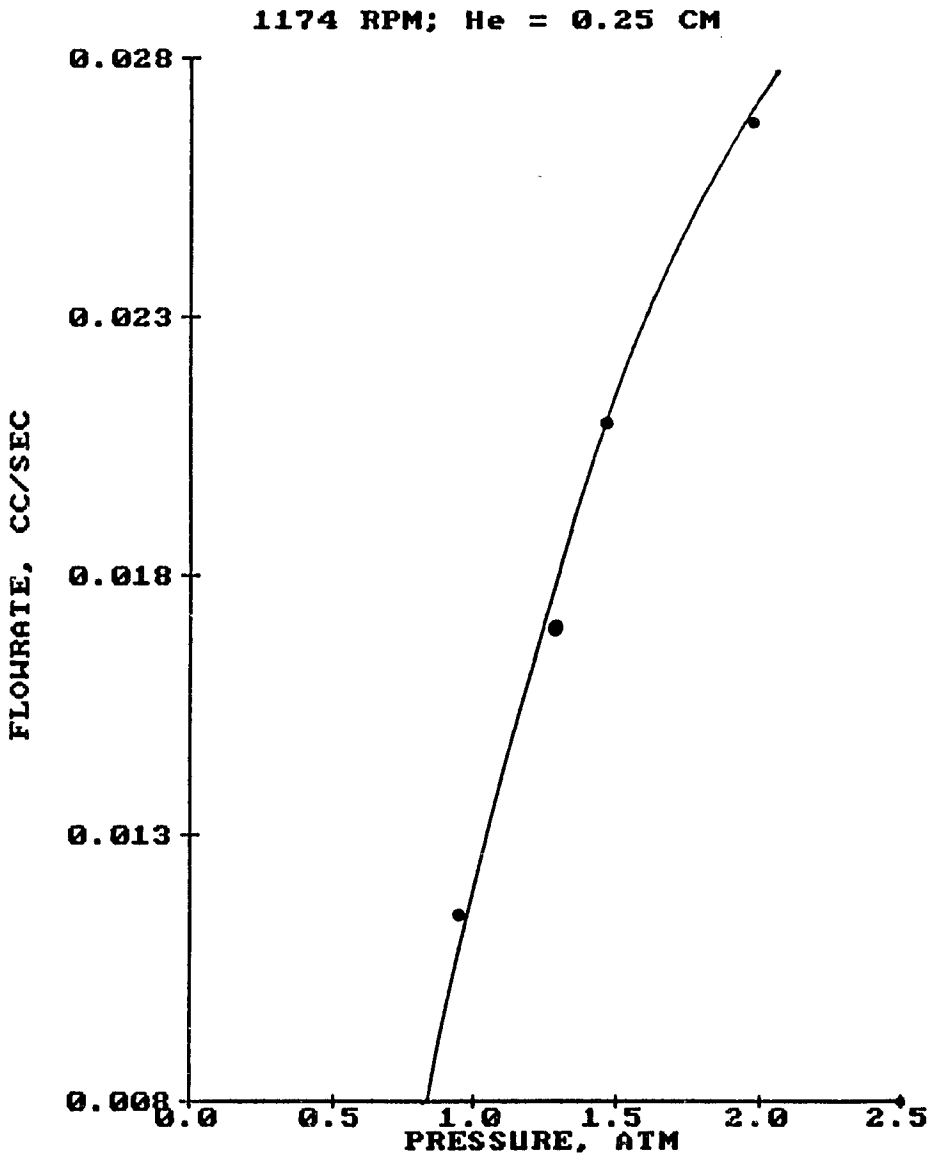

Fig. 2-1 Plot of flow rate vs. pressure during centrifugation

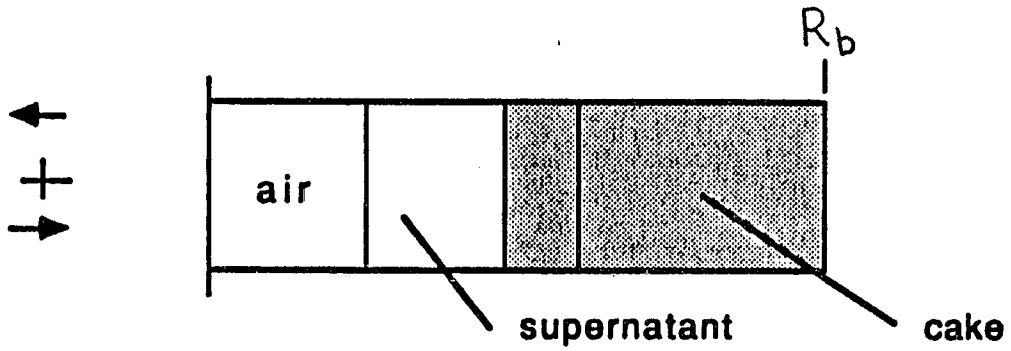

Fig. 2-2 Schematic of permeameter

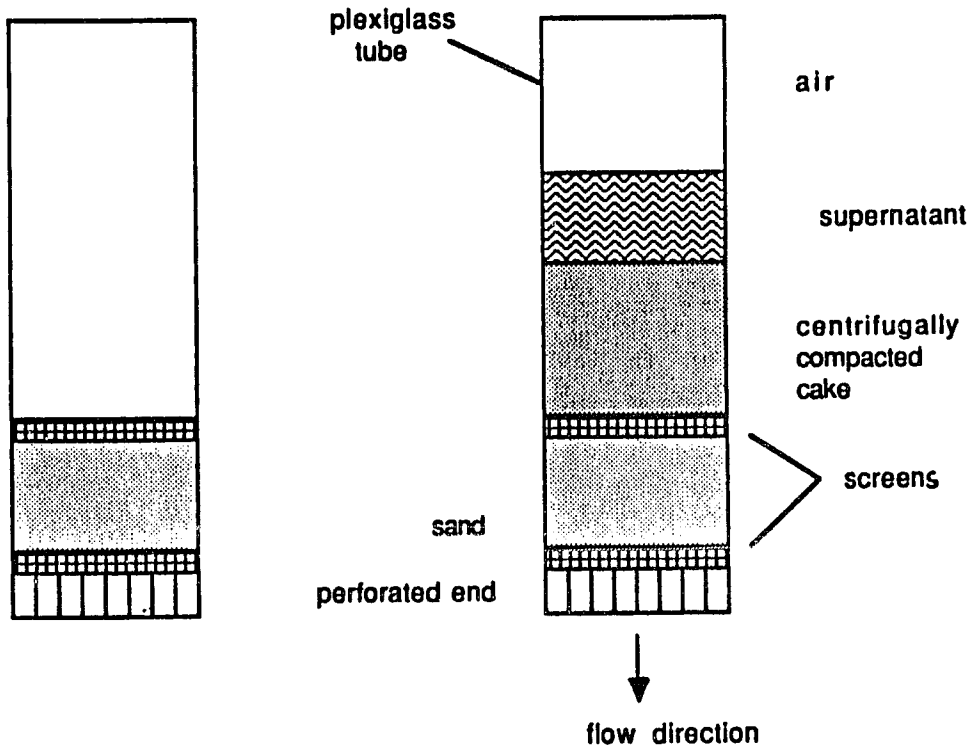

Fig. 2-3 Schematic showing centrifuge tube for centrifugal permeameter experiments

A second modification was to introduce (Fig. 2-4) the fluid while the centrifuge was rotating at constant rotational velocity rather than being accelerated from a still position as done previously (Alemi et al., 1976; Hinds et al., 1986; Wojtanowicz, 1988). The compressible sludge was poured into the rotating cylinder (doser); it then exited through a 1/2 inch diameter tygon tube to a transparent acrylic centrifuge tube. The transparent tube allowed visual observation and recording of flow rate versus time aided by a strobe light. The doser allowed the sludge to be accelerated rapidly to better simulate the introduction of drilling fluid into an industrial decanting centrifuge. Dosing in this manner was later discarded as imbalances were created between the two sides of the centrifuge. Consequently, fluid suspensions were introduced before rotation was initiated.

In addition to imbalances, measurement of permeability was not possible immediately following dosing of the fluid while rotating. Owing to the low permeability of the network, no flow was discernible until after the cake had been compacted. Figure 2-5 shows the rapid decline in the solid-liquid interface, whereas, little to no distinguishable movement in the air-liquid interface is observed. Permeability measurements were not significantly affected by the sand base as the permeability of the sand base was 47.9 darcies. This is two orders of magnitude higher than the

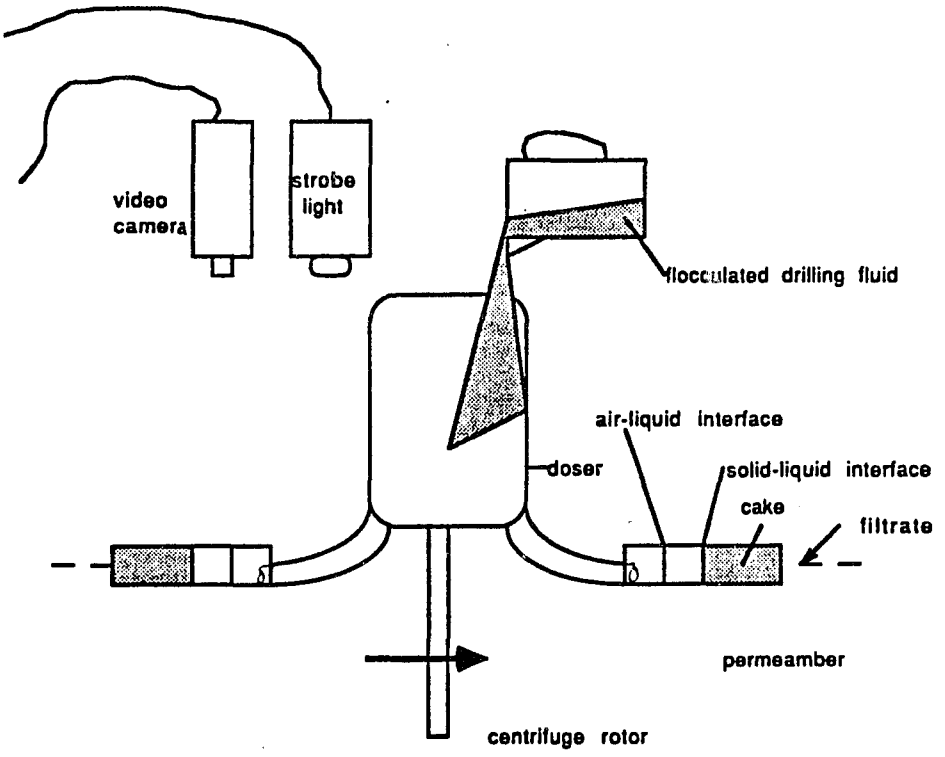

Fig. 2-4 Schematic showing centrifuge equipped with doser, strobe light, and video camera for performing centrifugal permeameter experiments

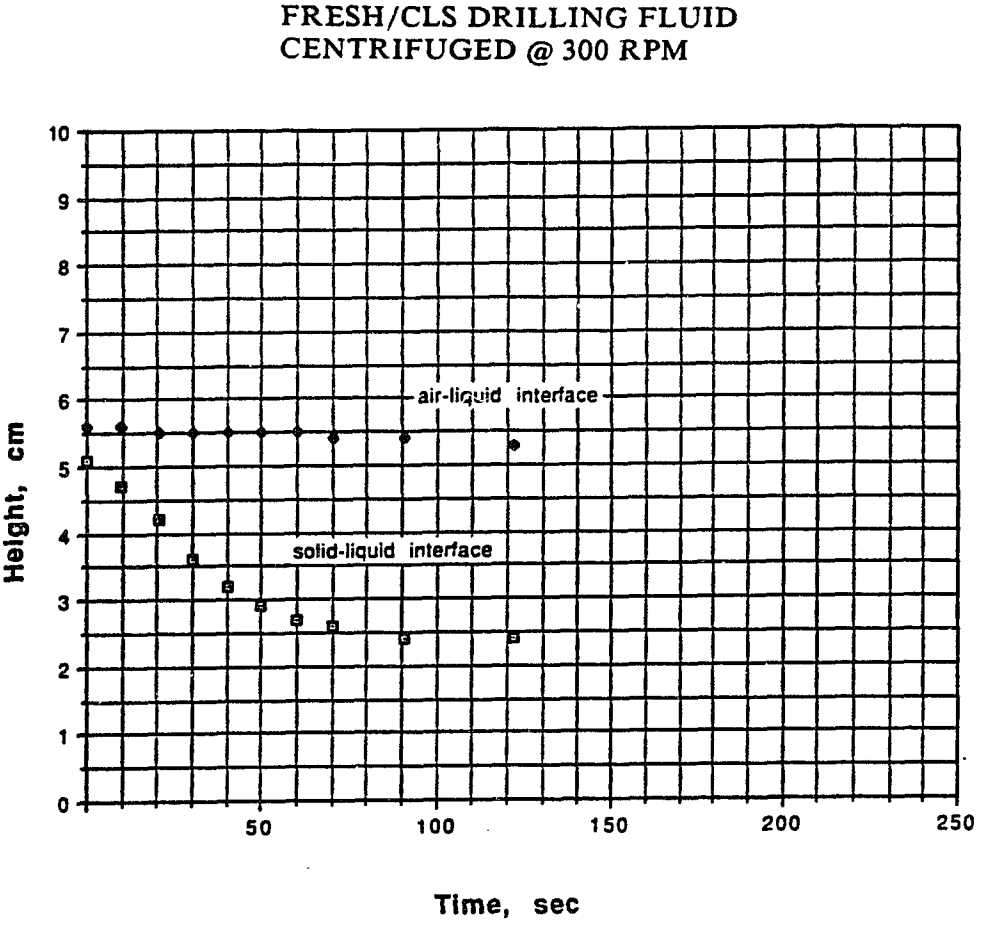

Fig. 2-5 Movement of air/liquid and solid/liquid interface in a centrifugal field

permeability of the fluids tested. Plugging of the sand matrix was not considered to reduce permeability as significantly as the adjacent, compressed clay matrix. Care was taken to select a sand grain size to prevent any migration. Upon examination of the sand matrix, no appreciable amount of clay had migrated.

2.1.2 Suspensions tested and preparation of sample

The permeability of six fluids was measured using the method described. Three were field samples and three were 100% mineral suspensions: bentonite, attapulgite and barium sulfate, or by its common name, barite. Mud properties for two of the field samples have been included in Appendix D: Fresh/CLS and Salt/CLS fluid systems. Some of the fluids tested and evaluated were simulated. The simulated fluids were formulated in the laboratory using recommended additives at respective concentrations which would make them similar to field muds of the same type. The 1:1 dilutions of field samples were prepared by adding a 1:1 volume of distilled water, adding $Fe_2(SO_4)_3$ to reduce pH (coagulation) to the level shown in Table 2-1, then adding a polymeric flocculant. All three of the previously mentioned mineral suspensions had a density of approximately 9 lb_m/gal before dilution. This density was selected to approximate that of unweighted field samples.

Table 2-1 Chemical treatments of fluid systems

Fluid System	Dilution	Chemical Treatment	pH	Dosage*
Starch	1:1	$Fe_2(SO_4)_3$ High M:high anionic PE	7.9	0.236
Salt/CLS	1:1	$Fe_2(SO_4)_3$ Very high M:non-ionic PE	5.9	0.262
Fresh/CLS	1:1	$Fe_2(SO_4)_3$ High M:high anionic PE	6.4	0.306
Attapulgite & water	1:1	$Fe_2(SO_4)_3$ High M:high anionic PE	6.3	0.219
Bentonite & water	1:1	$Fe_2(SO_4)_3$ High M:high anionic PE	4.6	0.175
Barite	1:0	None	NA	0.0

*pounds of dry polymer per barrel of actual mud
NA - not available
M - molecular weight
PE - polyelectrolytes
CLS - chrome lignosulfonate

The most difficult drilling fluid to treat chemically was the fresh/CLS fluid system. The pH had to be brought to a lower value and more polymer (0.306 lb_m) was required for flocculation. On a second treatment, however, less polymer (0.262 lb_m) was required to reach the flocculated endpoint. This meant the principal differences between the salt/CLS and fresh/CLS treatment were the molecular weight and the polyelectrolyte charge used.

The dosage variability is attributed to the method of mixing in which incremental amounts of polymer were added. Suspensions were mixed using a spatula to stir the samples. Typically, 40 mL of the 1:1 dilutions were mixed and placed

in the centrifuge tube for measurement. Incremental additions of 2% w/w mixtures of polymer varied from 0.5-1.0 mL.

2.1.3 Data interpretation

The slight curvature of the liquid surface versus time plot is evident (Fig. 2-5). In accordance with Darcy's law, flow rate declines with pressure. As stated in Appendix B, permeability is computed from the slope of the logarithm of Function R versus time, where Function R models observed flow and is the ratio of $(R_b + R_L)$ to $(R_b - R_L)$ (see Appendix B). The radius to the case base, R_b, is constant while the radius to the top of the liquid, R_L, increases with time as the fluid flows through the cake. Consequently, Function R increases with time. Hydraulic pressure results from the water mass being centrifugally accelerated. To illustrate, the following example is presented for an inhibitive drilling fluid containing starch.

At each level of compaction, the equilibrium cake thickness was measured and the rotational velocity noted.

Table 2-2 Equilibrium cake thickness at various rotational velocities

Data	H_e, cm	N, rpm
1	3.5	243
2	3.15	389
3	2.85	489
4	2.45	760
5	1.85	1228

Function R was plotted against time for each of the five data and the slope obtained.

Table 2-3 Permeability reduction with increasing rotational velocity

H_e, cm]	N [rpm]	slope, m	R	k, md
3.50	243	$6.089(10)^{-4}$	1.00	356.9
3.15	389	$3.212(10)^{-5}$	0.99	6.613
2.85	489	$1.495(10)^{-5}$	1.00	1.762
2.45	760	$1.017(10)^{-5}$	1.00	0.4266
1.85	1228	$9.706(10)^{-6}$	0.99	0.1178

R is the coefficient of correlation

A plot of permeability against H_e for this data is shown in Fig. 2-6. In Fig. 2-7, the characteristic shape of permeability and cake height plotted against rotational velocity is shown.

2.1.4 Verification and relation to other methods

Measurement of permeability in the centrifuge was compared with a conventional stationary or static permeameter. This was done to demonstrate the accuracy of the method as developed for this research.

For this comparison, flocculated bentonite was tested in both the static and centrifugal permeameter. The slurry was centrifuged at 470 rpm for sufficient time to achieve an equilibrium cake thickness of 2.2 cm, and the permeability was measured. The pressure applied by the centrifuge due to the accelerated mass of water was 0.23 atm. The sample was removed from the centrifuge and placed in the static permeameter. A similar hydraulic pressure was applied (0.33 atm). The tube was removed and centrifuged a second time at 470 rpm, and permeability was measured. In the second

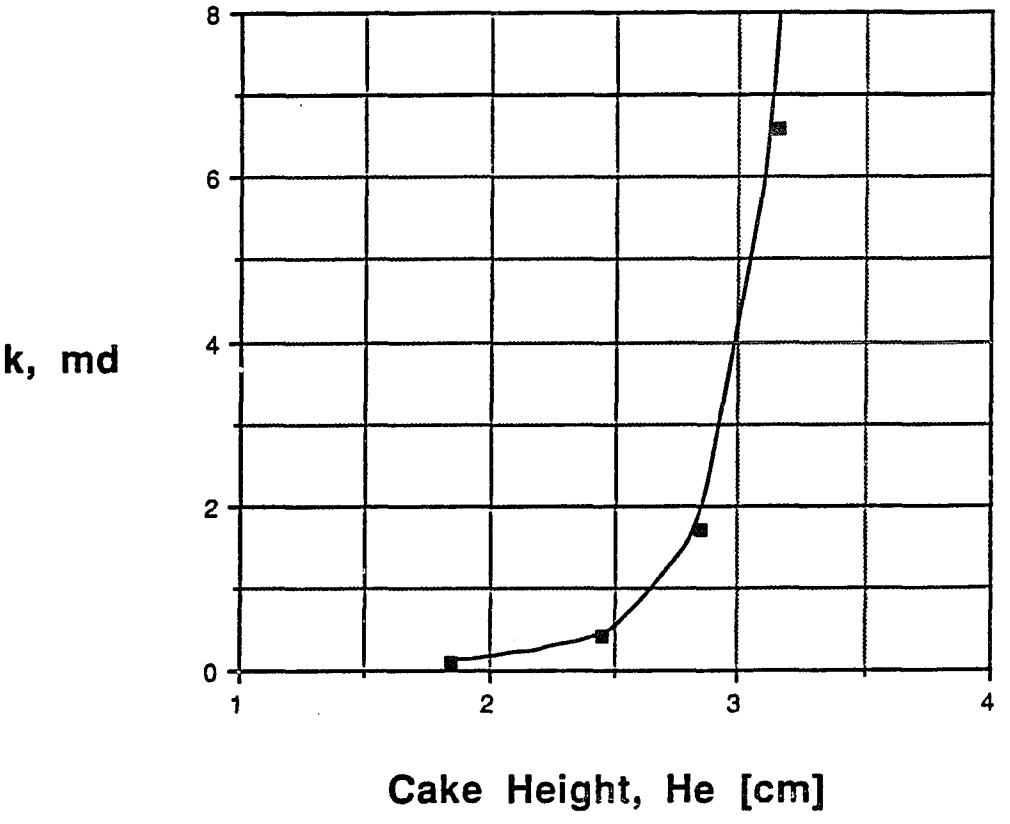

Fig. 2-6 Characteristic permeability vs. cake height plot due to centrifugal compression

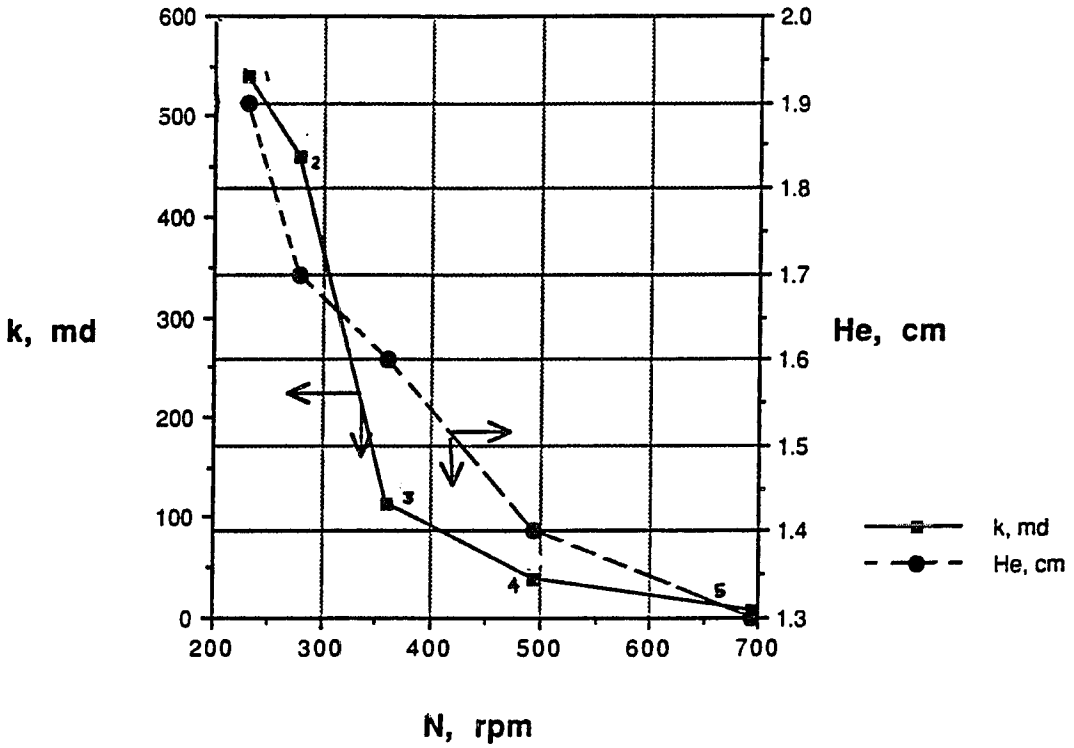

Fig. 2-7 Characteristic permeability and cake height against rotational velocity (RPM) due to centrifugal compression

centrifuge period, the cake height was reduced from 2.2 to 1.8 cm when the sample was centrifuge a second time. This reduction is attributed to a rearrangement due to stress re-application after relaxation. Permeability was measured a second time in the static permeability as shown.

Table 2-4 Similarity of centrifugal and static permeameter data

Permeameter Type	H_e	k, md	P, atm
Period 1			
Centrifugal	2.2	11.1	0.23
Static	2.2	10.9	0.33
Period 2			
Centrifugal	1.8	3.1	0.29
Static	1.8	2.5	0.33

The shortening of cake height in Period 2 to 1.8 cm may have been due to the extrusion of polymer-adsorbed onto clay surfaces into different voids under a reapplied compression (Gray, 1968).

2.2 Results and discussion

Past efforts employed the compression-permeability cell to measure specific resistance to filtration or to use the term adopted by Grace (1953), specific cake resistance. This term is related to permeability by Equation 1-1. Differences associated with the C-P cell provided the justification for the development of the alternate method outlined in section 2.1.

Certain differences exist between a centrifugally applied consolidating stress and that using the C-P cell.

First, the C-P cell applies stress to both sides of the network. Stress is greatest at the outer surfaces and decreases toward the center. The reason for this can be stated qualitatively. The only stress which can be applied to the center of the network is by compression of the network to either side. The network away from the center can be expected to absorb a certain level of stress due to its internal friction. Consequently, a lower stress level is applied to the network center.

The compression at each outer edge means expression of water is inhibited in two directions. Second, the application of stress is different. The stresses using the C-P cell are applied by deformation of the network at the surface contacting the porous plate. The centrifugal permeameter constrains the network on only one side. Stresses decrease inward from this outer radius. In this way, the expression of water toward the inner radius is not inhibited as severely as with the C-P cell. Third, the application of stress is due to centrifugal acceleration, which more directly simulates the application of stress in the industrial centrifuge. These differences motivated this new approach to quantify its benefits over using the C-P cell.

Similarities in network response are now made between fluids tested with the C-P cell and fluids tested using the centrifuge. C-P cell data is from Grace (1953) while cen-

trifugal permeameter data was obtained in this research.

Measurements of network permeability against consolidating stress were absent from the literature, therefore, data from this research were converted to specific cake resistance in order to compare with a previous study.

For ease in application, Eq. 1-1 was converted to practical units assuming a solids density of 2.6 g/cm^3,

$$\alpha_p = \frac{5.799\ (10)^{-17}}{k\ (\ 1 - \phi\ )} \quad [m/kg] \qquad 2\text{-}5$$

where k, without the subscript "s," is expressed in millidarcies. On the abscissa, Grace (1953) placed compressive pressure (P_c, lb_m/in^2) which is identical to effective consolidation stress (σ_v').

For data in this research, effective consolidation stress was computed as described in Appendix C, but was converted to lb_m/in^2 to better compare with Grace's data.

In Grace's analysis, contrary to Ruth's (1946) hypothesis, the plots were not linear at high compressive pressures. Following examination of various materials (Fig. 2-8, Fig. 2-9, and Fig. 2-10), Grace concluded they did not lend themselves to direct mathematical treatment. He also observed that values of α_p versus P_c varied widely for the same material. This was explained by the degree of flocculation existing in the prefilt (prior to filtration) because of the various electrolytes present. The flocculation differences were confirmed by microscopic examination on

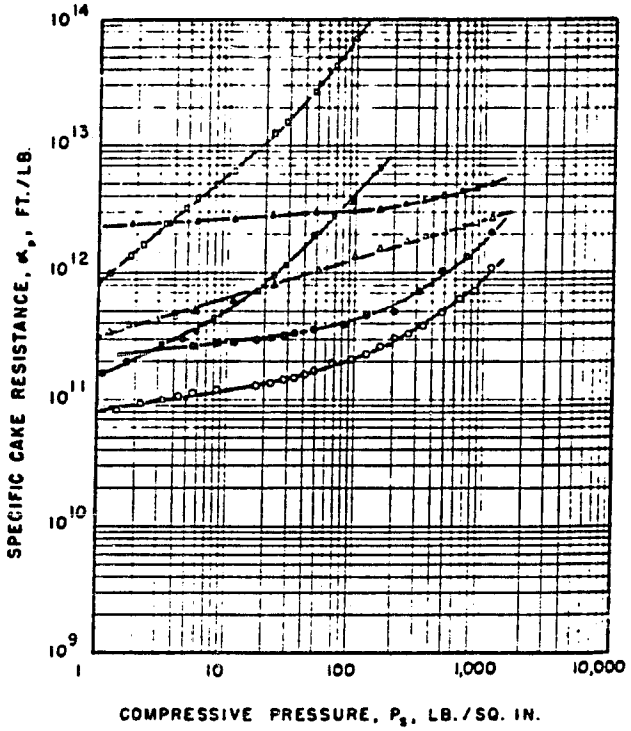

○ Superlight $CaCO_3$ (flocculated)
50 g./l. of distilled water pH = 9.8
● Superlight $CaCO_3$
50 g./l. of 0.01 M $Na_4P_2O_7$ pH = 10.3
△ R-110 grade TiO_2 (flocculated)
50 g./l. of distilled water, pH = 7.8
▲ R-110 grade TiO_2
50 g./l. of 0.01 N HCl pH = 3.45
⁼ ZnS
Type B pH = 9.07
■ ZnS
Type A pH = 9.10

Fig. 2-8 Specific cake resistance vs. compressive pressure and including flocculated TiO_2 (after Grace, 1953)

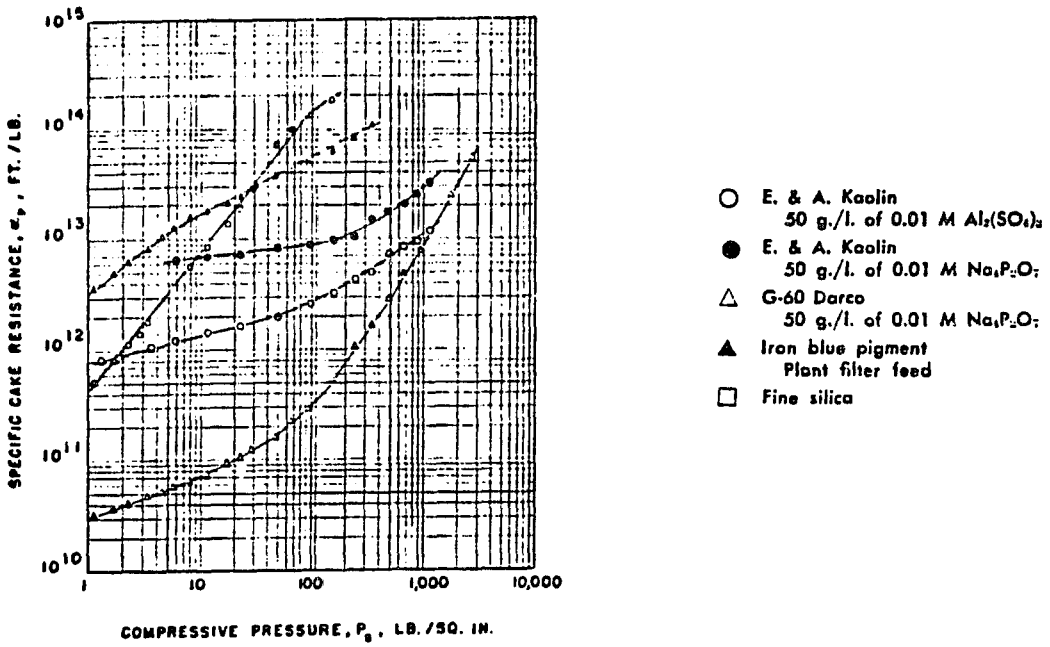

Fig. 2-9 Specific cake resistance vs. compressive pressure and including kaolin (after Grace, 1953)

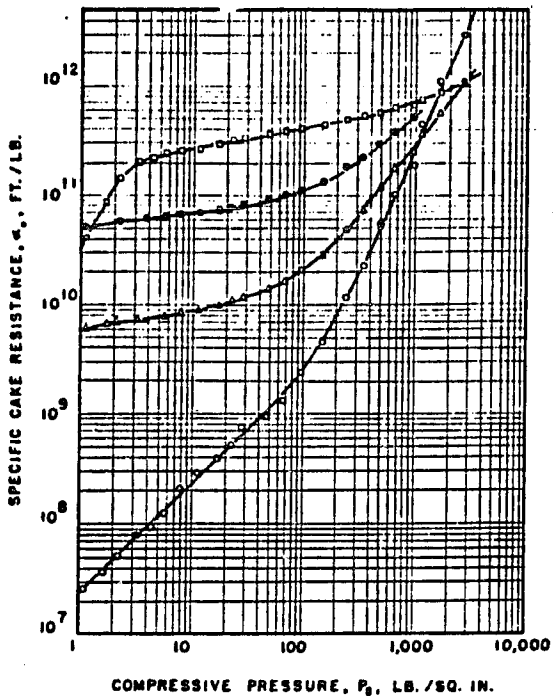

Fig. 2-10 Specific cake resistance vs. compressive pressure and including fine ilmenite (after Grace, 1953)

prefilt suspensions. This indicated that the response of the network depended upon the chemical treatment.

For the suspensions tested in this research, the least compressible was barite. The compression which did occur was due to packing as air was expelled from the network. Barite (Fig. 2-11) compared in trend with R-110 grade TiO_2 in 0.01 N HCl (Fig. 2-8). Concave up indicates the medium is yet to reach ultimate compaction. It can be dewatered further with increased compressive pressure. Concave down indicates the material is approaching ultimate compaction.

When all drilling fluids were combined on the specific resistance against compressive pressure plot (Fig. 2-12), the trend was practically linear. A best fit straight line as shown had a coefficient of correlation of 0.819 (Fig. 2-13).

The most pronounced compactible drilling fluid system (concave up) was that of flocculated bentonite (Fig. 2-11). It compared most closely in trend to E. & A. kaolin (Fig. 2-9).

The most pronounced least compactible drilling fluid system (concave down) was the inhibitive mud containing starch (Fig. 2-12), and compared most closely with fine silica (Fig. 2-9) and fine ilmenite (Fig. 2-10). Flocculated attapulgite compared closely with lignosulfonate (Fig. 2-12) which were both fluids tested in this research.

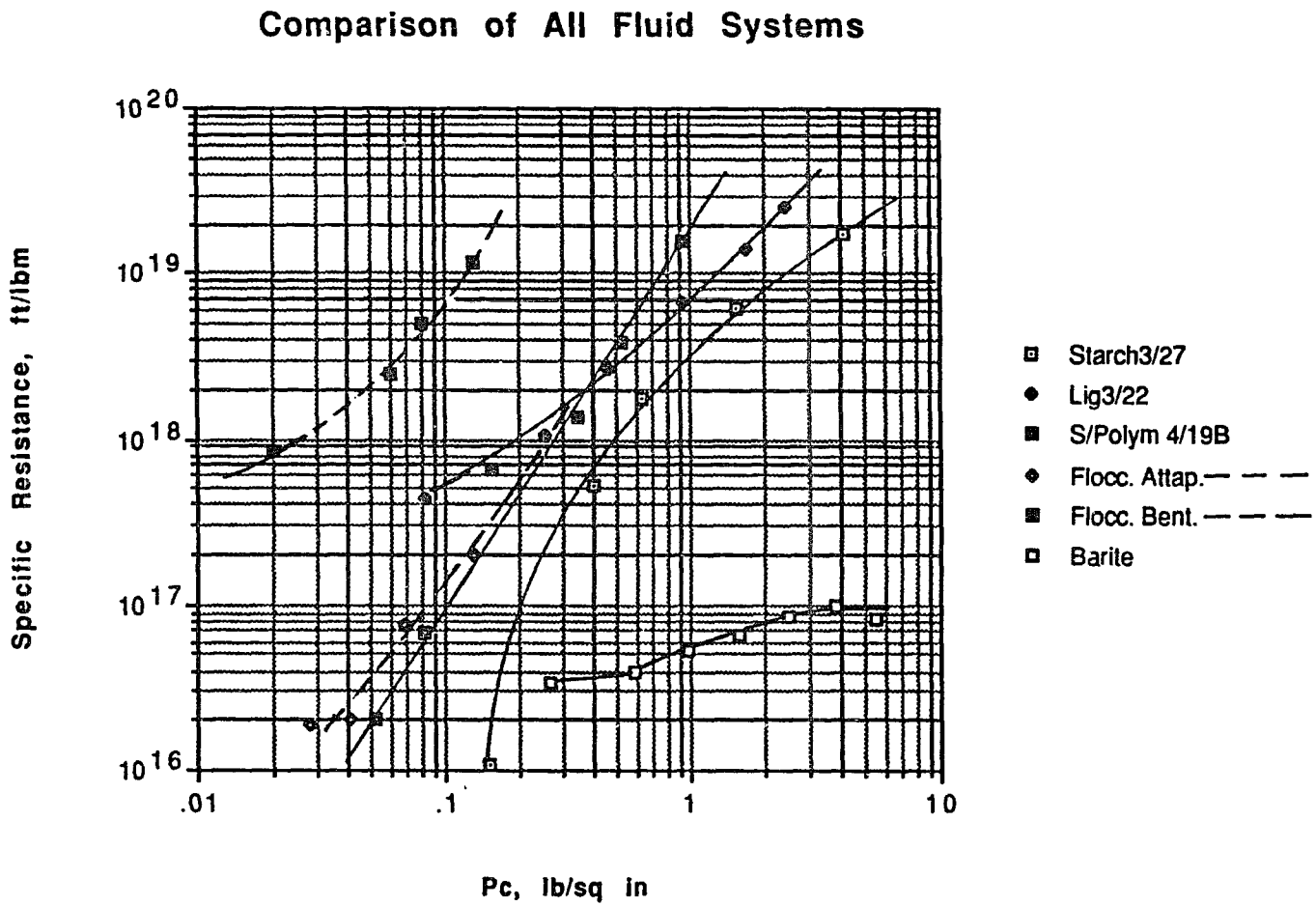

Fig. 2-11 Comparison of all fluid systems on a specific resistance against compressive pressure

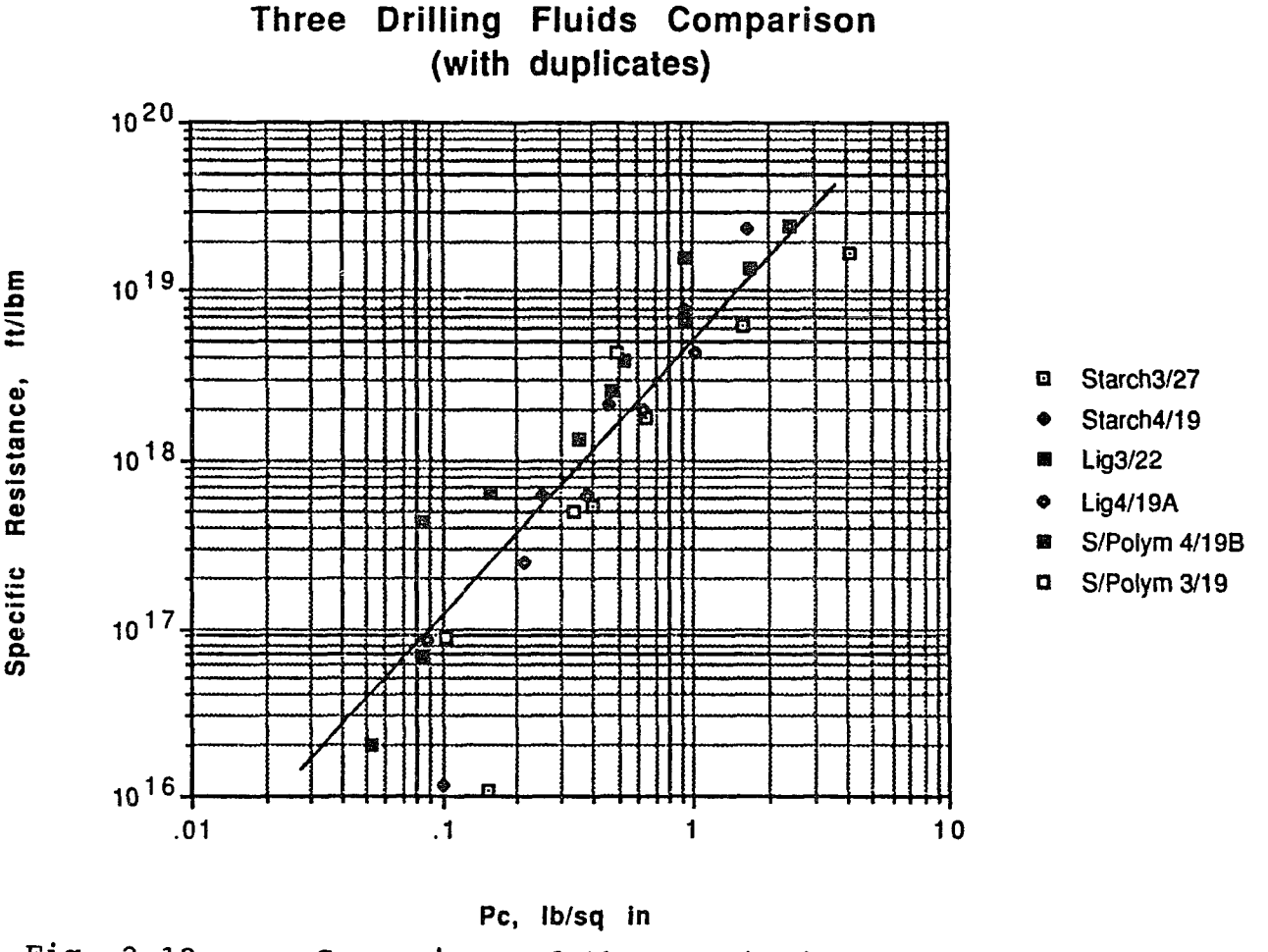

Fig. 2-12 Comparison of three drilling fluid systems on a specific resistance vs. compressive pressure plot

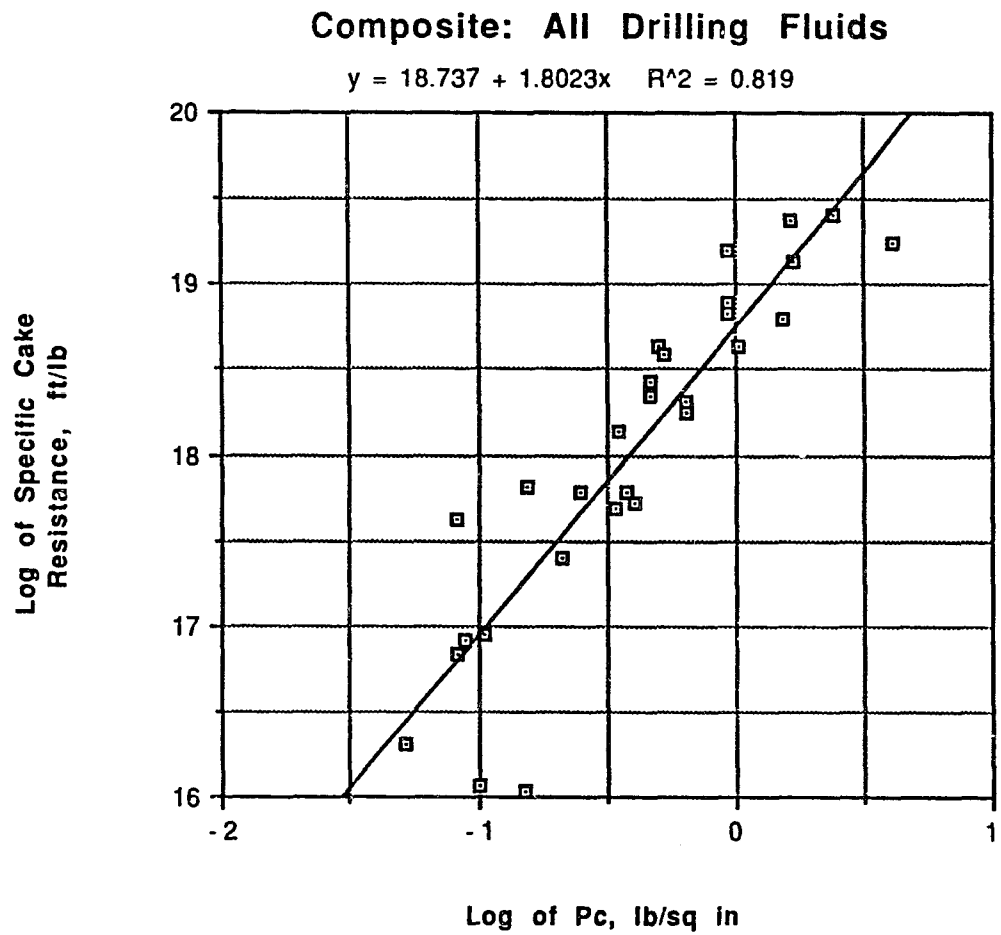

Fig. 2-13 Log-log plot showing similarity of specific cake resistance-compressive pressure responses for various drilling fluids

2.2.1 Permeability and porosity tables

The characteristic shape of permeability against rotational velocity is presented in Fig. 2-14. Flocculated networks are typically highly permeable when initially mixed. The maximum measured permeability among the drilling fluid systems tested was 357 md @ 243 rpm and was for an inhibitive drilling fluid system containing starch. The maximum permeability of a mineral suspension was flocculated attapulgite, and was 539 md at 235 rpm.

The following table is a typical example, and these data are graphically presented in Fig. 2-15.

Table 2-5 Dewaterability characteristic for lignosulfonate

H_e cm	N rpm	k md	ϕ %	σ_v' kPa
3.8	235	15.95	91.56	0.58
3.1	550	2.13	89.65	3.21
2.6	770	0.6902	87.66	6.38
2.25	1035	0.2920	85.74	11.62
1.85	1233	0.1333	82.66	16.67

In Fig. 2-16 flocculated attapulgite is shown in comparison to the other samples tested. For each of the fluid systems tested, several measurements were made. As the data in Table 2-5 are fairly typical, a discussion of particulars is useful before an enlarged table is shown.

The final porosity of 83% equates to 65% by weight water content which compares closely with the 65% by weight water minimum obtained in controlled full-scale studies where the sludges contained active clay solids (Wojtanowicz, 1988).

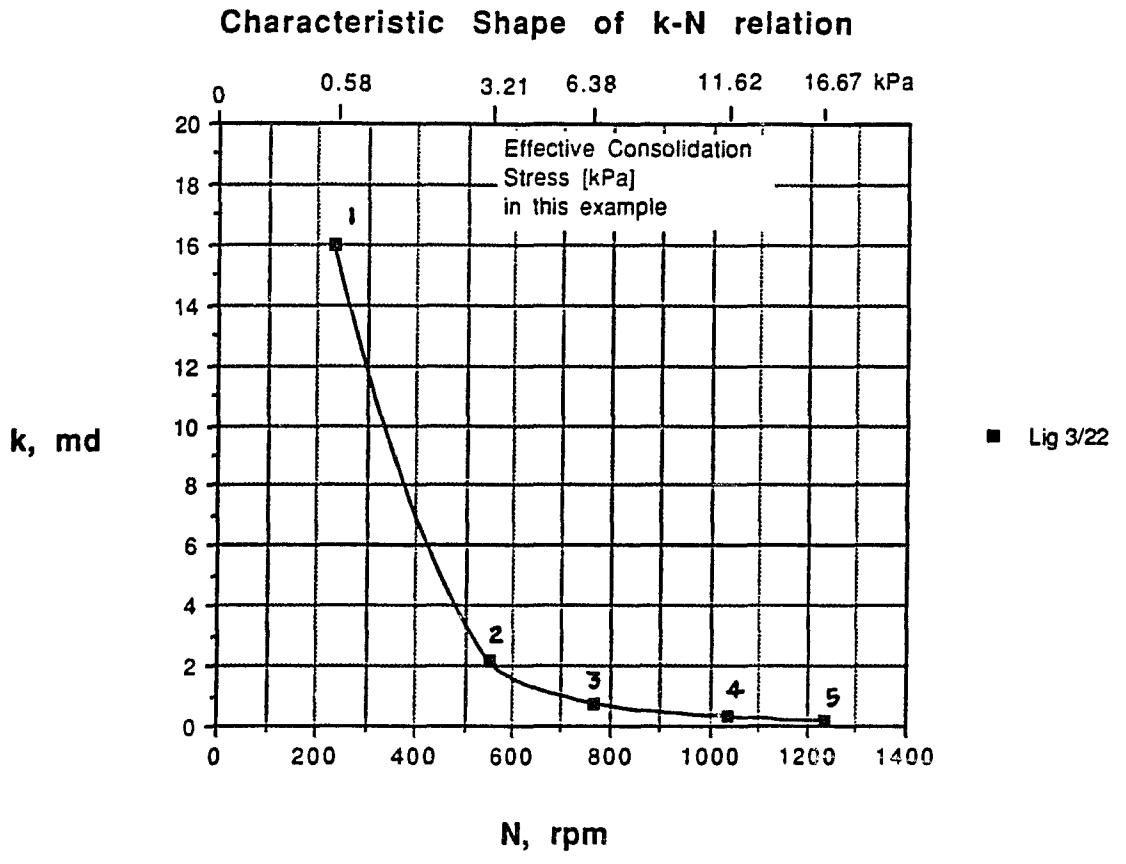

Fig. 2-14 Characteristic plot showing effect of rotational velocity (RPM) on permeability combined with effective consolidation stress

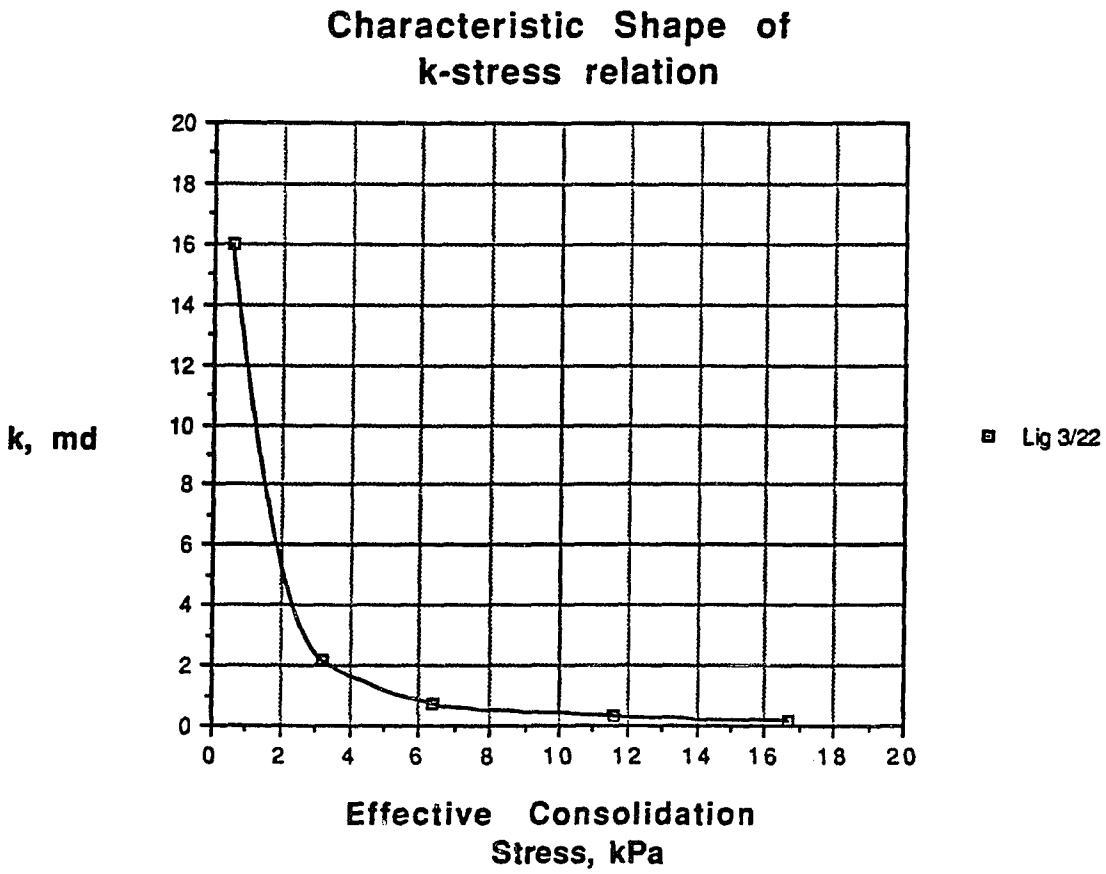

Fig. 2-15 Characteristic plot showing effect of effective consolidation stress on permeability

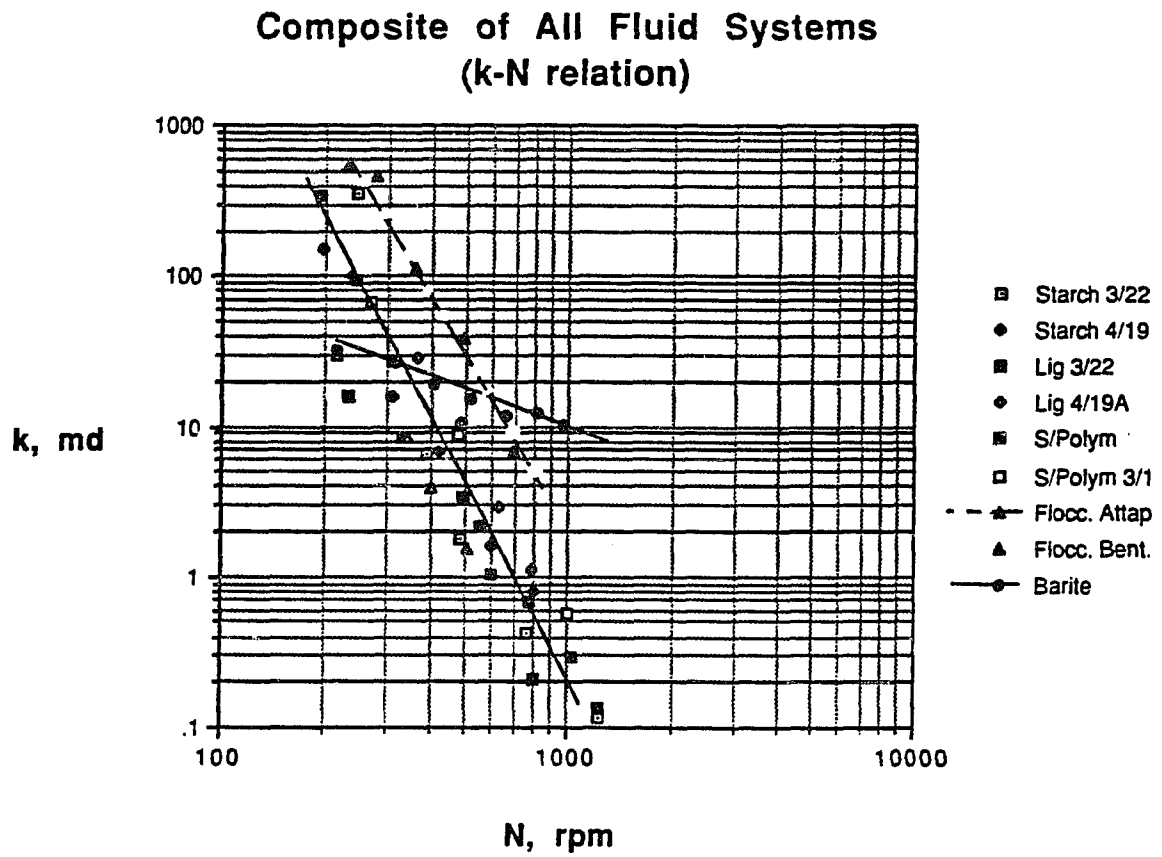

Fig. 2-16 Plot showing log-log relation for permeability-rotational velocity of all fluids tested

The following table compares the weight percent water of the same fluid systems tested at an equivalent 800 rpm as calculated from an interpolation of data.

Table 2-6 Water content (% w/w) of fluid systems tested at 800 rpm

Fluid System	Water Content, % w/w
Inhibitive with starch 1	58%
Inhibitive with starch 2	59%
Lignosulfonate 1	74%
Lignosulfonate 2	74%
Salt-polymer 1	65%
Salt-polymer 2	65%
Flocc. Bentonite	92%*
Flocc. Attapulgite	81%+
Barite	23%

* @508 rpm
\+ extrapolated from 694 rpm

For each drilling fluid system, the duplicates were in excellent agreement, and showed the greater difficulty in dewatering the lignosulfonate fluid system. Overall, it can be concluded that moderate increases in centrifuge speed drastically reduce permeability. This is borne out in all data as presented in the following table for all fluid systems.

Table 2-7 Experimental data from all fluid systems tested

He cm	N rpm	σ_v' kPa	k md	ϕ fraction	Weight % Water
Run 1 1:1 Inhibitive with starch					
3.5	243	1.07	357.0	0.85	68%
3.15	389	2.76	6.6	0.83	65%
2.85	489	4.39	1.8	0.82	63%
2.45	760	10.7	0.43	0.78	58%
1.85	1228	28.3	0.12	0.72	49%
Run 2 1:1 Inhibitive with starch					
3.7	196	0.68	152.0	0.86	70%
3.7	312	1.71	15.7	0.86	70%
3.5	422	3.15	6.71	0.85	68%
3	595	6.34	1.59	0.82	64%
2.5	795	11.5	0.79	0.79	59%
Run 1 1:1 fresh/CLS					
3.8	235	0.58	15.9	0.91	81%
3.1	550	3.21	2.13	0.89	77%
2.6	770	6.38	0.69	0.88	73%
2.25	1035	11.62	0.29	0.86	70%
1.85	1233	16.67	0.13	0.83	65%
Run 2 1:1 fresh/CLS					
4.6	238	0.61	99.4	0.93	84%
4	366	1.46	29.0	0.92	81%
3.6	486	2.59	10.5	0.91	80%
3.2	628	4.37	2.86	0.90	77%
Run 1 1:1 salt/CLS					
3.5	194	0.36	340.	0.91	81%
3.2	243	0.57	92.5	0.91	79%
2.8	330	1.06	8.54	0.89	76%
2.3	493	2.41	3.32	0.87	72%
2	604	3.64	1.02	0.85	69%
1.7	799	6.42	0.21	0.83	65%
Run 2 1:1 salt/CLS					
3	270	0.72	67.3	0.90	78%
2.2	480	2.32	8.8	0.87	71%
1.25	1000	10.33	0.56	0.76	55%
1:1 flocculated Bentonite					
4.55	217	0.16	29.4	0.98	94%
3.9	345	0.42	8.47	0.97	93%
3.65	400	0.57	3.94	0.97	93%
3.3	508	0.93	1.55	0.97	92%

Table 2-7 (cont.)

He cm	N rpm	σ_v' kPa	k md	ϕ fraction	Weight % Water
1:1 flocculated Attapulgite					
1.9	231	0.20	539.0	0.94	87%
1.7	279	0.28	459.0	0.94	85%
1.6	360	0.47	114.0	0.93	84%
1.4	493	0.89	37.9	0.92	82%
1.3	694	1.77	6.74	0.92	81%
1:0 barite					
2.25	215	1.86	31.9	0.47	25%
2.15	316	4.03	27.0	0.44	23%
2.1	407	6.70	19.4	0.43	22%
2.1	520	10.93	15.5	0.43	22%
2.1	655	17.34	11.9	0.43	22%
2.1	810	26.53	12.1	0.43	22%
2.1	968	37.88	10.2	0.43	22%

2.2.2 Effect of effective stress on permeability

A comparison of Fig. 2-16 and Fig. 2-17 shows that the decrease in permeability is more pronounced when viewing the data on a k-σ_v' plot as opposed to a k-N plot. This is due to the dependence of σ_v' upon the square of rotational velocity. The drilling fluids tested show a similar trend on the log-log plot of permeability-rotational velocity (Fig. 2-18).

An excellent linear fit for a salt/polymer (sample 4/19B) fluid system is evident over the rotational velocity range tested (Fig. 2-19). The salt/polymer fluid system, as expected, is one of the most compressible because of the presence of polymer in the continuous phase and also present as the flocculating medium.

As mentioned, a sample of each drilling fluid system is presented with all other fluid systems on a plot of

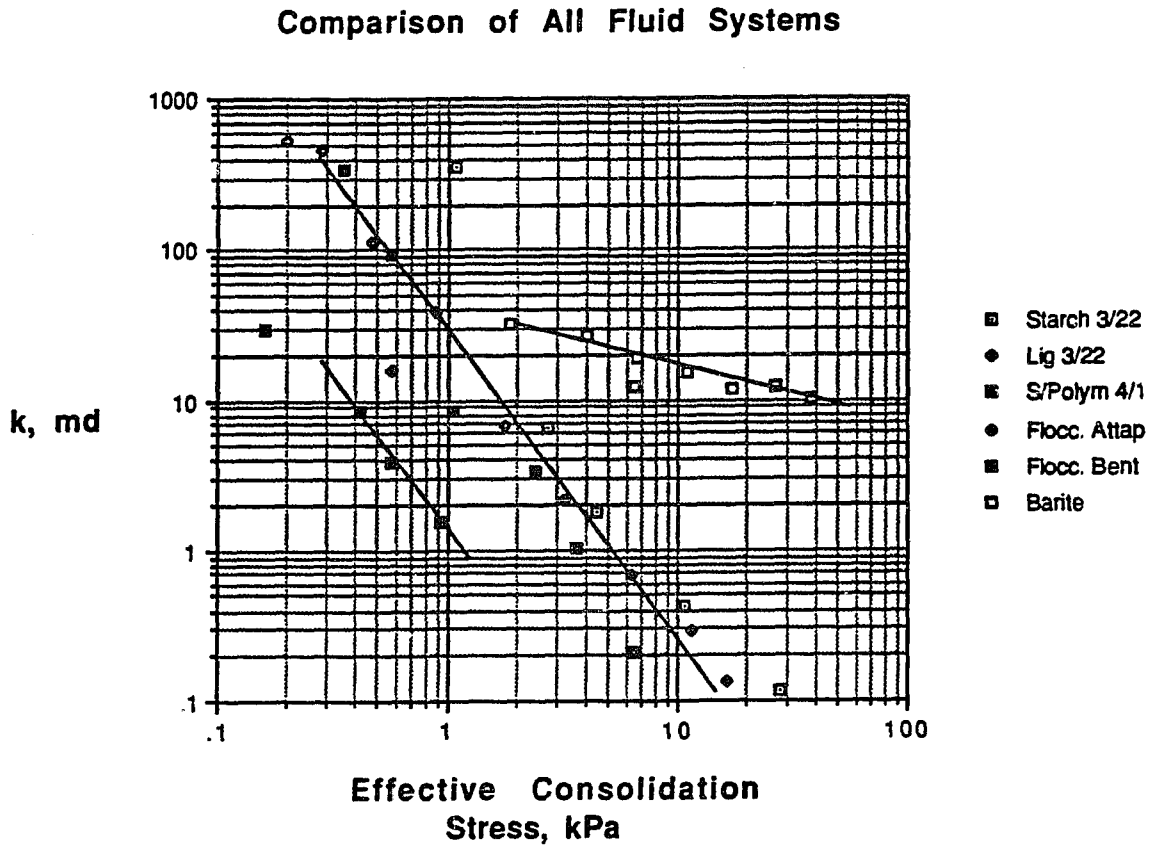

Fig. 2-17 Linear relation for permeability-effective consolidation stress of all flocculated drilling fluids tested

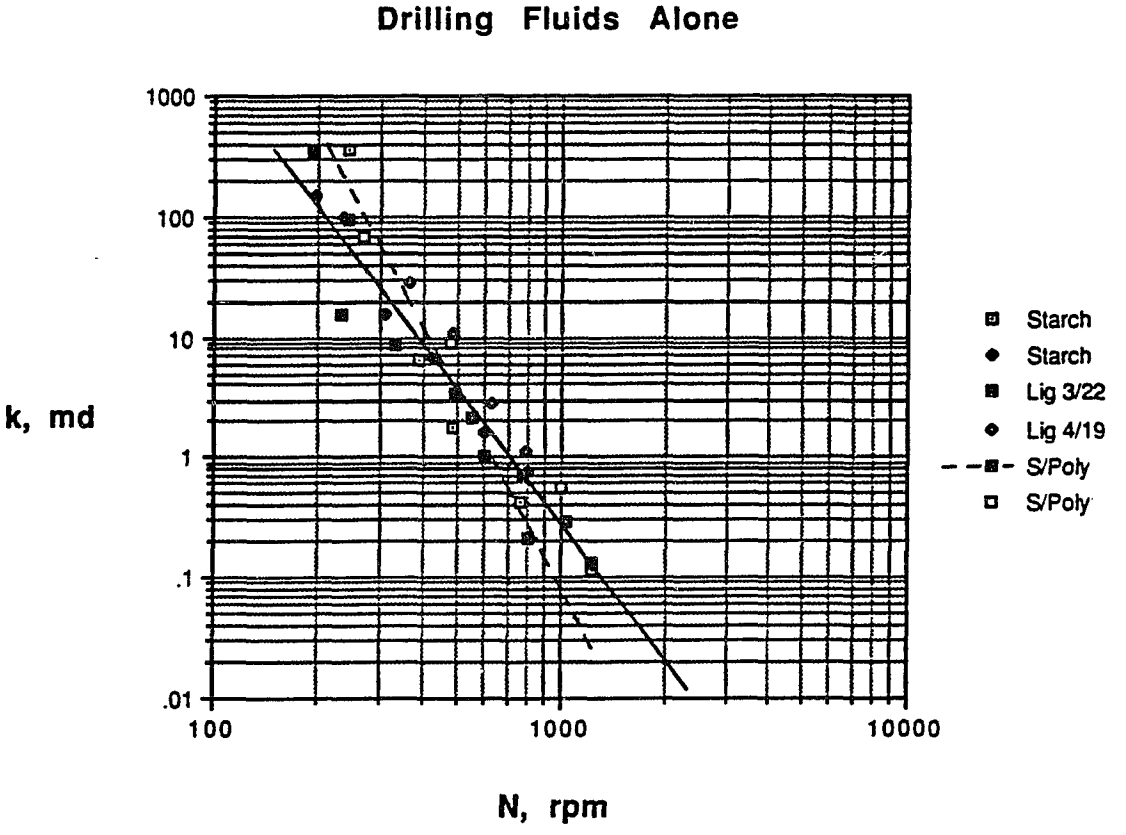

Fig. 2-18 Linear relation for permeability-rotational velocity (RPM) of all flocculated drilling fluids tested

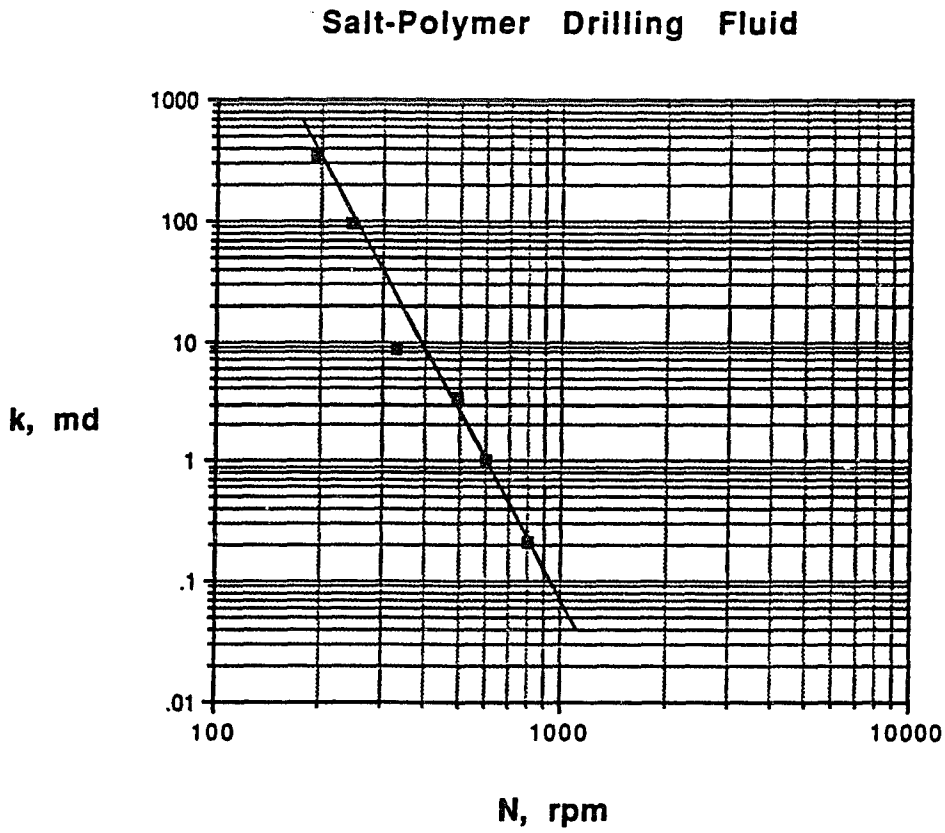

Fig. 2-19 Linear relation for permeability-rotational velocity (RPM) of 1:1 flocculated salt/CLS fluid

permeability against σ_v' (Fig. 2-17). The less compactible barite is divergent from the trends of other samples. While flocculated attapulgite is similar to the drilling fluid systems, flocculated bentonite has a similar slope on the log-log plot, but it is displaced, showing that its permeability reduction is more sensitive to increases in effective consolidation stress.

2.2.3 Discussion

The mutually opposing nature of compressible networks is obvious. The rate at which dewatering can occur is dependent upon its permeability, which decreases with compaction. To reduce water content, the network must be compressed. However, as the network is compressed, its permeability is reduced. As permeability is reduced, flow rate out of the compressed cake is reduced. It is likely that a permeability reduction will occur such that the cake will not be in the centrifuge long enough to achieve ultimate compaction. This is equivalent to saying that residence time is insufficient to allow stresses to be equilibrated. Future studies should address the optimum application of consolidating stress for achieving the minimum water content.

Nomenclature

A = cross sectional area of cake, cm^2
k = permeability, md
k_s = permeability, m^2
dL = cake thickness, cm
N = rotational velocity, rpm
dP = pressure drop across the cake, atm
P_c = compressive pressure, lb_f/in^2
q = flow rate of liquid through cake, cm^3/s
R_b = radius to top of cake (liquid-cake interface), cm
R_L = radius to top of air-liquid interface, cm

α_p = specific resistance to filtration, m/kg
μ = viscosity of fluid, cp
ϕ = porosity, void volume to total volume, cm^3/cm^3
ρ_s = solids density, kg/m
ρ = density, g/cm^3
σ_v' = effective consolidation stress, kPa
ω = rotational velocity, sec^{-1}

Chapter III

Deformation Properties of Dewatering Sediments

Permeability measurements and their analysis was described in Chapter II. Resistance to compression will be addressed in this chapter. For a specified compression, the response of the network can be quantified by its bulk modulus of elasticity. In this manner, it is conceivable that ultimate compaction at a specified compression level can be predicted. This assumes sufficient residence time in the centrifuge be allowed for water expression.

For various drilling fluids, this chapter describes and applies the measurement of bulk modulus in a centrifugal field. From these results, a comparison with C-P cell data from other investigators is performed.

3.1 Methodology of measurements

3.1.1 Description of experimental investigation

In Chapter II, permeability measurements on six fluids (Table 2-1) were described. Data from these experiments can also be used to calculate bulk modulus.

3.1.2 Calculation of bulk modulus

In this section, the derivation for the computation of bulk modulus measurement is presented and parallels one

developed by Buscall (1982). The one presented here is more direct and can be more readily applied to experimental data.

The derivation begins with a definition of bulk modulus, K, (Streeter and Wylie, 1975, p. 17).

$$K = \frac{d\sigma_v'}{dV/V} \qquad 3\text{-}1$$

where σ_v' = effective consolidation stress

dV/V = differential volume change due to applied differential stress

The volume change can be considered in one dimension as the network is constrained by the sides of the centrifuge tube during compression. Consequently, the denominator dV/V can be written as

$$dV/V = \frac{A\ dH_e}{A\ H_e} = \frac{dH_e}{H_e} \qquad 3\text{-}2$$

where A = tube cross-sectional area

H_e = equilibrium cake height

Stress is force acting on an area, and the force is due to the mass (m) accelerated by the centrifuge, where $\omega^2 r$ is centrifugal acceleration. Mass over area (m/A) can be replace by ρH_e. The density causing compression (ρ_{eff}) is the difference between the density of the saturated suspension and the liquid phase density (ρ_w = 1.0 g/cm^3 for water),

$$\rho_{eff} = \rho_{sat} - \rho_w \qquad 3\text{-}3$$

The calculation of ρ_{sat} was based upon the known mud density and mud volume, and the known volume of dilution water and chemicals. Throughout the cake compression, the mass of

solids remained constant. Thus, ρ_{sat} could be known at any compression level. The assumption of all solids having a specific gravity of 2.6 g/cm^3 was also included in these computations. The density relation in Eq. 3-3 can be derived from the definition of effective consolidation stress described in Appendix C. This definition is

$$\sigma_v' = \sigma_{TOT} - P \qquad C\text{-}1$$

Stress can be written as

$$\sigma = (m\omega^2 r)/A \qquad 3\text{-}4$$

and replacing m/A by ρH_e

$$\sigma = \rho H_e \omega^2 r \qquad 3\text{-}5$$

Substituting the density term into Eq. C-1, we can write

$$\rho_{eff} H_e \omega^2 r = \rho_{sat} H_e \omega^2 r - \rho_w H_e \omega^2 r \qquad 3\text{-}6$$

which, upon removal of similar terms, yields Eq. 3-3. If the terms r, H_e, A and ρ_{eff} are taken as constant, then the numerator of Eq. 3-1 ($d\sigma_v'$) is

$$d\sigma_v' = \rho_{eff} H_e r d\omega^2 \qquad 3\text{-}7$$

This is a reasonable assumption due to the small relative change as compared with the change in rotational velocity (ω). Differentiating Eq. 3-7 yields,

$$\rho_{eff} H_e r d\omega^2 = \rho_{eff} H_e r 2\omega d\omega \qquad 3\text{-}8$$

The radius, r, is best handled by replacing it with the radial distance to the network midpoint,

$$r = R_b - H_e/2 \qquad 3\text{-}9$$

where R_b = radial distance to the bottom of the sedimented cake

Substituting this value for the radius into Eq. 3-8 and combining the numerator (Eq. 3-8) and denominator (Eq. 3-2) into the definition of K (Eq. 3-1),

$$K = (R_b - H_e/2)\ \rho_{eff}\ H_e^2\ \omega\ d\omega/dH_e\ [g/(cm\text{-}sec^2)] \qquad 3\text{-}10$$

Or in alternate units to be used in experimental computations,

$$K = (R_b - H_e/2)\ \rho_{eff}\ H_e^2\ \omega\ d\omega/dH_e^*\ (0.0001)\ [kPa] \qquad 3\text{-}11$$

where kPa are units of stress.

Data obtained for moduli measurements provide the data for the ω versus H_e relation. The slope of ω against H_e provides $d\omega/dH_e$ for use in solving Eq. 3-11. Thus, an experimental method for measuring bulk modulus (K) as a function of rotational velocity (ω) is readily available.

The assumption of homogeneous sediment density is maintained throughout the data analysis. However, a method for quantifying the variable density of sediment for a centrifugally sedimented cake was discovered. This method was applied in one instance; however, it was not incorporated into the bulk modulus computation. A description of this method follows.

3.1.3 Determination of variable density

Previous investigators (Bear, et al., 1984; Buscall, 1981) made the assumption of constant density throughout the compressed cake. This approximation was made for at least two reasons. First, it was expected that accuracy would not

be significantly affected, and second, no method was readily available for measuring the density variation in such a small mass. However, a means was discovered for quantifying the variability of cake density. The method was made on a single sedimented sample, a flocculated field fresh/CLS drilling fluid. This CLS mud was chemically treated as described in Table 2-1.

The mass and volume of the dried sample provides the data from which original cake density in the saturated state can be computed. The geometry of the compacted cake once it had dried was a frustrum of an homogeneous right circular cone. This method for estimating the original density distribution is simplified by assuming that the sedimented dried cake has homogeneous density. This assumption is defended by considering the relation between capillary pressures and soil shrinkage theory.

Shrinkage depends upon particle size and geometric arrangement (Holtz and Kovacs, 1981, p. 96,183). The mechanism governing particle distance upon drying is the equilibrium between capillary pressure and interparticle compressibility. During evaporation, menisci form in pore throats. The retention of capillary menisci hanging on the particles increases contact between the particles (Fig. 3-1). With evaporation, the capillary pressure (u_c) increases and draws the solid particles together. Pressure can be described by the following relation (Holtz and Kovacs, 1981, p. 170),

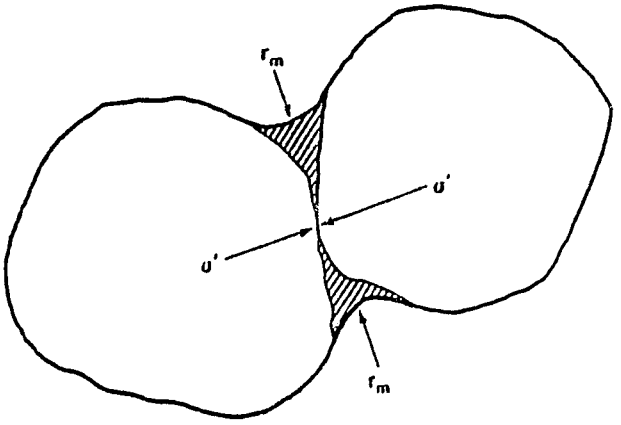

Fig. 3-1 Effect of capillary film on soil grains (after Holtz and Kovacs, 1981)

$$u_c = h_c \rho_w g \quad [kPa] \qquad 3\text{-}11$$

where u_c = capillary pressure, kPa

h_c = height of capillary rise, m

ρ_w = density of water, g/m^3

g = acceleration due to gravity, m/sec^2

This equation can also be expressed in terms of the meniscus radius (r_m) and surface tension (T) of the air-water interface which acts around the circumference of the pore (Holtz and Kovacs, 1981, p. 170),

$$u_c = h_c \rho_w g = -2T/r_m \qquad 3\text{-}12$$

where T = surface tension (73 dynes/cm for water at 20°C)

r_m = meniscus radius, cm

To illustrate the magnitude of capillary pressure, consider a pore opening of one micron which can be expected in a sedimented clay network. According to Eq. 3-12, a capillary pressure (u_c) of -1500 kPa would result.

Particle sizes in drilling fluids before entering a centrifuge are typically from 0.7 to 10 microns. As drying continues, capillary forces are relaxed, but the network shows no evidence of expanding. Consequently, the dried cake of a flocculated compressible network is believed to have homogeneous density.

Two physical observations can be related to support this conclusion. First, when an incompressible network of similar sized particles (barite) was centrifuged and dried,

the resulting shape was that of the original saturated cake. Its shape was cylindrical and not conical. Second, the density of an upper layer of dried cake compares closely with the density of a lower layer.

Upon calculating the saturated density of the "reconstructed" cake, the density of the upper layer was 1.76 g/cm^3 while the bottom layer had a density of 1.84 g/cm^3. These densities are sufficiently equal. Thus, the conclusion of homogeneous density of the dried cake is supported.

The measurement of variable density allowed for an increase in accuracy for calculating effective consolidation stress (σ_v'). This expression was applied to the aforementioned flocculated field fresh/CLS drilling fluid.. Its geometry was adequately modeled by a cylinder atop a conical frustrum (Fig. 3-2).

Assuming constant density, the mass of solids in each section is dependent only upon its volume ($m = \rho V$). The slice is conceptually expanded both horizontally and vertically to fill the volume the cake originally occupied.

A procedure for calculating density distribution is as follows:

Step 1 Measure cake height following centrifugation.

Step 2 Dry the cake.

Step 3 Measure the top diameter (x_t), base diameter (x_b), and height (z_{tot}) of the dried cake. The shape of the dried cake is parabolic with a typically

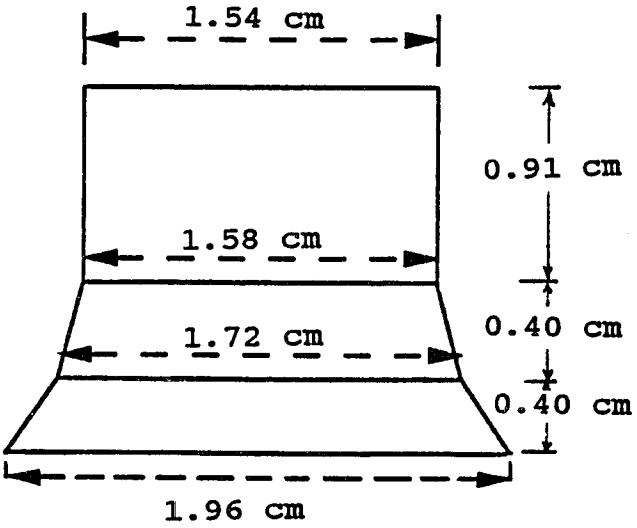

Fig. 3-2 Dimensions of dried centrifuged cake

flattened top and base. It can be adequately modeled by frustrum sections in this analysis.

Step 4 Measure the mass of the dried cake.

$m_{cone\ tot}$ = 6.483 g

Step 5 Measure the dried cake diameter (x_{cone}) at points along the height. In this example, four diametric measurements sufficed to accurately characterize its geometry. The height (z) for each section is also measured.

Step 6 Plot the height (z) versus diameter (x_{cone}) values as measured in Step 5.

Step 7 Calculate the volume of the dried sections (V_{cone}) and sum the volume of these sections (V_{tot}) (Fig. 3-3).

Step 8 Calculate the mass of each section from $m = m_{cone} * V_{cone}/V_{tot}$ for the topmost section. In this example 6.48 g *(1.75/3.67) = 3.09 g which is the mass of solids in that section.

Step 9 Calculate the mean diameter (x_{mean}) at one third the section height. This approximation is typical for cones of similar geometry and gives good results. For the top section, x_{mean} = 1.56 cm. Obtaining this mean directly from a plot of height (z) against diameter (x) is adequate.

Step 10 Calculate the thickness for each conical section (z_{cyl}) the cake was occupying when saturated

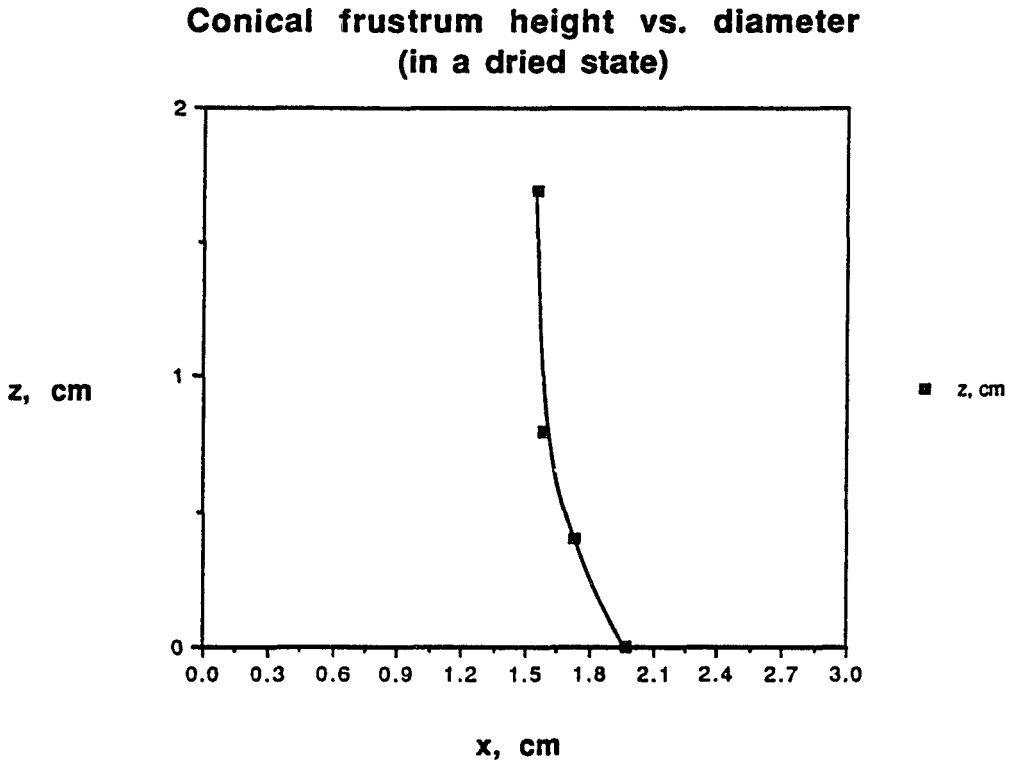

Fig. 3-3 Shape of a flocculated bentonite mud after centrifuging at 800 rpm and drying

(initially).

$z_{cyl} = (x_{cyl}/x_{mean}) * z_{cone} = (2.75/1.56) * 0.91 = 1.57$ cm

Step 11 Using a spreadsheet computer program with the following columns allows the density for each saturated cylindrical section to be computed.

A) $V_{cyl} = 2.75^2 * (\pi/4) * z_{cyl}$ for each cylindrical (wet) section, $cm^3 = 2.75^2(\pi/4) * 1.59 = 9.44\ cm^3$

B) $m_{cone\ tot} = 6.48$ g

C) m from Step 8 = 3.09 g

D) $V_{solids} = m/(2.6\ g/cm^3) = 3.09\ g/2.6 = 1.18\ cm^3$

E) $m_{water} = m + (V_{cyl} - V_{solids}) * 1.0\ g/cm^3 = 3.09\ g + (9.44 - 1.18) * 1.0\ g/cm^3 = 8.25$ g

F) $\rho_{cyl} = (m + m_{water})V_{cyl} = (3.09\ g + 8.25\ g)/9.44 = 1.201\ g/cm^3$

One shortcoming in this procedure is that density distribution can only be calculated for the final ω_f.

Saturated density of the mixture is obtained from Step 11-F.

$$\rho_{sat} = (m_s + m_w)/V_{cyl}$$

The results for this particular cake are shown:

Table 3-1 Summary and calculations of original wet cake density from dried cake measurements

Δz_{dry}	Δz_{cyl}	m_{solids}	V_{cyl}	$m_s + m_w$	ρ_{sat}
cm	cm	g	cm^3	g	g/cm^3
0.91	1.52	3.09	9.01	11.34	1.26
0.40	0.62	1.51	3.68	4.84	1.31
0.40	0.55	1.88	3.29	4.67	1.41
Σ 1.71	2.69	6.48	15.99	20.85	

As mentioned earlier, the $\Delta\rho$ would be obtained in computation of bulk modulus from bulk density. In this particular experiment on a field fresh/CLS drilling fluid, the bulk density was 1.30 g/cm^3, which compared quite closely with the density at the sedimented cake midpoint. Bulk density is equivalent to saturation density (ρ_{sat}) and was computed for this example as follows:

$$\sum_{i=1}^{3} \frac{\Delta z_{cyl\,i}}{2.69} \rho_{sat\,i} = 1.30\ g/cm^3$$

In all other cases, ρ_{sat} could be computed as mentioned, i.e., from the known mass of solids throughout all compression levels. The density of the cake bottom as compared with the cake top has been quantified, and the two differ by less than 13%. Therefore, the assumption of an homogeneous cake is reasonable, especially considering the variability in response of the various fluid systems. Additional experiments would be required to make conclusions regarding variation of 13%. However, the variation would be expected to be higher for more compressible drilling fluids like a flocculated bentonite, and less for less compressible sus-

pensions. A visual observation the sedimented barite, showed no conical shape; it had retained its cylindrical geometry after centrifuging.

3.2 Results and discussion

3.2.1 Bulk modulus versus solids fraction

Before analysis of the various data is presented, a comparison is included between the computation method of bulk modulus for this research and that of Buscall (1982) in Fig. 3-4. The difference between the samples is that Buscall tested attapulgite while this research tested flocculated attapulgite. To compare, the data in this research will be plotted as Buscall did using bulk modulus versus fraction of solids. The presence of polymer made the network more compressible as evidenced by its greater volume change under the same or less compressive stress. This occurred even though the fraction of solids was considerably greater.

Figure 3-5 shows the results of experiments performed on all fluid systems (except barite). These are the same experiments from which permeability data was obtained (Table 2-7). It is noted that at zero bulk modulus, the initial solids fraction can be observed. Figure 3-6 shows only the drilling fluids tested. The fresh/CLS fluid system is least affected by compressive stress.

The driest cake is clearly barite. This is due in part

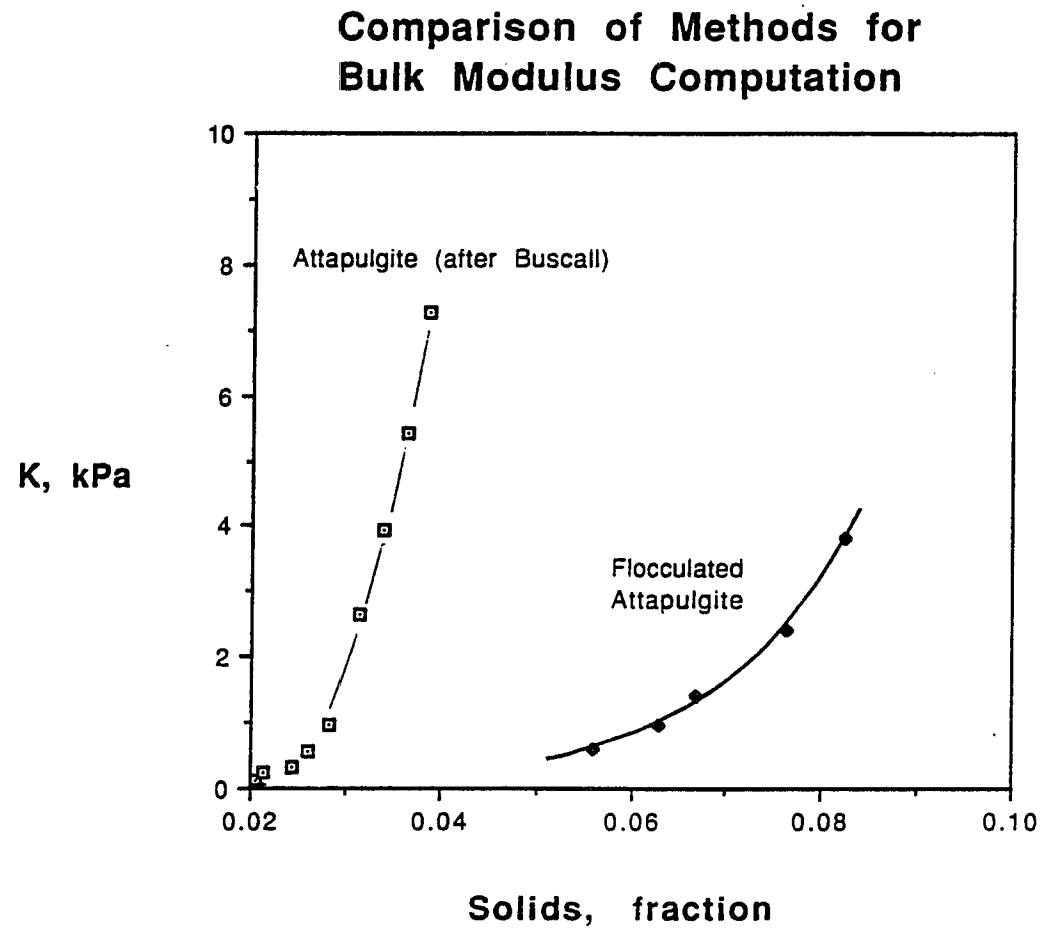

Fig. 3-4 Comparison of methods for bulk modulus computation

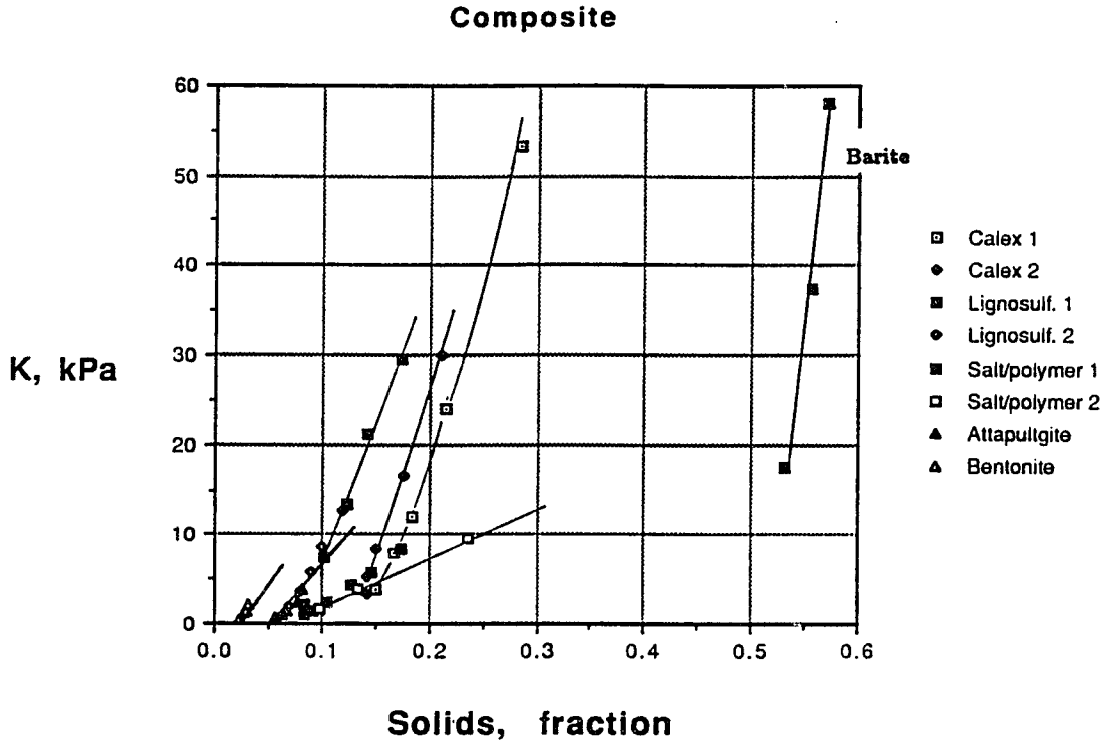

Fig. 3-5 Bulk modulus vs. volume of solids fraction for six fluid systems

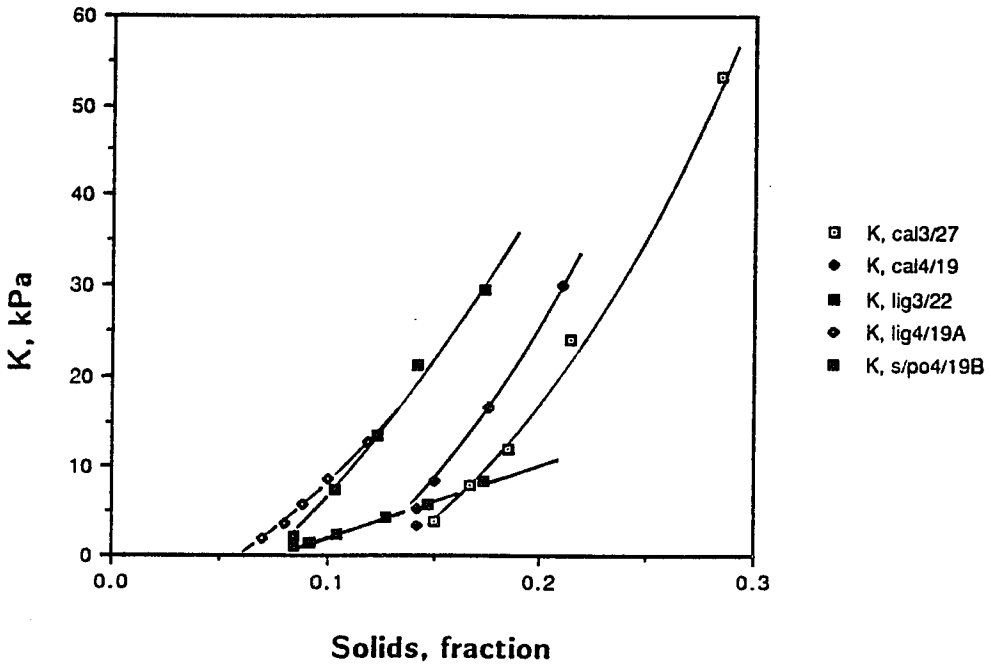

Fig. 3-6 Bulk modulus vs. volume of solids fraction for three fluid systems

to its relatively high initial solids fraction of 0.532. The fresh/CLS system shows no sign of reaching ultimate compaction owing to the linearity of the data. In contrast is the starch-3/27 sample which above a solids volume fraction of 0.25 (a void ratio of 3), its limit of dewaterability is imminent as observed from the exponential increase of bulk modulus.

In addition to bulk modulus measurement, the response of compressible networks is often related to void ratio (e) which is the ratio of void volume (V_v) to solids volume (V_s),

$$e = V_v/V_s \qquad 3\text{-}13$$

It was computed at each compaction level to allow a comparison of centrifugal compression with C-P cell compression. Void ratio can be related to porosity (ϕ) by the equation,

$$e = \phi(V_v+V_s)/V_s \qquad 3\text{-}14$$

3.2.2 Void ratio versus effective consolidation stress

Two terms commonly used by geotechnical engineers to estimate soil settlement are compression index (C_c, Holtz and Kovacs, 1981, p. 313) and compressibility (a_v, Holtz and Kovacs, 1981, p. 311).

The respective definitions are

$$C_c = \frac{-de}{d\log\sigma_v} = \frac{e_1-e_2}{\log\frac{\sigma_2}{\sigma_1}} \qquad 3\text{-}15$$

$$a_v = -\frac{de}{d\sigma_v} \qquad 3\text{-}16$$

Equation 3-15 is a semi-log plot of e versus σ_v' while Eq. 3-14 is a cartesian plot of e versus σ_v'. The latter term (a_v) can be related to bulk modulus by the equation

$$a_v = \frac{-V\,de}{K\,dV} \qquad 3\text{-}17$$

The slope of a semi-log plot of void ratio versus effective consolidation stress yields compression index. A cartesian plot of void ratio versus effective consolidation stress yields compressibility (a_v). Plots illustrating compression index and compressibility are shown in Fig. 3-7 and Fig. 3-8 respectively.

From published data on San Francisco Bay mud (Holtz and Kovacs, 1981), the compression index using the C-P cell was 0.986. This sample was included to compare with the values of the various drilling fluids tested and shown in Fig. 3-7. From the slope of this figure, compression index was obtained, and the results are contained in the following table. Only the last item was measured using the C-P cell; all others were made using the centrifuge.

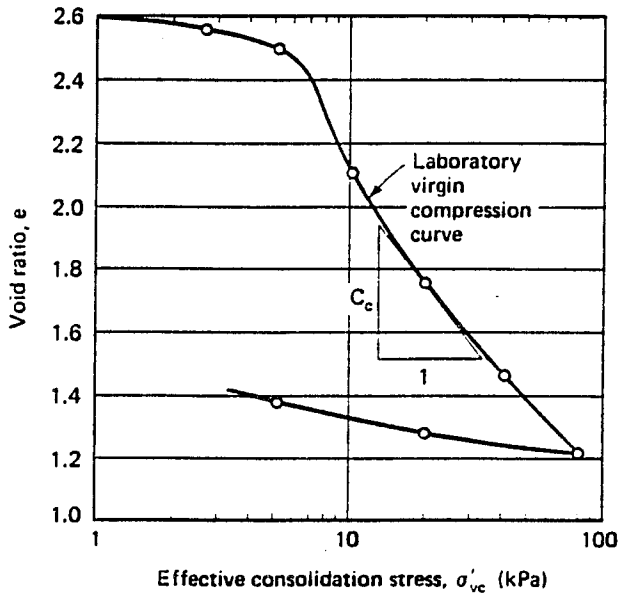

Fig. 3-7 Example showing computation of compression index (after Holtz and Kovacs, 1981)

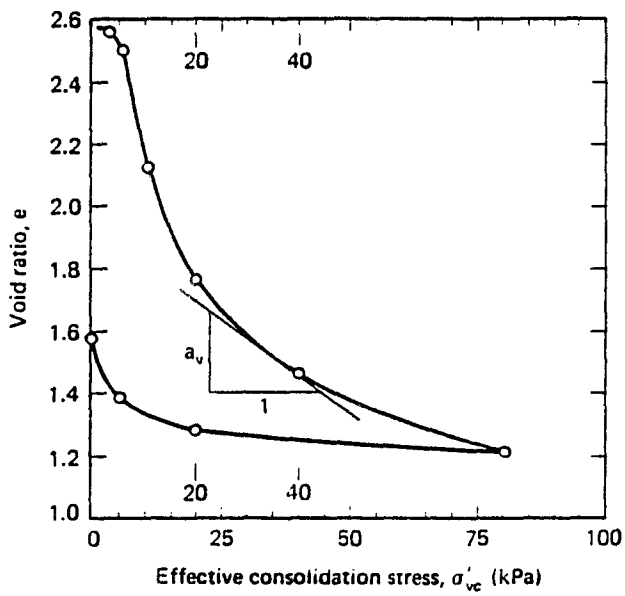

Fig. 3-8 Example showing computation of coefficient of compressibility (after Holtz and Kovacs, 1981)

Table 3-2 Compression index of various fluids

Fluid System	Compression Index, C_c
Fresh/CLS and flocc. attapulgite	6.17
Salt/CLS	5.24
Starch samples	2.46
San Francisco Bay mud	0.99

From a qualitative sense, networks can be classified as (Tiller, et al., 1990):

1. Incompressible
2. Slightly to moderately compactible
3. Highly compactible
4. Super compactible

A comparison of the slopes on the semi-log plot of void ratio versus effective consolidation stress (Fig. 3-9) for the various suspensions allows for a qualitative comparison. Using Tiller et al. classification, the fluids tested were grouped as follows:

Table 3-3 Compactible cake quality of fluid systems

Fluid System	Compactible Quality
Barite	Low
Starch, Fresh/CLS	Moderate
Salt/CLS, flocc. attapulgite and flocc. bentonite	High

Several examples of compressive solids are shown in Fig. 3-10. A comparison of the data obtained in these experiments is compared with data from a C-P cell and shows the magnitude of the compression obtained.

A comparison is made for attapulgite and barite, as these two minerals were common between the two investigations.

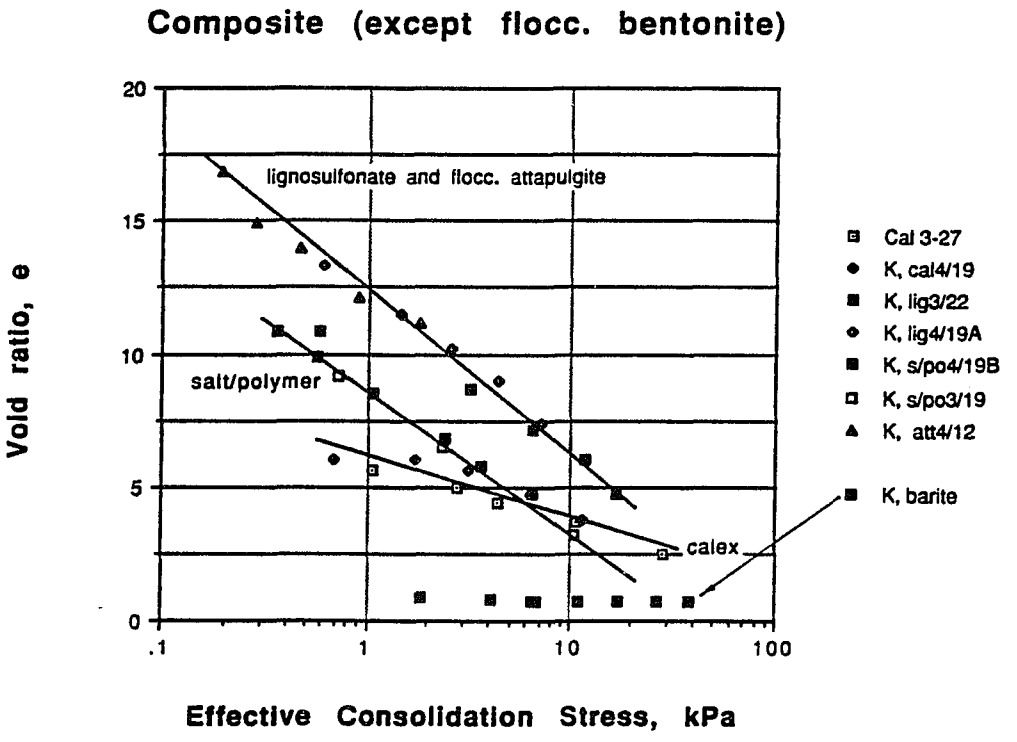

Fig. 3-9 Response of void ratio to effective consolidation stress for all fluid systems tested

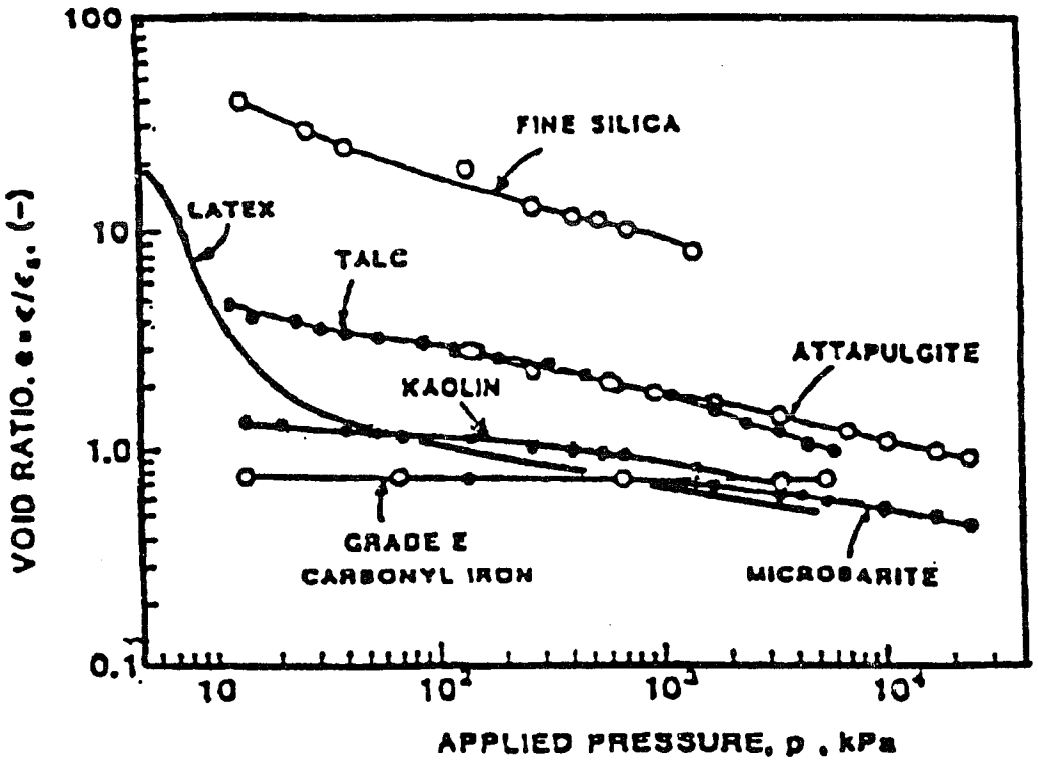

Fig. 3-10 Response of void ratio to applied pressure using the C-P cell and including attapulgite (after Tiller et al., 1989)

Figure 3-11 presents a comparison with data from Tiller's (1989) investigation.

For attapulgite, its compactibility in the C-P cell was compared with a flocculated attapulgite suspension compacted in the centrifuge in this research. As compactibility is conventionally presented as void ratio against applied pressure or effective consolidation stress, σ_v', this format is followed.

Greater stress was applied with the C-P cell. The slope for flocculated attapulgite in the centrifuge is greater than for attapulgite compacted in the C-P cell. This is due to the presence of adsorbed polymers. Another similarity for the two investigations is that the range of void ratio is of the same order of magnitude.

A comparison of barite compaction for the two methods shows excellent agreement. The barite in this research was not flocculated. These comparisons illustrate the validity of the centrifugal method for measurement and analysis of bulk modulus. Figure 3-12 shows a composite of all data presented in this format with duplicates, and Fig. 3-13 is a simplified version without duplicates.

Thus, the centrifuge can be used to obtain both compressibility index and coefficient of compressibility, and to classify qualitatively the compactible quality of the networks. To compare the drilling fluid systems quantitatively, they were compared at a single void ratio

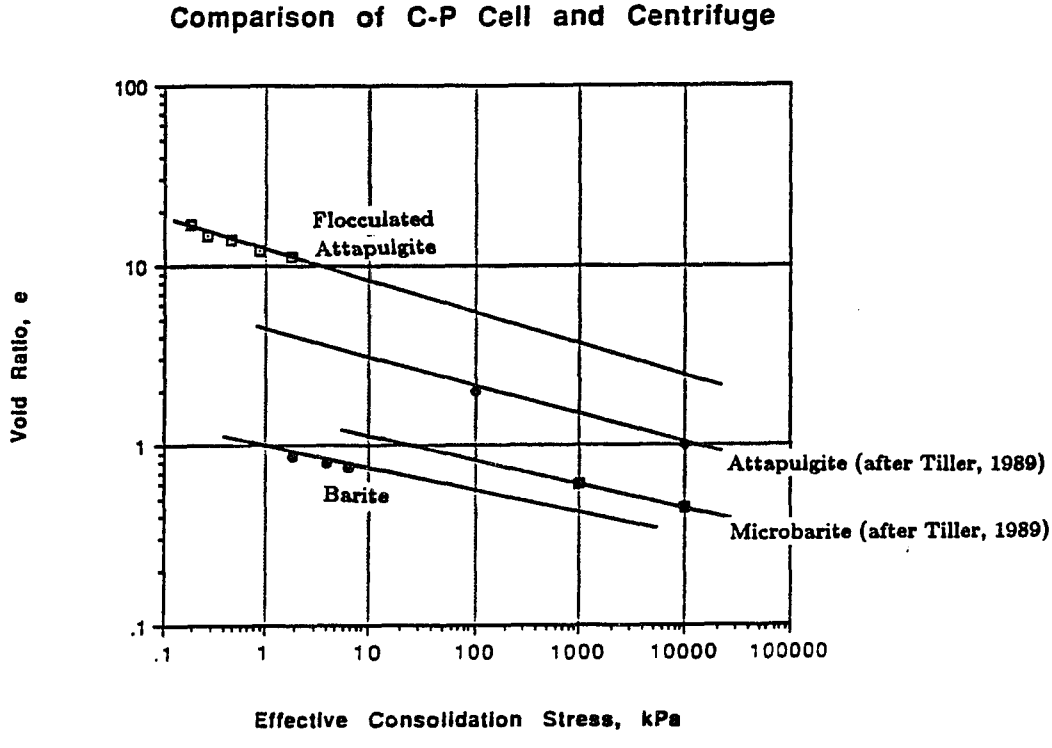

Fig. 3-11 Comparison of void ratio response using C-P cell and the centrifuge

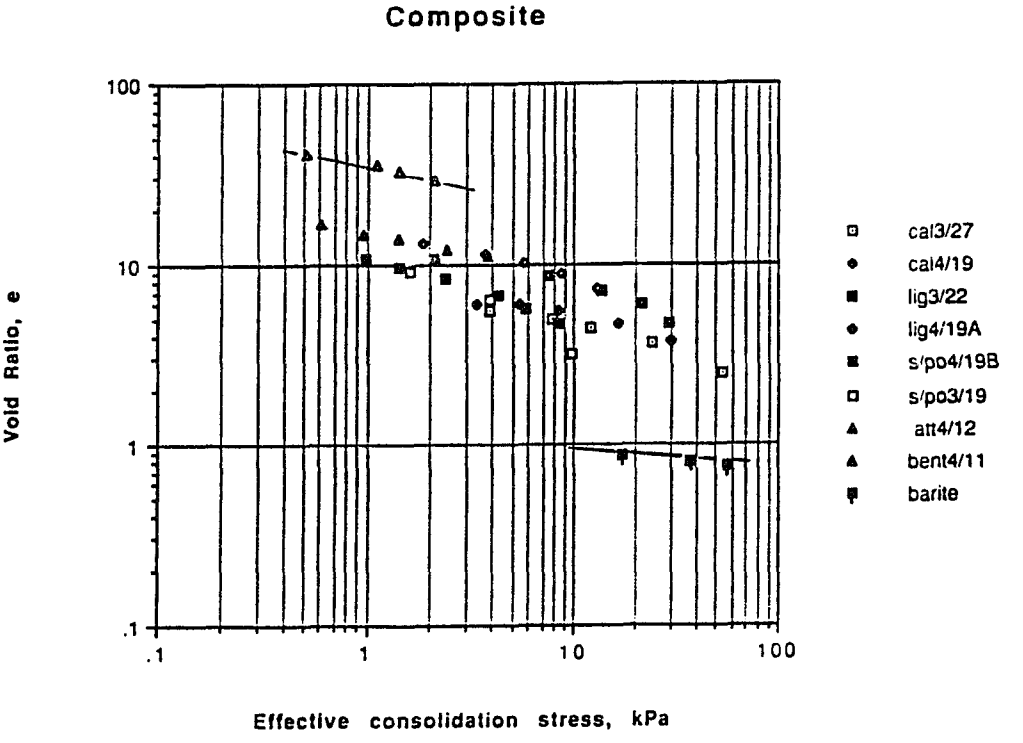

Fig. 3-12 Response of void ratio to effective consolidation for all fluid systems tested and including duplicates

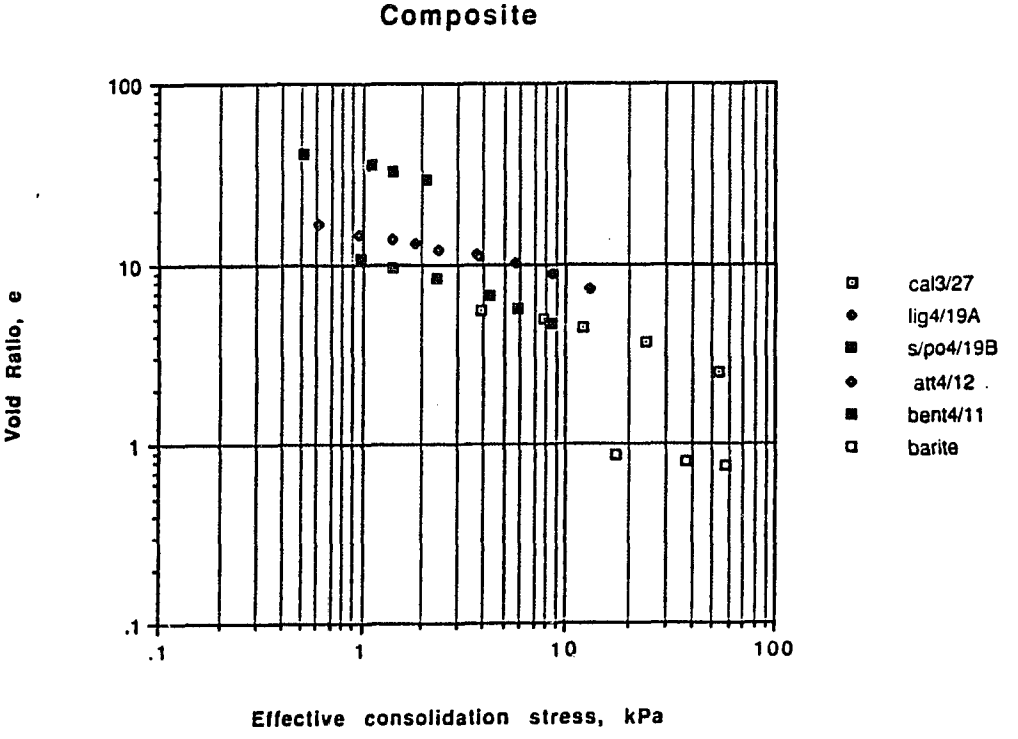

Fig. 3-13 Response of void ratio to effective consolidation for all fluid systems tested without including duplicates

(Table 3-4). This strict comparison was not possible with bulk modulus due to its variability over a short range of void ratios.

3.2.3 Minimum void ratio for drilling fluids

Below some minimum void ratio, increasing stress produces no substantial volume change. The flocculated networks tested herein appear to reach a minimum void ratio between 3-4 which is equivalent to a porosity of 75% to 80%, respectively. Porosity is equivalent to moisture content on a volume basis. Moisture content is 60% w/w for a void ratio of 4. It is interesting to observe that this matches the minimum water content reported under full-scale controlled dewatering conditions when a high volume of active solids was present (Wojtanowicz, 1988).

Using a void ratio of four, the fluid systems are compared in two ways: effective consolidation stress and rotational velocity required to achieve this void ratio.

Table 3-4 Comparison of effective consolidation stresses at a void ratio of four

	At void ratio = 4	
Fluid System	Effective Consolidation Stress, kPa	ω, sec^{-1}
Starch 3/37	6.74	68
Starch 4/19	10.2	77

The large void ratios at the highest level of compaction applied for the two flocculated clays alone are shown in Table 3-5.

Table 3-5 Large void ratios for compaction of flocculated mineral suspensions

Fluid System	Void ratio	Effective Consolidation Stress, kPa	ω_{max}, sec^{-1}
Flocc. Attapulgite	11	1.8	72.66 (694 rpm)
Flocc. Bentonite	30	0.93	53.19 (508 rpm)

A composite plot of void ratio against stress on a cartesian coordinate system (Fig. 3-14) provides an excellent cluster of data over a wide range of conditions. Flocculated bentonite at the most compactible end and barite to the lower right at the least compactible end forms the border for the other fluid systems tested.

A comparison of dewaterability for two flocculated clay mineral species reveals the extreme difficulty in dewatering flocculated bentonite. This is the most hydrophilic of clay families owing to its high montmorillonite content. Montmorillonite exhibits a greater degree of interparticle swelling than is present in other clays. Its swelling is believed to account for its low dewaterability despite the fact that less polymer was used to achieve flocculation.

The flocculated attapulgite overlays the fresh/CLS samples. This similarity is attributed to the fact that attapulgite has a specific surface lower than most clays, particularly montmorillonite (Gray and Darley, 1980, p. 151). Certain of its mechanical properties are dependent upon particle-particle interference rather than on electrostatic interparticle forces so highly influential in more active clays. Therefore, the explanation that attapulgite

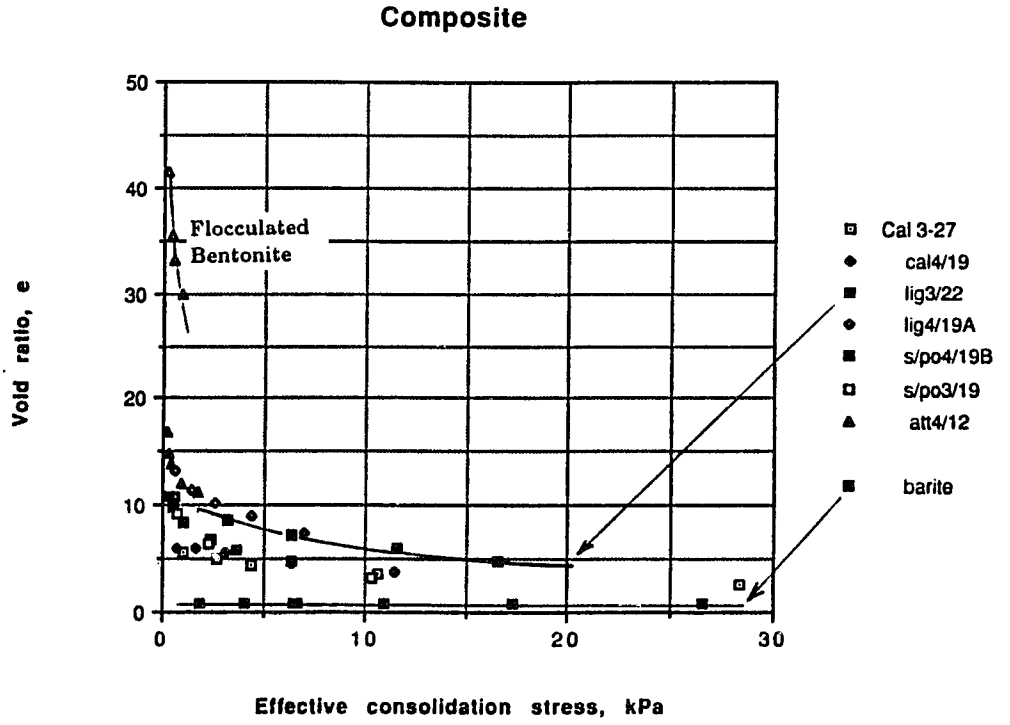

Fig. 3-14 Response of void ratio to effective consolidation for all fluid systems with duplicates on cartesian coordinates

has a compressibility less than bentonite is largely attributed to its lack of electrostatic charges. Consequently, less ionic polymer is required to flocculate attapulgite, because less is adsorbed onto the clay surfaces.

This chapter described the second and final parameter required to characterize a compressible network. Thus, a method is available for quantifying both the permeability (Chapter II) and the resistance to consolidation stress for a chemical pre-treatment. The viability of this method for evaluating other types of pre-treatments is tested in the next chapter, which describes an electric field pre-treatment.

Nomenclature

a_v	=	coefficient of compressibility, kPa^{-1}
C_c	=	compressibility index, dimensionless
e	=	void ratio, dimensionless
e_o	=	initial void ratio, dimensionless
E	=	constrained modulus, kPa
g	=	gravitational acceleration, $[l/t^2]$
H_{ei}	=	equilibrium cake height corresponding to ω_i
h_c	=	height of capillary rise, m
H_o	=	original cake height, cm from Casagrande's procedure
K	=	bulk modulus of a viscoelastic solid, kPa or $g/(cm\text{-}sec^2)$
m	=	mass of solids in each section, g
$m_{cone\ tot}$	=	total mass of the dried cake, g
m_{water}	=	mass of water in wet section, $g\text{-}sec^2$)
N	=	rotational velocity, rpm
P	=	hydrostatic or neutral stress, kPa
r	=	radius in centrifuge, cm
r_m	=	radius of the meniscus
R_b	=	centrifugal radius to cake bottom, cm
R_c	=	centrifugal radius to cake top, cm
V	=	bulk volume of a viscoelastic solid undergoing compression, cm^3
V_{cone}	=	dried cake volume - final, cm^3
V_{tot}	=	total volume of wet cake, cm^3
V_{cyl}	=	cake volume of wet section, cm^3
V_s	=	volume of solids, l^3
V_{solids}	=	volume of solids in the jth section, cm^3
V_{tot}	=	total volume of the dried cake, cm^3
V_v	=	volume of voids, l^3
x_t	=	diameter of top of conical section, cm
x_b	=	diameter of bottom of conical section, cm
x_{cyl}	=	diameter of a wet cake cylindrical section, cm
$x_{cone\ midpt}$	=	diameter of a dried cake conical section, cm
z_{cyl}	=	thickness of a wet cake cylindrical section, cm
z_{cyl}	=	thickness of a dried cake conical section, cm
z	=	thickness of cake, cm
z_{tot}	=	total thickness of the dried cake, cm
z_{cone}	=	thickness of conical section, cm
dz	=	differential thickness of sedimented cake, cm

Nomenclature (cont.)

ϵ	=	longitudinal strain, cm/cm
ρ_{cyl}	=	density of the final section, g/cm^3
ρ	=	density, g/cm^3
ρ_{eff}	=	unsupported density of the solids causing consolidation, g/cm^3
ρ_{sat}	=	density of the saturated sedimented network, g/cm^3
σ_v'	=	effective stress, kPa
σ_{tot}	=	total stress, kPa
ω	=	rotational velocity, sec^{-1}

Chapter IV

Dewatering Enhancement of Drilling Fluids Using Electrocoagulation

Chemical coagulants and flocculants can enhance removal of colloids in the centrifugation of drilling fluids. However, these chemicals are themselves waste and necessarily add to waste volume. Removal of colloids without the addition of chemicals would be beneficial. Elimination of chemical coagulants has been reported by placing colloidal suspensions in an electric field (Berry and Justice, 1987). This process, electrocoagulation (EC), has proved more successful when using alternating current (AC) as compared to direct current. Without the addition of chemicals, electrocoagulation has provided a phase separation through gravity settling over several hours or days; waste has been reduced, and treated water has been recycled (Ryan et al., 1989).

This chapter addresses process mechanisms, reviews industrial and pilot-scale experiments, and evaluates the electrocoagulation process as applied to drilling fluids. Finally, the permeability and bulk modulus of the sedimented cake is measured following electrocoagulation treatment. These measurements are then compared with similar suspensions that were chemically pre-treated.

The hypothesis investigated is the elimination of chemical pre-treatments prior to centrifugal dewatering.

4.1 Electrocoagulation mechanisms and applications

Clay suspensions are chemically and electrically stable. Clays are typically surrounded by an ionic layer of uniform, negative electric charges (Fig. 4-1). The origin of these negative charges is isomorphous substitution of ions into the tetrahedral or octahedral sheets in the clay lattice and/or imperfections in the crystal lattice (Holtz and Kovacs, 1981, p. 93).

Electrostatically attracted to the clay surface are various exchangeable cationic species. This layer of both negative and positive charges comprises the double layer and is responsible for interparticle forces between clay colloids. This characteristic is behind the reason clays are called "active" solids.

Electrostatic forces in the double layer cause particle repulsion. They are stronger at larger particle separations than are van der Waals or London forces, which tend to agglomerate particles. An approximation of the effects of these forces and their resultant is shown in Fig. 4-2. For particle agglomeration to occur, this charge surface must be neutralized.

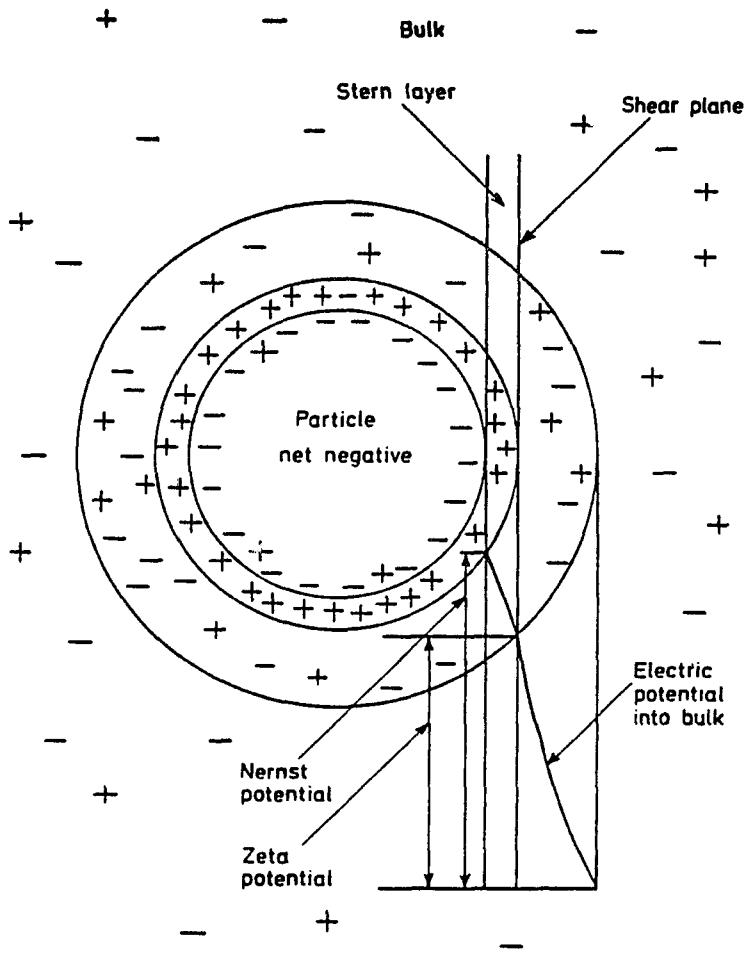

Fig. 4-1 Diagram showing zeta potential in relation to a charged colloid

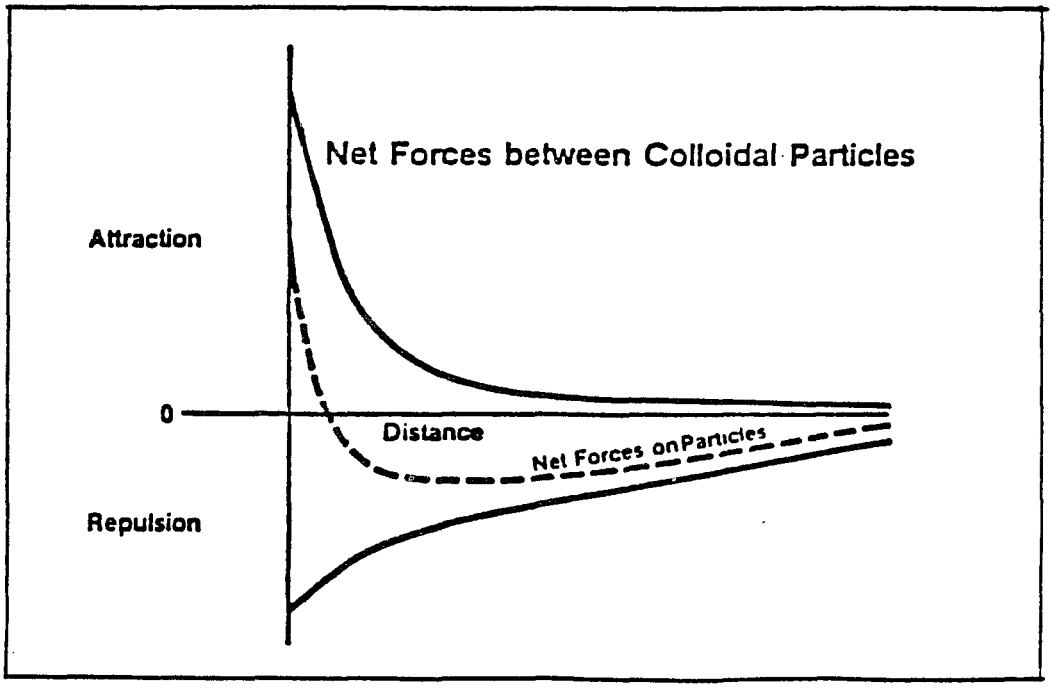

Fig. 4-2 Effect of distance on interparticle forces

4.1.1 Mechanisms and discussion

Electrocoagulation has been explained by two mechanisms: electrostriction and ionization.

In electrostriction, a term used by Schwarz (1962), the applied electric field forces surface charges to be displaced forming a dipole. A dipole consists of two equal electric charges of opposite sign which are separated by a specified distance. For clays, this length is typically on the order of one micron. Dipole linking results in particle agglomeration.

Hoekstra et al. (1969) observed the dielectric relaxations of colloidal suspensions at radio-frequencies (30 and 300 gigahertz) in an AC field. The counter-ions on the surface of the colloidal particles are acted upon by electrical forces. To escape from the surface into the free solution, the ions must overcome a high electrical potential barrier, however, along the surface they can move freely. They are moved tangentially by an external field. The result of this tangential movement of ions is polarization of the ionic atmosphere surrounding the colloid. Further, the external field induces an electric dipole moment along the particle. Once dipoles are formed, a dipole-dipole interaction, or dipole linking occurs from which the effect of coagulation can be observed.

Coagulation is the chemical destabilization of sols. It is effected by the addition of electrolytes which reduces

the charge on the particles. This reduction allows the particles to aggregate (La Mer, 1964). The effects of dipole linking include increase in particle size accompanied by more rapid settling.

The mechanism of electrostriction was also proposed by Lavrov et al. (1975). Upon observing a decrease in the dielectric constant, Schwann et al. (1962) concluded that the applied electric field had altered the double layer associated with the colloid. This decline in dielectric constant occurred with an increase in the frequency of the field. Dielectric constant (ε) is the ratio of the force in free space to the force in the medium. It is a measure of the ability of a material to resist the formation of an electric field within it. It is frequently reported as the ratio of ϵ/ϵ_0 where ϵ is the permittivity of the medium and ϵ_0 the permittivity of free space. As Schwann (1962) reported, a decrease in permittivity with treatment, causes an increase in interparticle attraction.

In contrast to electrostriction, the ionization mechanism states that the electric field causes ionization of the suspension. Freed ions participate in chemical bonding which leads to coagulation. Horgan and Edwards (1961) reported that certain electro-hydrodynamic phenomena observed in dielectric liquids are most likely due to the ionization of the fluid, rather than polarization of the dielectric. Concurring, Pierce (1959) stated that copious ionization

occurs in an applied [electrical] field, especially if bubbles of gas exist within the liquid. During electrocoagulation treatments in this research, bubbles were present. During industrial applications, Berry and Justice (1987) stated the effect of electrocoagulation treatment was time-dependent and not instantaneous as with chemical coagulants. In one experiment, 24 hr was required to insure the full effect of electrocoagulation as judged by settling which clarified the treated fluid. But, the diffusion of cations into the bulk of the fluid, following ionization of the suspension, is also time-dependent.

Ionization of the suspension can be attributed to the electrolysis of water (Gale, 1990). During electrolysis, two reactions occur at the cathode and anode respectively:

$$2H_2O - 4e^- \text{------>} 2O + 4H^+$$

$$4H_2O + 4e^- \text{------>} 2H_2O + 4OH^-$$

In the application of an AC electric field, each electrode acts alternately as a cathode and anode on each swing of the cycle. From these chemical reactions it can be seen that pH should be affected only to the degree one reaction is more efficient than the other. These reactions occur only at the electrodes, and not in the bulk suspension.

If electrolysis of water is the mechanism, then this suggests a preferential anodic reaction because pH in virtually all cases increased with treatment. As clays are amphoteric, i.e., dissolve in either acids or bases, it has

been postulated by Gale (1990) that the presence of the H^+ and OH^- ions from electrolysis of water explains clay dissolution. When dissolved, cations such as Na^+, K^+ and Ca^{+2} are released, they act as electrolytes to coagulate colloids. In support of this concept an experiment is cited in which a shale containing 11% w/w bentonite was mixed in distilled water (Griffin et al., 1986). This resulted in the release of cations as reported (Table 4-1):

Table 4-1 Cation concentration in water after 24 hours of hot rolling shale in water

		Percentage
Potassium	K^+	1.25
Sodium	Na^+	1.62
Calcium	Ca^{+2}	$0.23(10)^{-4}$

Measurements were made using atomic absorption spectrophotometry.

These freed cations behave as electrolytes in which the double layer is compressed and promotes chemical coagulation.

The consistent increase of conductivity indicates the suspension is undergoing ionization as shown in Table 4-2.

Table 4-2 Increases of conductivity following electrical treatment

Fluid type	σ_i[1]	σ_f[2]
Bentonite % w/w		
0.10%	48	72
0.26%	50	110
0.50%	86	620
1.00%	140	650
2.00%	240	750
4.00%	440	1400
Calex Drilling Fluid 1:1[3]	4380	7200

1 σ_i conductivity initially, before treatment, μmhos/cm
2 σ_f conductivity following, after treatment, μmhos/cm
3 the 1:1 refers to one part test fluid and one part water

In an industrial application cited in section 4.1.2 to follow, an electrocoagulation treatment of only 13.5 sec resulted in coagulating a volume of 8 gal (Table 4-3). Three hours was required to observe coagulation of the entire volume. Had the mechanism been wholly electrical, then it is proposed the individual colloids would have been interlinked instantaneously in the dipole-dipole manner described, and coagulation would have resulted. The extensive time required suggests the migration of ions into the solution, and supports the ionization mechanism.

Several industrial and pilot-scale electrocoagulation treatments motivated this investigation for drilling fluids, although the following applications are from the coal mining industry.

4.1.2 Applications

Water is frequently used in coal washing applications

and, consequently, is contaminated with colloidal particles. These colloids must be removed before discharging the water.

Industrial applications have employed a patented device (Fig. 4-3) in which the fluid enters the bottom of the apparatus then rises up the electrodes. Fluid enters a weir before exiting. Processing variables include: current, voltage, electrode spacing, and flow rate or treatment time.

However, during a treatment, electrode spacing is not varied. An experiment performed on a coal mining slurry follows (Justice, test: 9-9-1988):

Table 4-3 Kerr Mine 9-16-1988 electrocoagulation results

Solids	1.5% w/w
Voltage	25 V
Current	120 amperes (A)
Frequency	60 hz
Conductivity	2000 μmhos/cm
Electrode spacing	0.5 in
Evaluation	Liquid clarity after 1.5 hr settling
Treatment time	13.5 seconds.

Settling was evaluated as it simulated the thickener which is normally used for chemically treated coal wash water. The test showed results similar to chemical treatment could be achieved. A second evaluation was performed a short time later:

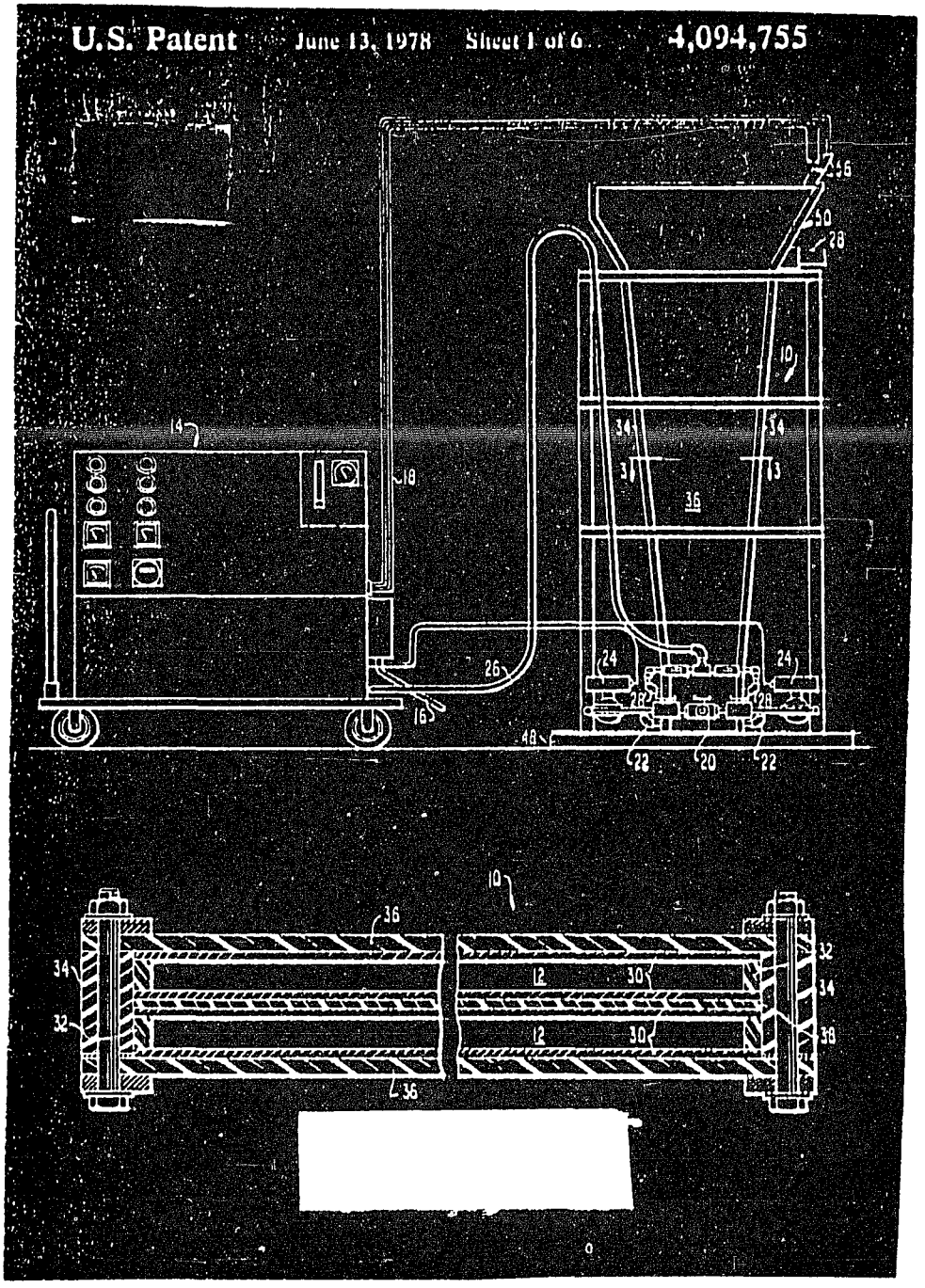

Fig. 4-3 Electrocoagulator for industrial applications (after Moeglich, 1979)

Table 4-4 Kerr Mine 10-13-1988 electrocoagulation results

Solids	2% w/w
Voltage	38 V
Current	21 A
Frequency	100 hz
Conductivity	2000 μmhos/cm
Electrode spacing	0.5 in
Evaluation	770 to 48 NTU* after 4 hr and to 4.5 NTU after 22 hr
Treatment time	4.6 min

* nephelometric turbidity units (NTU) measures light intensity scattered by particles

Snyder and Gregory (1979) tested a mineral suspension washed from a coal refuse pile. The suspension was compositionally similar to those above. Their bench scale tests showed electrocoagulation treatment could reduce chemical flocculants. The treated fluid contained 3% w/w bentonite. They found it advantageous to increase conductivity, and did so with the addition of graphite particles. The test was useful in determining the maximum solids content which could be used for a specified electrode spacing.

Table 4-5 Effect of solids content on operational difficulties

Solids content, % w/w	Remarks
< 7%	No plugging
9-11%	Required intermittent backflushing
18%	No operation possible

For comparison, an unweighted 9.6 lb_m/gal mud has 9.5% w/w solids, and this is considered a lower density mud. Following treatment, the authors reported these clays settled to a hard dense layer. For the colloid tested and shown above,

settling rate was dependent upon time and intensity of electrical treatment. The concept of threshold current density was proposed. Once this level is reached, the process is relatively insensitive to further increases. In another application, a detailed analysis of chemical constituents was performed before and after electrocoagulation treatment. Treatment reduced the metals content of the liquid phase as the metals precipitated onto the settled clay (Culberton, 1986). With treatment, total suspended solids (TSS) from 195,000 ppm to 15 ppm.

These successes motivated this research into the feasibility of electrically treating drilling fluids to enhance phase segregation in the centrifuge. However, there are two major differences between coal wash water and drilling fluids: drilling fluids are chemically and electrically stable suspensions and of higher density.

The next section describes the experimental investigation into the effect of electrocoagulation treatment on drilling fluids.

4.2 Effect of electrocoagulation on drilling fluid properties

4.2.1 Apparatus and measurements

A modification of the patented device was made by replacing the plate electrodes with concentric electrodes (Fig. 4-4). This alternate arrangement takes advantage of

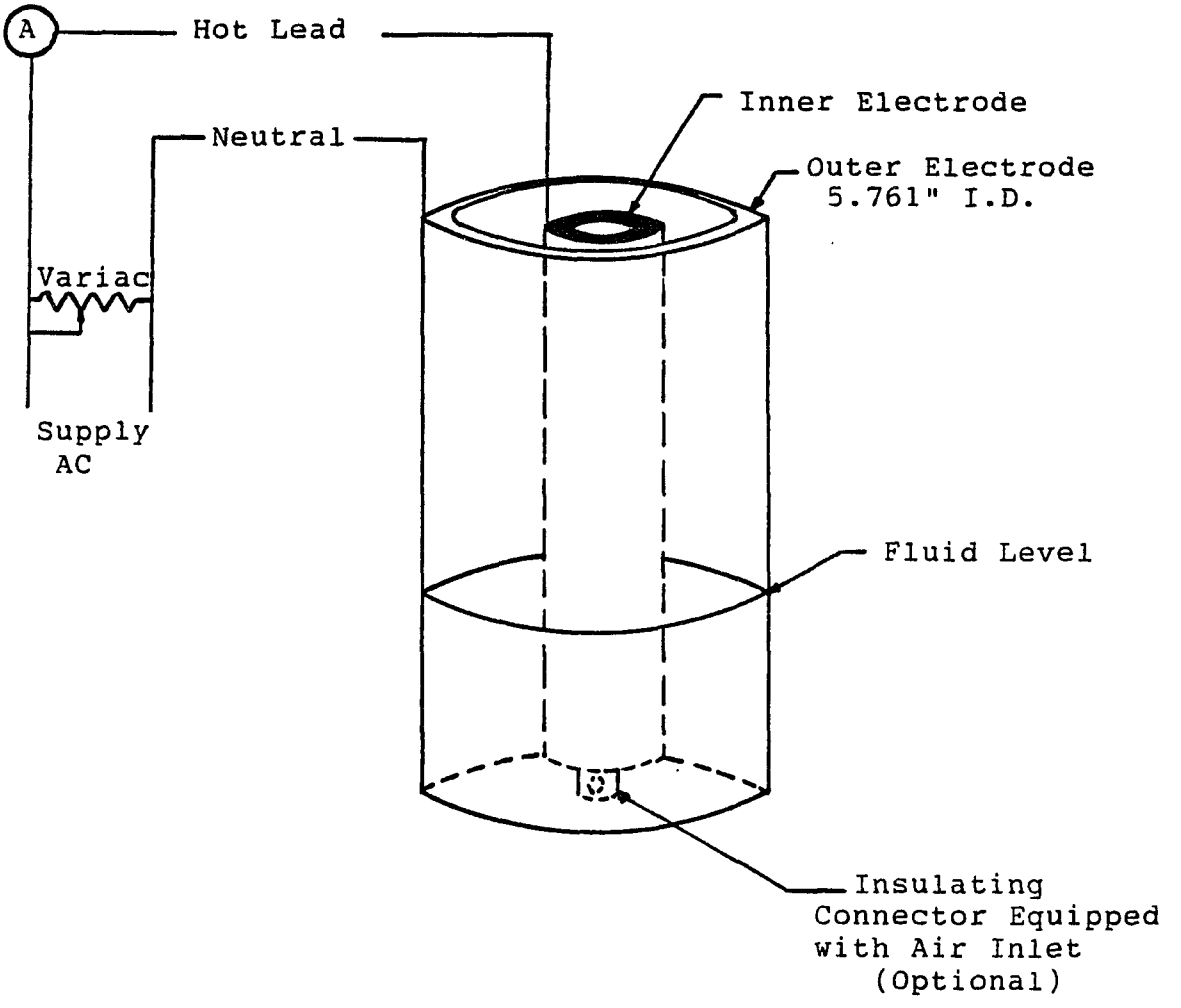

Fig. 4-4 Schematic of experimental set-up with concentric electrodes

existing oilfield piping, servicing, and experience. Consistent with industrial applications, aluminum electrodes were used.

The experimental set-up includes a variable voltage supply (variac), ammeter, and optional air inlet. The injection of air was purported in the literature to create turbulent flow in the inner electrode space and aid in fluid mixing to decrease plugging of the space. However, air injection did not reduce the amount of solids deposited upon the electrode surfaces. Consequently, it was not employed further.

To compare with other investigators a comparison plot of sludge volume percent against settling time is shown (Fig. 4-5 Sludge volume against settling time of Mine waste and a 0.26% w/w bentonite suspension). This dashed line shows a sludge containing less active solids than the solid line representing a 0.26% w/w bentonite suspension. Both underwent similar current densities expressed as amps/ft^2. Current density is later expressed as (amps/ft^2)/(L/min). Since Snyder and Gregory did not measure volume and time, a comparison of these two parameters was not possible. This difference in active solids is believed responsible for the difference in the curves. With clays present, the two differences are

(1) lower settling rates are observed. It can be seen that 40 minutes is required for clays

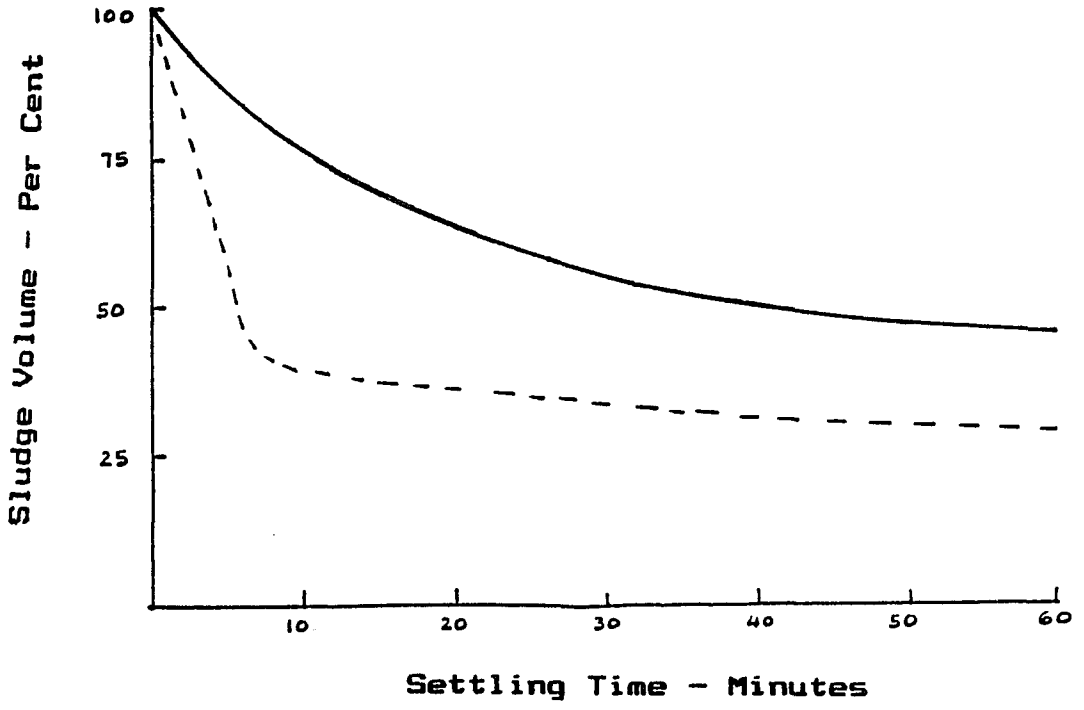

Fig. 4-5 Sludge volume against settling time of two EC treated samples: (i) 0.26% w/w bentonite suspension (solid line), (ii) mine waste (dashed line, after Snyder and Gregory, 1979)

while less than 10 minutes for the other case. (2) the settled sludge volume is less. Fifty-two percent for the clays while less than 30 percent in the other case.

As instantaneous effects were sought, a means was required for evaluating partial success. The selection of zeta potential (ζ) measurement was selected based on it being an indicator of the potential for solids to coagulate (Hinds et al., 1986). From electrochemical theory, if ζ is sufficiently low (near the isoelectric point), van der Waals and London forces are able to effect a bond resulting in coagulation.

Zeta potential of a particle is the potential difference between the outer limit of the shear plane and the bulk phase. The shear plane or slipping plane has a tendency to lag behind a clay particle in motion. Its ions are readily sheared or removed and replaced by others in the bulk solution (Everett, 1988, p. 90).

Both thickness of the double layer and ζ are affected by the addition of an electrolyte. An increase in ionic strength (I) results in compression of the double layer thickness (d), such that $d \alpha 1/I^{1/2}$ (Alexander and Johnson, 1948, p. 298). As electrolyte concentration increases, the thickness of the double layer decreases. Experiments showed dilute suspension (0.26% w/w bentonite) could be phase segregated following electrocoagulation, but higher concen-

trations of bentonite (6% w/w) could not. This is explained by the inability of the freed ions to migrate due to interference between particles. Ions are free to migrate in the suspension as long as the particle concentration is low. However, if too concentrated, as with a 6% w/w bentonite suspension, the movement of ions is retarded by interferences between the electric fields of the particles.

The device selected for measurement of zeta potential was the Micromeritics ζ Analyzer Model 1202 (Fig. 4-6). The unit has the advantage of analyzing undiluted mud with a solids content as high as 15% w/w; other units require excessive dilution. Sample fluid was placed in a 147 mL reservoir adjacent to a filled and weighed 6 mL chamber containing the same sample. A direct current is placed across the fluid. This current causes negatively charged particles to migrate into or out of the sample chamber. Admittedly, a direct current applied to mud can alter its zeta potential. The zeta potential computation is based on the mass change of the sample chamber.

A relationship exists between electrolyte concentration and dielectric constant of the dispersion medium, in this case, water. Electrolytes have the ability to cause a molar depression of the dielectric constant of water. The assumption for computation of ζ by Micromeritics assumed only temperature to effect a change in the dielectric constant of water. Electrolyte presence effected specific resistance,

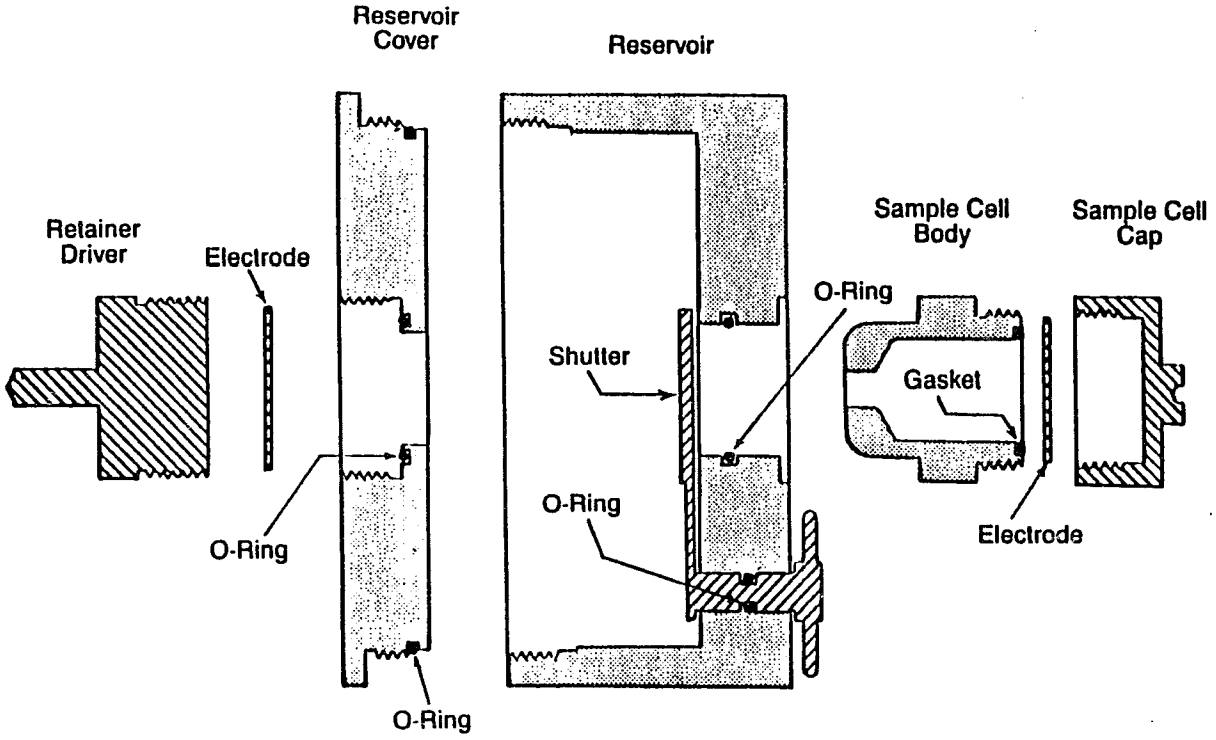

Fig. 4-6 Diagram of Micromeritics Zeta Potential Analyzer

which was taken into account for the ζ computation using the Micromeritics device.

One disadvantage of this device is that operator technique is extremely influential. Torquing of the sample cell body to the sample cell cap, presence of air/gas bubbles, homogeneity of sample has significant effects on measurement repeatability. It is recommended that at least a mass change of 0.03 g be obtained before reliable results can be achieved. Unless zeta potential is zero, this mass change can be obtained either by increasing field intensity or by extending test duration.

If barite is present in the sample, it should be removed as much as possible. Otherwise, clay particles flowing into the sample chamber can displace more dense barite particles. This results in a mass loss in the sample cell, which loss is indicative of a positive ζ, when, in fact, the movement of clay particles into the cell should reflect a negative ζ. The net mass loss is due to differences in clay specific gravity (2.6) and barite specific gravity (4.2).

Therefore, the use of zeta potential as a means of evaluating extent of electrocoagulation treatment has merit. Its use is justified in the evaluation of electrocoagulation on various drilling fluids.

4.2.2 Electrocoagulation effect on routinely tested properties of drilling fluids

4.2.2.1 Drilling fluids tested

Fluids tested were

1. simulated spud mud with caustic soda and containing 6% w/w bentonite without dilution
2. 1:1 simulated salt/polymer fluid formulated using:

Item	lb_m/bbl
CMC	1
NaCl	18.67
Bentonite	20.02
Drispac	0.36

CMC = Carboxymethylcellulose
Drispac is a polyanionic cellulose and is used for fluid loss control.

3. 1:1 simulated fresh/CLS fluid formulated using:

Item	lb_m/bbl
Bentonite	20
Q-Broxin	9
Caustic soda	1.5
Soltex	3

Q-Broxin is a modified lignosulfonate which acts as a deflocculant and protective colloid. Soltex is a sulfonated residuum, which in water base drilling fluids, lowers fluid loss and minimizes heaving shales. Caustic soda (NaOH) increases pH which increases fluid viscosity.

One of the fluids tested was a field mud containing CLS in a fresh water system. This type of mud was mixed and diluted 1:1 to formulate a fluid having similar components, and the whose mixture could be accurate known. The effect of the various components could then be better understood.

With a field mud, the precise components are not accurately known. The formulated fluid was a 1:1 simulated fresh/CLS system (Table D-3).

The next two listed fluids were obtained on-site from the active mud system while a well was being drilled.

4. 1:1 field fresh/CLS fluid (Table D-4)
5. 1:1 field salt/CLS fluid (Table D-5)

4.2.2.2 Results and discussion

The experimental data described in this section were performed per API guidelines for field testing of drilling muds (NL Baroid, 1975). In addition, conductivity, zeta potential, solids percent by weight, and CST were measured. Centrifugation effects are addressed in section 4.3.3.

In each table of Appendix D the "BEFORE" column represents the sample prior to treatment by electrocoagulation, but after a 1:1 dilution with water. For purposes of discussion, each fluid will be discussed in the context of measured properties. In this way, noteworthy differences will be evident. The areas include:

1. filtration and electrical stability (CST, filtrate volume, and zeta potential)
2. suspension ionization (conductivity and chlorides)
3. Rheology (plastic viscosity and yield point)

Due to negligible or insignificant changes, the discus-

sion of several mud properties is omitted. They are included in the tables, as they are mud properties which are routinely tested.

CST and filtrate volume measure different aspects of filtration, and are expected to be similarly effected by treatment. However, a difference is that filtrate volume is dependent upon cake deformation. This deformation is believed to mask subtle differences which occur in interparticle forces. Therefore, filtrate volume is not deemed to be a useful indicator of subtle changes in suspension stability.

CST, on the other hand, is more sensitive to interparticle forces. There is an evident change in CST values with treatment. With treatment, CST is typically reduced while filtrate volume is typically increased when the suspension is destabilized. CST is reduced by 50% in each case except for the 1:1 field fresh/CLS (Table D-4). As explained earlier, the chemical treatment with thinners/deflocculants renders this fluid system the most chemically and electrically stable. Consequently, it is least affected by electrocoagulation treatment.

Zeta potential was reduced from -110 to -40 mV on this CLS fluid. This large value still indicates an electrically stable suspension, and can be considered an unsuccessful treatment. While consistent measurements of zeta potential following increased levels of electrocoagulation treatment

were not obtained, it is believed that drastic reductions can occur from large negative values, however, as the isoelectric point is approached, additional reductions were not realized.

Consistent with the ionization mechanism, suspension ionization is indicated following electrocoagulation treatment of certain fluids. Two measurements for its observation are increases in conductivity and chlorides. The most marked change occurs for the bentonite suspension which simulates a spud mud with caustic soda (Table D-1). This change was addressed earlier and related to freeing of ions in the presence of an electrical field (Table 4-1). The salt/polymer fluid (Table D-2) was not measurably affected. This was due to the high concentration of ions already in suspension. These ions inhibited the removal of additional ions. The CLS fluid systems (Tables D-3,4, and 5) were unaffected by treatment. Electrocoagulation treatment cannot remove ions if the colloids have been coated with deflocculants. This coating inhibits ion exchange or removal.

Rheology is unaffected except for the 1:1 field salt/CLS fluid (Table D-5). Plastic viscosity increased while yield point decreased. This is believed due to some amount of particle agglomeration. With growth in particle size, interparticle interference increases as measured by a viscosity increase. However, the interparticle attraction

would necessarily be reduced to account for agglomeration. With this reduction, a reduction in yield point is effected.

Methylene blue capacity is unchanged. Evidently, the coagulation which occurs does not markedly alter the surface area of the bentonite present. This suggests a very loosely coagulated particle. This loose association is evident. When a treated sample is stirred after it has settled with clear water having been separated, gentle stirring immediately makes the mixture turbid.

The pH increase is largest (7 to 9.5) with the bentonite suspension (Table D-1). This increase is explained by the removal of hydroxyl ions. Hydroxides are present in montmorillonite ($(Al,Mg)_8(Si_4O_{10})_3(OH)_{10} * 12H_2O$), a principal component of bentonite. The next largest (8.5 to 10.5) increase occurred with the 1:1 field salt/CLS. The increase in alkalinity of the filtrate, and the fact that this increase is accompanied by a reduction in hardness, suggests a chemical reaction has occurred. If calcium carbonate dissolution accounted for the increase in alkalinity from one to nine, the hardness would be expected to have increased, rather than decreased as observed.

In summary, routinely tested mud properties have limited utility in evaluating changes in interparticle forces. This suggests the need for new properties to be investigated and methods standardized in order for dewaterability to be evaluated. Particularly indicative of change are CST, zeta

potential, and conductivity. Particle size measurements are also recommended.

In order to more clearly ascertain electrocoagulation effects not evident from routinely tested mud properties, zeta potential measurements and centrifugation effects were investigated.

4.2.3 Effect of suspension stability

The choice of zeta potential was made for two reasons. (1) zeta potential is an accepted measure of interparticle forces, and (2) zeta potential is affected by chemical coagulants. Therefore, it is reasoned that since the effect of chemical coagulation can be evaluated in this manner, so can electrical coagulation. First, then, it will be shown that the addition of a coagulant reduces zeta potential.

Lavrov et al. (1975) measured zeta potential following the addition of alum ($KAl(SO_4)_2*12H_2O$) on refractory materials. Addition of electrolyte produced an increasing conductivity and a declining zeta potential (Fig. 4-7). A similar trend was noted when alum was added to a 6% w/w bentonite suspension (Fig. 4-8). The mean for each set of tests is plotted, and is bracketed by an error bar indicating one standard deviation above and below the mean. A similar trend was observed when alum was added to the undiluted field fresh/CLS fluid (Fig. 4-9). This suspension contained 11% w/w solids.

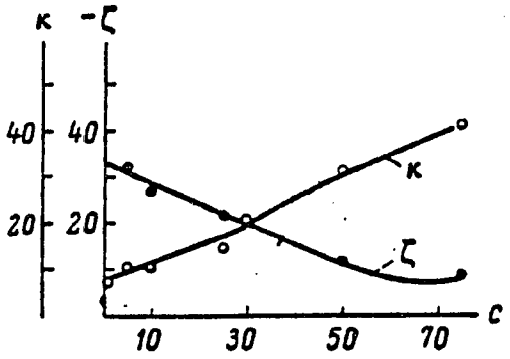

Fig. 4-7 Dependence of conductivity (K) on zeta potential of the refractory suspension on the $Al_2(SO_4)_3$ concentration (C) (after Lavrov et al., 1975)

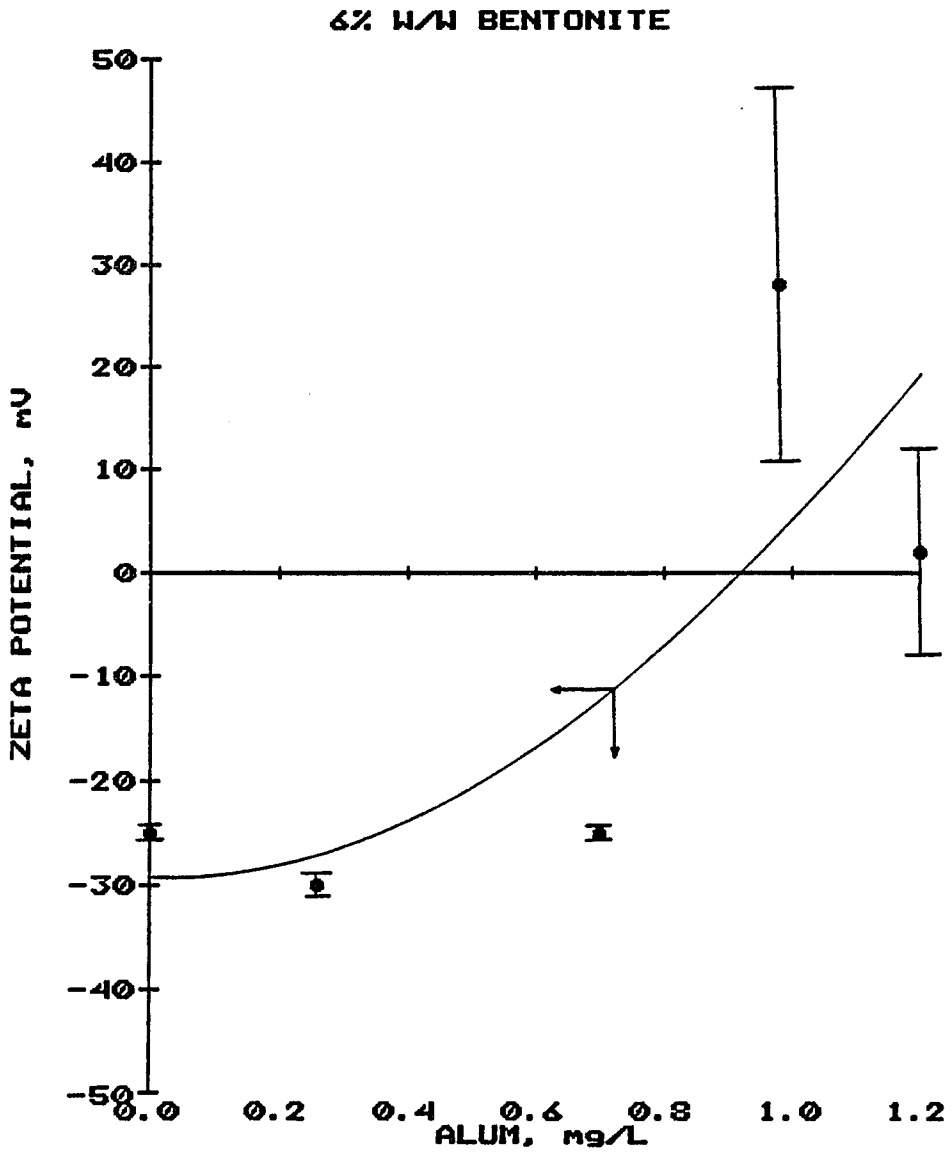

Fig. 4-8 Dependence of conductivity and zeta potential of a 6% w/w suspension of bentonite on alum concentration

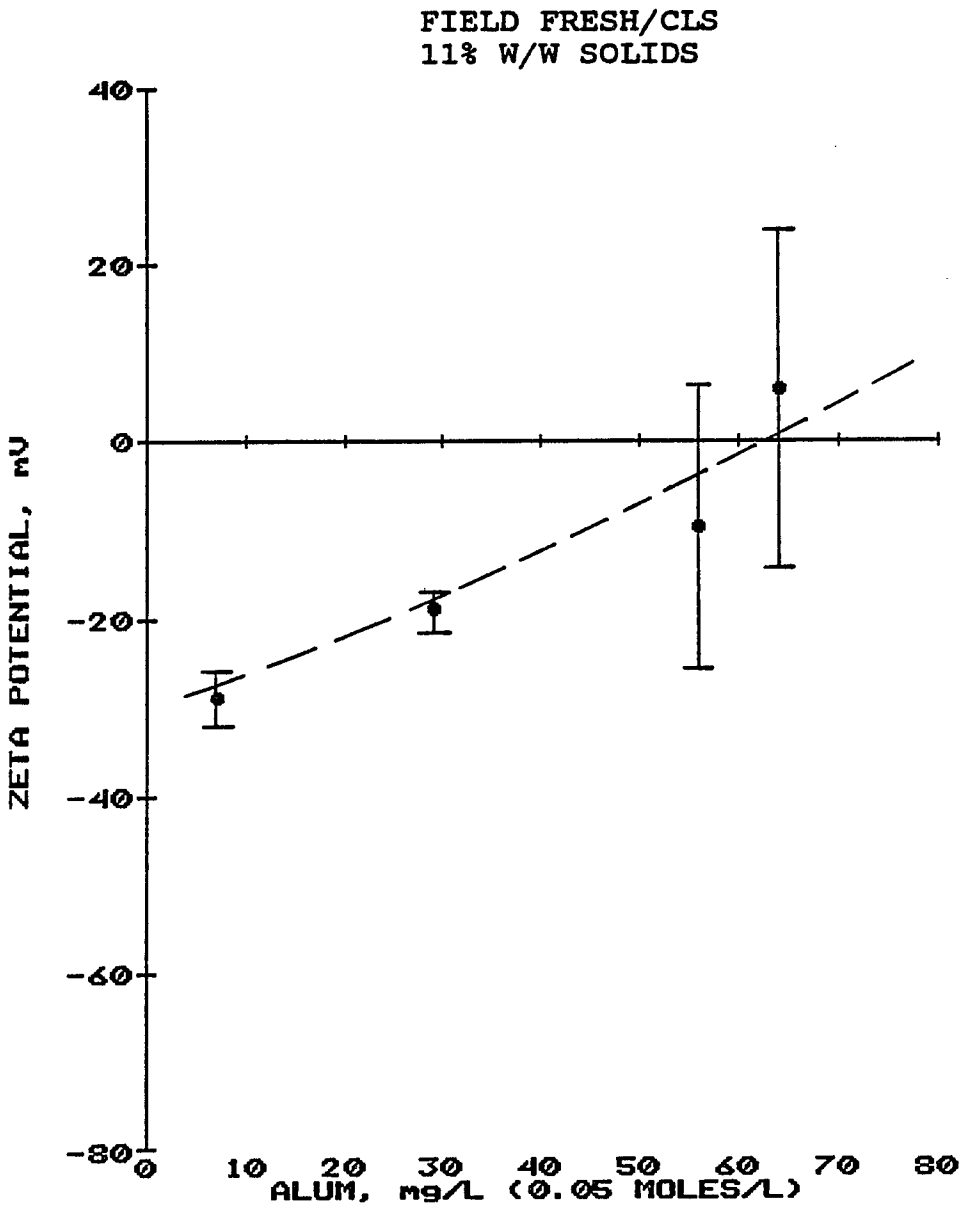

Fig. 4-9 Dependence of zeta potential on 0.05 moles/L alum additions to a field fresh/CLS fluid containing 11% w/w solids

A similar trend was reported by Hinds et al. (1986) for a ferric electrolyte added to a drilling fluid sample from a reserve pit (Fig. 4-10).

Others have demonstrated the reduction of ζ by adding a coagulant (Hughes, 1981; and Coca et al., 1982). A ζ reduction is typically accompanied by a pH reduction as Fig. 4-11 indicates. The pH reduction, in this case, was due to alum additions. These data compared well with published graphs shown earlier, and explain further why a pH of neutral or below is required before the minimum volume of a flocculant can be added. This is because this level of pH approximates the isoelectric point. For the fresh/CLS sample, a pH of neutral reflects the isoelectric point. Reduction of ζ to near its isoelectric point is required before a sol can be coagulated or flocculated.

In summary, experimental data confirm that chemical coagulants can reduce ζ. Further, it is supported by theory and experimentation, that reduction of zeta potential accompanies chemical coagulation. The effect of electrical treatment is similar.

4.2.3.1 Effect of electrical energy

The response of a fresh/CLS fluid when electrical energy is applied is shown in Fig. 4-12. The most effective treatment resulted from the highest applied energy. ζ was reduced from -745 to -52 mV, yet the suspension remained

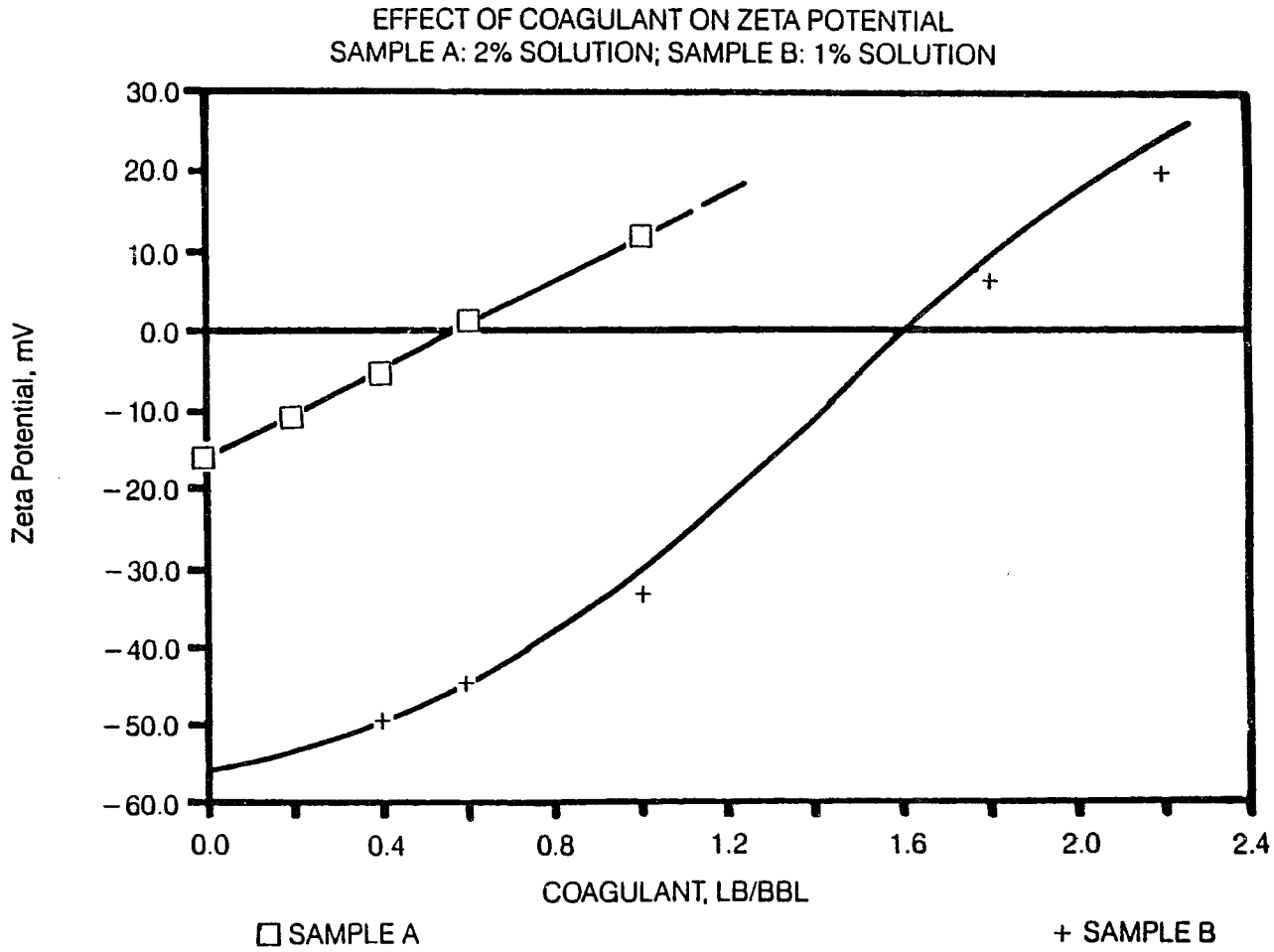

Fig. 4-10 Dependence of zeta potential on coagulant additions to diluted reserve pit samples (after Hinds et al., 1986)

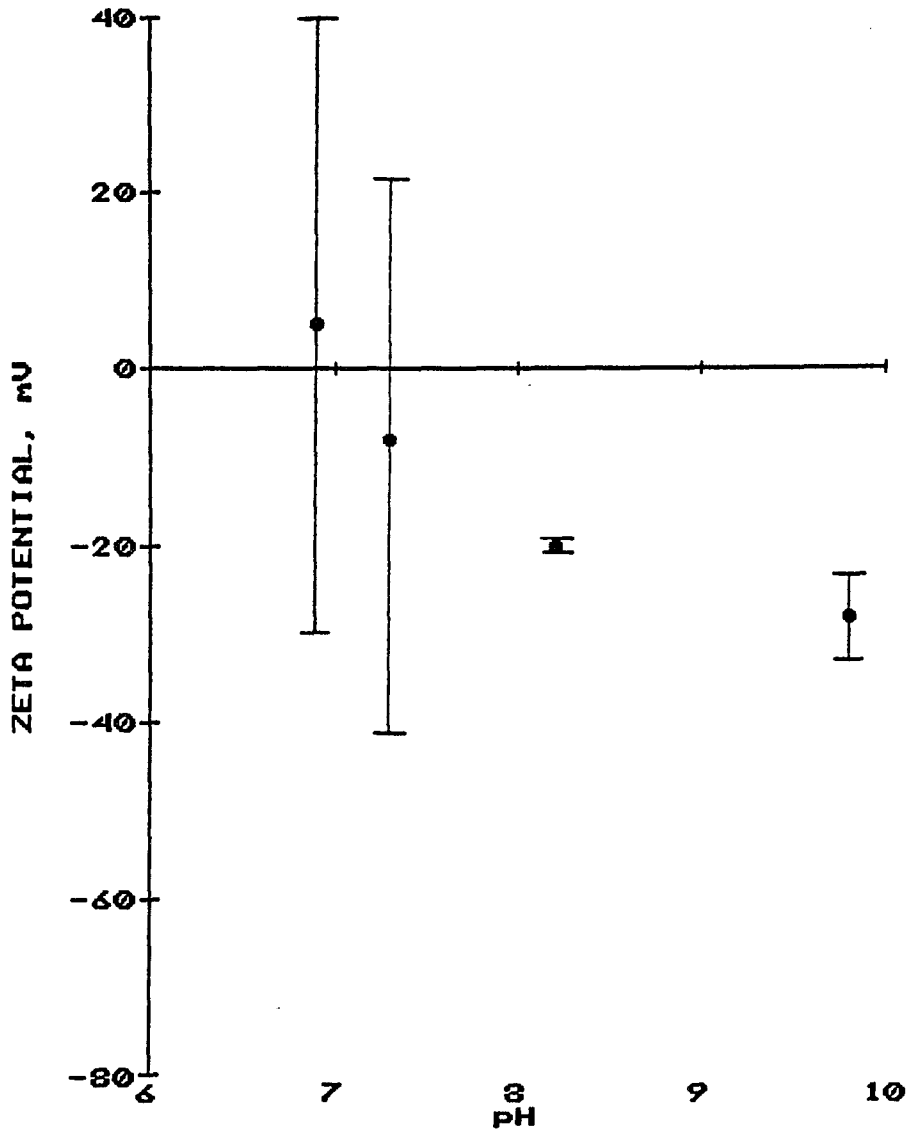

Fig. 4-11 Relation of zeta potential to pH (from alum additions) for a 6% w/w bentonite suspension

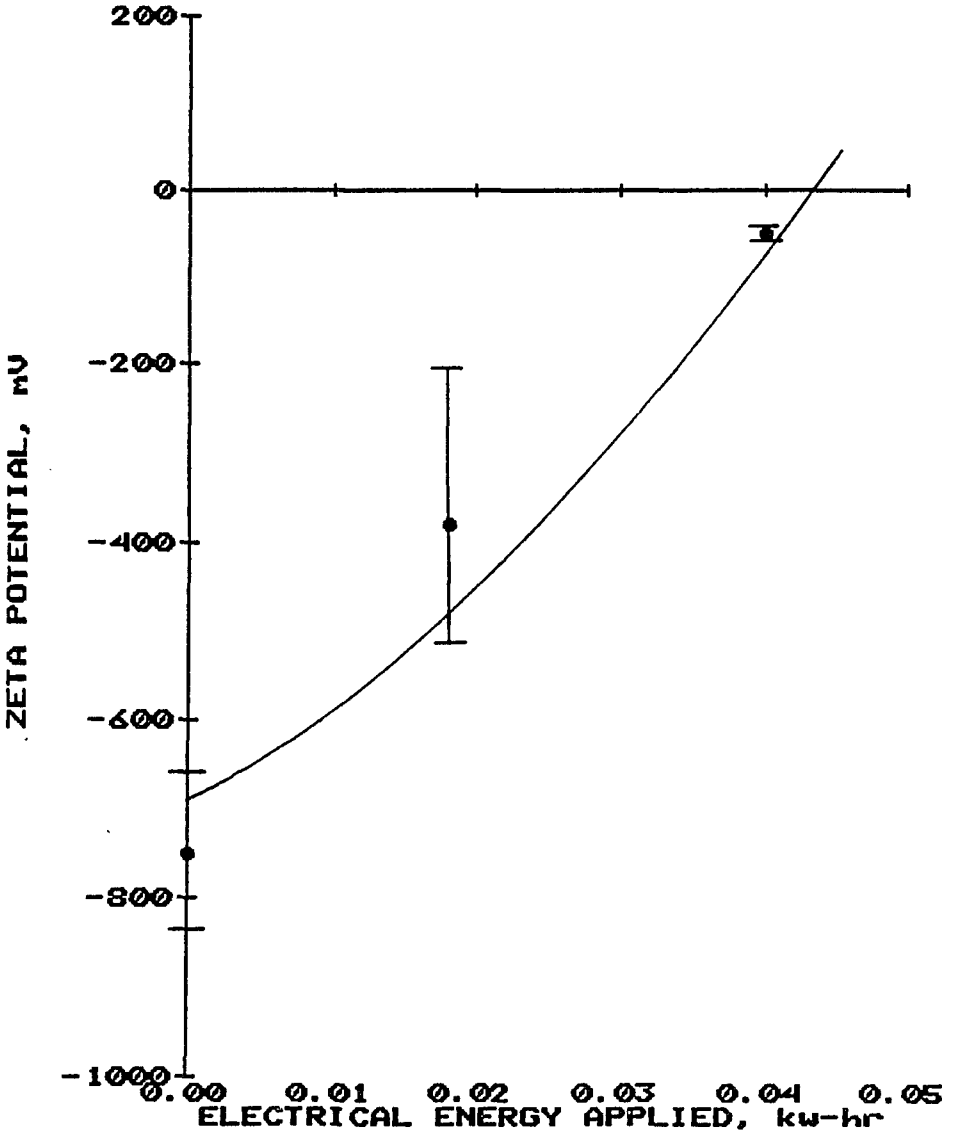

Fig. 4-12 Relation of zeta potential to electrical energy from EC treatment of a field salt/CLS fluid

chemically stable.

The 1:1 simulated spud mud without caustic was electrically treated in a series of experiments. In each treatment, one liter was the treated volume. Times and currents varied and CST was selected as the criterion for evaluating coagulation effects. CST measurements were adequate for initial screening of the optimum current level and treatment time. The results are plotted in Fig. 4-13. Greater amounts of treatment time do not show promise for substantially reducing CST, as a leveling of the effect is evident between 225 and 180 sec.

CST is affected by solids content, and solids content is affected by treatment time. Electrocoagulation treatment removes solids as solids plate onto electrodes. This is especially true for bentonite suspensions, and necessitates adjustments in CST when solids content varies.

To determine the effect of current, it was increased while treatment time was kept constant at 5 min. Maximum allowable current was 19 A with the particular setup used in this phase of testing, and showed the minimum CST value. As no leveling of data occurred, the application of greater current levels was justified and applied in subsequent tests (section 4.3.3 Electrocoagulation effect on dewatering performance).

The next fluid tested was a 1:1 simulated fresh/CLS fluid. This mixture was and treated by utilizing varying

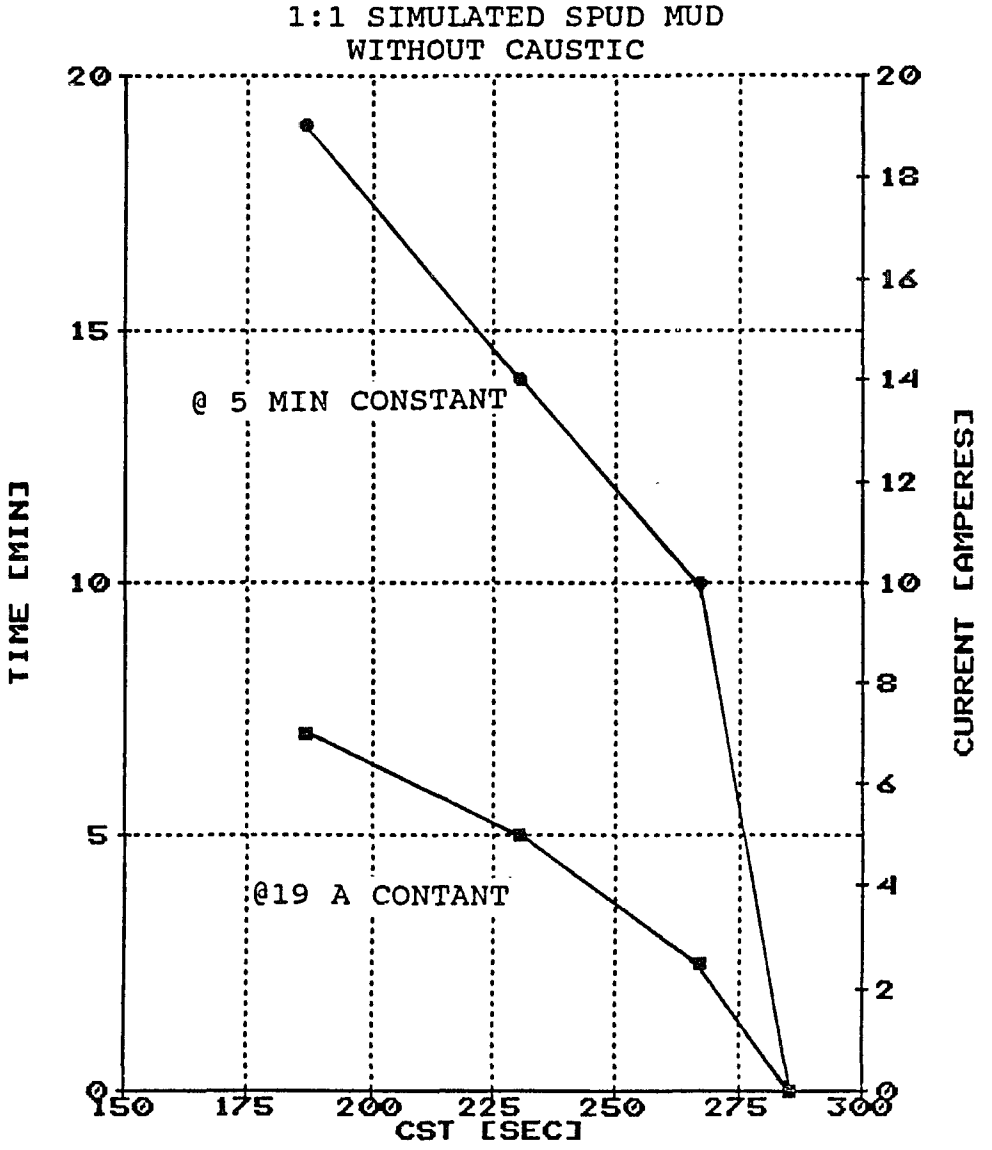

Fig. 4-13 Dependence of Capillary Suction Time to time and current level of EC treatment upon 1:1 simulated spud mud (6% w/w bentonite) without caustic soda

currents while holding treatment time constant. Following treatment, CST was measured with results as shown in Fig. 4-14.

Figure 4-15 shows that additional treatment time offered no benefit. Similar to the bentonite suspension, greater current is suggested but not greater time. This suggests that the ionization which will occur does so relatively quickly. A simulated salt/polymer fluid was formulated to evaluate electrocoagulation treatment on this type of fluid system. A field counterpart was not tested. After dilution and treatment, CST was measured with results shown in Fig. 4-16. These data were plotted in a similar manner as the earlier figure for the 1:1 simulated spud mud without caustic. The best results were again for 19 A, and the best time was the longest used, which in this instance was 7 min. These and other fluids were electrically treated with higher currents using a welding machine. A discussion of this series of experiments is in section 4.3.3.

In summary, the beneficial effects on CST resulting from the maximum level of current (19 A) suggested that reater levels of current were justified. In addition, a reduction in zeta potential with increased electrical energy suggested greater current levels.

However, before addressing effects of higher current levels, the electrode configuration which influences the maximum effect is addressed. Electrode spacing should be

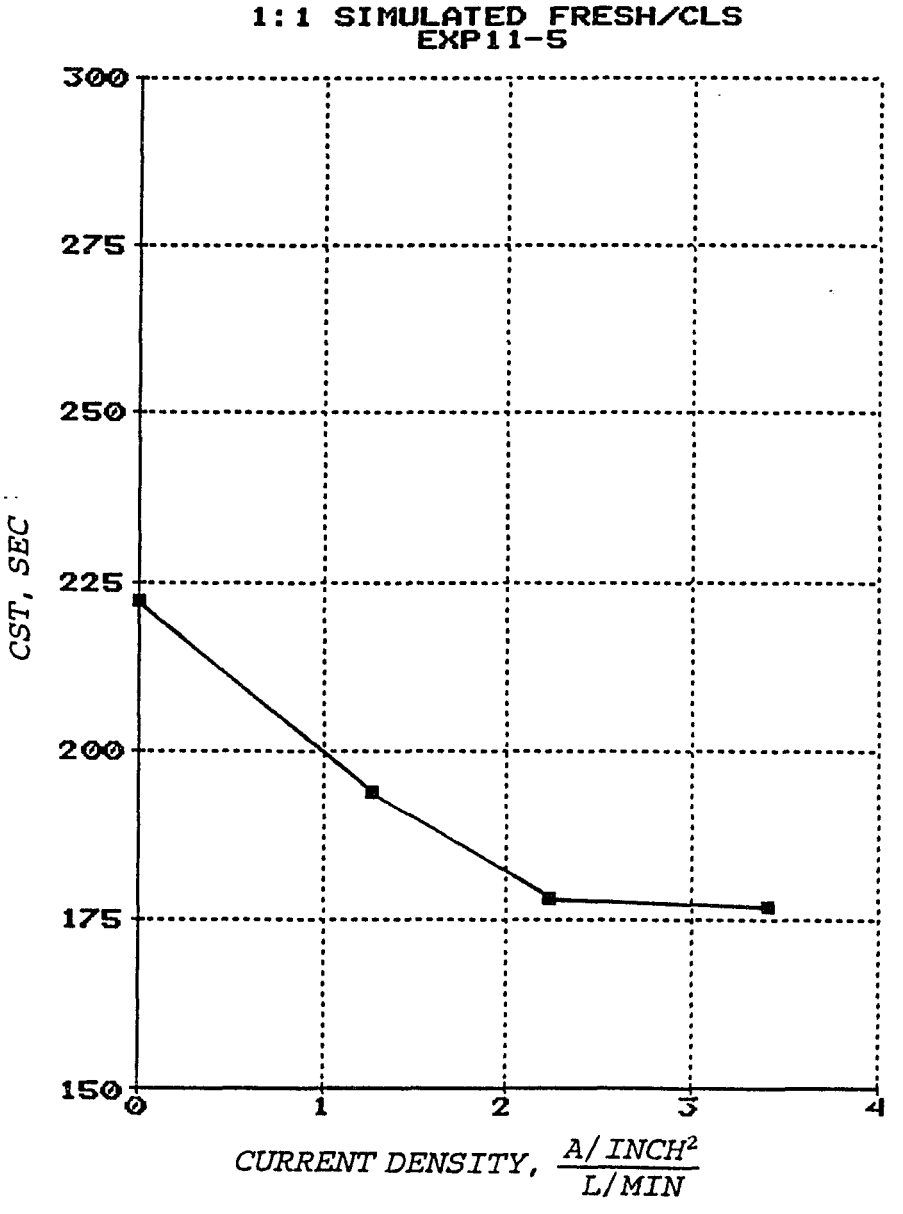

Fig. 4-14 Dependence of Capillary Suction Time to current density for EC treatment of a 1:1 simulated fresh/CLS fluid

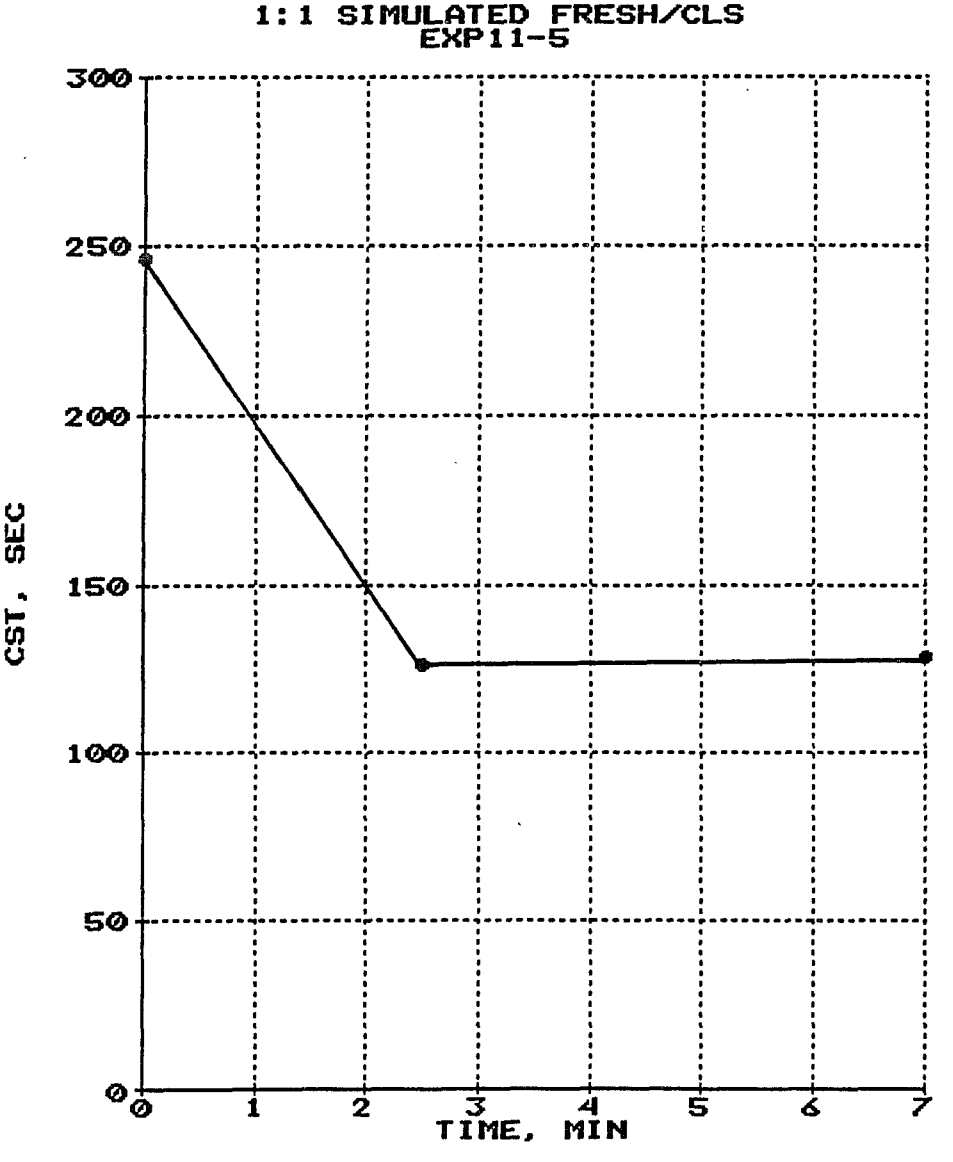

Fig. 4-15 Dependence of Capillary Suction Time to treatment time for EC treatment of a 1:1 simulated fresh/CLS fluid

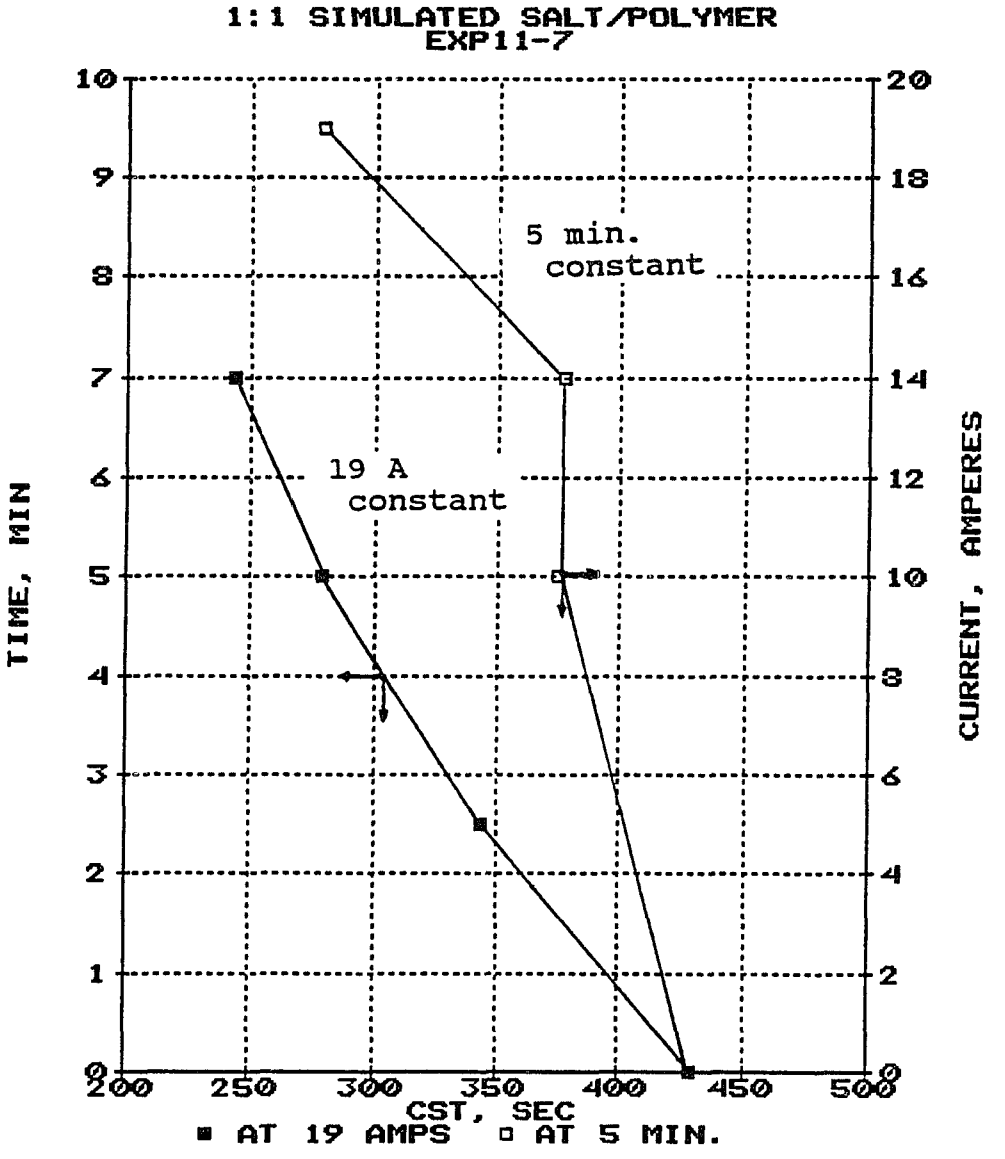

Fig. 4-16 Dependence of Capillary Suction Time to time and current level of EC treatment on a 1:1 simulated salt/polymer fluid

close enough to minimize resistance without reducing it to such a value that an electrical short is possible.

4.2.3.2 Effect of electrode spacing

Various electrode configurations were available, and with the exception of one configuration, all configurations had the outer electrode in common. Its inner diameter was 5.761 in. The outer diameters of the three available inner electrodes were 1.9 in., 3.5 in., and 4.5 in. The 4.5 in. offered the shortest electrode spacing for lowest resistance as evident from the following equation. Fluid resistance for a radial application of electrical energy can be expressed as (Branson, 1967, p. 75):

$$R = \rho \frac{\ln \frac{r_o}{r_i}}{2\pi h} \qquad 4\text{-}1$$

where R is resistance, ohm
ρ is resistivity, ohm-cm
h is depth of fluid in electric field, cm
r_o is outer electrode inner radius, cm
r_i is inner electrode outer radius, cm

replacing resistivity with conductivity, ($\rho = 10^6/\sigma$)

$$R = \frac{\ln \frac{r_o}{r_i}}{\sigma 2\pi h} 10^6 \qquad 4\text{-}2$$

where σ is conductivity, μmhos/cm.

When changing electrode sizes for the same fluid system, the denominator is a constant, consequently,

$$R \alpha \ln(r_o/r_i) \qquad 4\text{-}3$$

Thus, as r_i declines, R increases.

The diameter of the inner electrode can be easily varied, which means r_i can be varied. For conductive fluids, the resistance is low; conseqently, the distance between the electrodes will be enlarged. This is accomplished by minimizing r_i. For resistive fluids, it is important that the electrodes be spaced more closely. This is done by maximizing r_i. Power is the product of voltage and current. For the experimental apparatus in which voltage could be kept constant, current was maximized by reducing resistance. Thus, from these equations it can be seen that greater power can be applied when the smaller diameter electrodes are used.

4.3 Feasibility of electrocoagulation conditioning of drilling fluids for centrifugal dewatering

4.3.1 Selected drilling fluids

Fluids which were evaluated by centrifugal separation were:

1. Bentonite and water
2. 1:1 simulated spud mud with caustic soda
3. 1:1 simulated fresh/CLS
4. 1:1 simulated salt/polymer
5. 1:1 field fresh/CLS
6. 1:1 field salt/CLS

Bentonite and water is a simple system. It was used intially to develop an experimental methodology. Spud mud is essentially bentonite and fresh water with caustic soda added; it is commonly used to begin drilling a well. The CLS systems are chemically dispersed systems; the most difficult to dewater. The easiest to dewater is the salt/polymer. The suspensions tested included a variety of conductivities.

Table 4-6 Conductivity and resistivity of various suspensions

Fluid system	Conductivity, μmhos/cm	Resistivity, ρ ohm-m
1:1 salt/CLS	86400	0.116
1:1 fresh/CLS	7900	1.26
6% w/w bentonite	840	11.90

4.3.2 Method of evaluation

As electrocoagulation treatment was investigated as a means for centrifugal pre-treatment, samples were centrifuged following electrocoagulation treatment. The samples were centrifuged @ 800 rpm for 2 min. Afterwards water and cake quality were measured. These measurements included TS (total solids) of the cake, TSS or TS of the supernatant, and TS of the transition zone if present as per Standard Methods (1985). Height or volume of each was also routinely measured.

Cake is that sedimented portion which remained in the centrifuge tube when inverted. Supernatant is the remainder whether turbid or clear unless a transition zone was pres-

ent. If a transition zone was present, it was turbid and classified as a transition zone when a distinctly clearer supernatant was present. The cake in each case was much wetter than with chemical pre-treatments. When stirred with a spatula, for example, the particles did not settle readily as with a chemically treated sample. This suggests difficulty in the full-scale decanting centrifuge. The presence of the conveyor could possibly prevent a compact cake from forming. Transition zone would be discharged as effluent with the supernatant.

4.3.2.1 Selection of dilution level and the sequence of dilution

The sequence of dilution referes to whether the dilution water was added before or after the electrical treatment. Dilution provided some improvement. A 1:1 level was selected and is a commonly employed level for chemical treatments.

Early experiments with electrocoagulation treatment of bentonite indicated dilution was beneficial. Experimentation on a 6% w/w bentonite suspension revealed a 1:1 dilution was more affected by electrocoagulation treatment when no dilution was used. This is explained by referring to the double layer theory. The 6% w/w mixture was a highly gelled suspension. Gelation indicates an interaction of the diffuse double layer. If upon electrocoagulation treatment,

the ions were freed from the individual clay particles, their mobility would be severely retarded by the ionic atmospheres surrounding each particle. With a more dilute suspension, an atmosphere void of double layer ions exists between particles. This allows ions to migrate and become bonded to clay particles.

With chemical treatments, dilution precedes treatment. However, with electrocoagulation treatment the benefit of dilution following treatment was investigated and tested on a 6% w/w bentonite suspension. When cake solids content was compared following centrifugation, no improvement was observed. An adverse effect was that cake volume for the dilution after treatment was reduced from 66 to 25 percent.

Another variation in treatment was also attempted, but without success. The procedure followed was to first treat, centrifuge, and retreat the supernatant and transition zone. Retreatment of two concentrations of bentonite (1.41% w/w and 3.55% w/w) showed no improvement in supernatant quality.

Coagulation occurs as clays dissolve, release ions, and these ions form colloidal groups. To explain the failutre of this experiemental variation, it is postulated that those ions most susceptible to being removed enter the suspension first. Upon retreatment, the more strongly bonded ions remain and are not released.

4.3.2.2 Selection of electric current level and effect of electrical treatment upon dewatering performance

As stated previously, TS and TSS of the treated and centrifuged samples were selected as the criteria for treatment evaluation. This is due to the testing of the original hypothesis, which was the ability of electrocoagulation to replace chemicals as a means for destabilizing a suspension.

The value called dissolved solids is total solids less suspended solids. Previous evaluations of chemical pretreatments has focused on supernatant quality or clarity (Malachosky et al., 1989). In this investigation, TSS of supernatant was evaluated whenever possible. If solids were too high to make TSS measurement feasible, TS alone was measured.

Caustic soda (NaOH) was added to a bentonite suspension to simulate a spud mud, and had the benefit of increasing conductivity from 800 μmho/cm to 2500 μmho/cm. Caustic additions also increased pH to 10 prior to the 1:1 dilution.

For the electrode spacing selected (4.026 in. X 3.5 in.), and using the welding machine, a maximum current between 30-35 A was applied. This electrode spacing was 0.263 in. which calls to question the practicality of such a narrow spacing as the space could easily become plugged with solids. The electrode configuration of 5.761 in. X 4.5 in. meant that resistance was too high. Higher levels were applied using a welding machine capable of 225 A, but with a

voltage limitation of 77 V.

Maximum treatment time was one minute due to frothing from Joule heating. Joule heating was present in all treatments. To illustrate:

Table 4-7 Dependence of applied electrical energy upon electrode configuration

Outer Electrode Diameter	Inner Electrode Diameter	Elec. Energy kw-hr	T_f, °C
5.761 in.	3.5 in.	0.0148	27
5.761 in.	1.9 in.	0.0182	32
5.761 in.	1.9 in.	0.0391	40

T_f is the final temperature following electrocoagulation treatment, initial temperature in all cases was 25°C

To determine if heat contributed to the electrocoagulation process, a 0.26% w/w bentonite suspension in distilled water was heated to 51°C. As shown, this temperature compared well with temperatures which resulted from Joule heating:

Table 4-8 Joule heating from electrical treatment

Bentonite Suspension, % w/w	T_f after 10 min. of EC treatment
0.5%	39°C
1.0%	54°C
2.0%	48°C
4.0%	62°C

Upon cooling, the suspension was observed for seven days. No coagulation and consequent settling was visible. Therefore, heat, under these conditions, is unable to promote coagulation, even in the most dilute of clay suspensions.

The untreated and treated samples were centrifuged and results compared. Both evidenced poor quality. Three zones

were apparent, a supernatant, transition, and cake (loosely aggregated). In the 35 A treatment, the following separation was seen:

Table 4-9 Solid/liquid separation using the centrifuge

	supernatant	transition	cake
TS (% w/w)	0.76%	2.2%	6.7%
Height, cm	1.6%	5.5%	1.0%

CST of the treated suspension before centrifuging was reduced from 111 to 50 sec. No phase segregation was visible after centrifuging the untreated sample.

To the 1:1 simulated fresh/CLS with an electrode configuration of 5.761 in. X 4.5 in., and a conductivity of 3850 μmho/cm, the maximum current applied was 30 A @ 65 V. As the treatment progressed, current increased to 48 A (nominal 50 A for plotting) at 41 V due to the conductivity of the suspension increasing. Power was similar for these two cases and was 2000 watts in each case. Treatment duration was 5 min., but frothing occurred after 4 min. Final temperature was 79°C.

For the 1:1 simulated fresh/CLS in order to obtain a larger current without decreasing current density, the spacing of electrodes was reduced, using a 4.026 in. X 3.5 in electrode configuration. This enabled 60 A to be applied, increasing to 70 A. However, due to excessive frothing and spillage, the test was terminated after 24 sec. of treatment. These two treatments showed no differences in centrifugal separation. Figure 4-17 shows the effect of

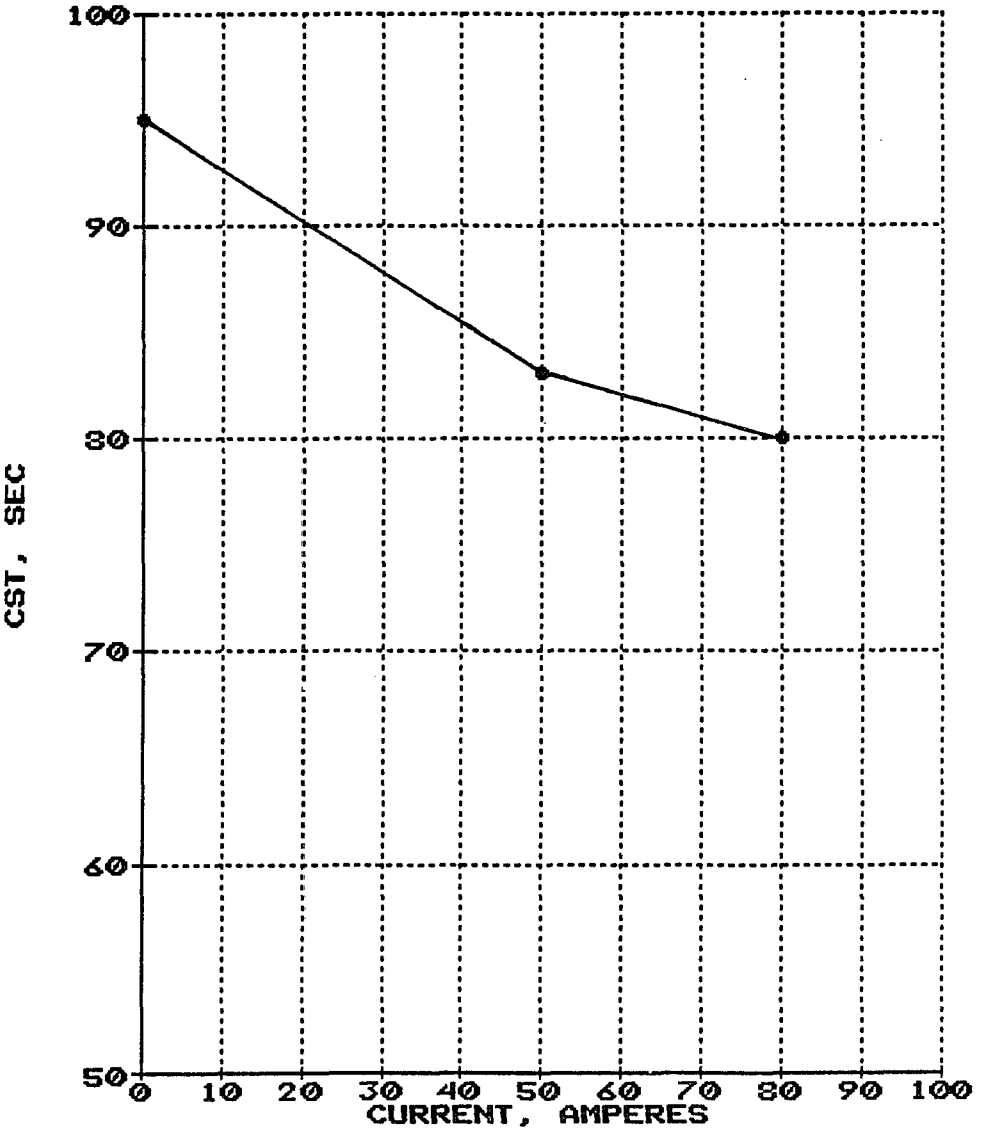

Fig. 4-17 Dependence of Capillary Suction Time to level of current of EC treatment on a 1:1 simulated fresh/CLS fluid

current upon CST. The similarity between the 50 A and 70 A treatments is explained by the brief duration of the latter.

For the 1:1 simulated salt/polymer, a plot of CST against current shows a consistent decline as the suspension is increasingly destabilized (Fig. 4-18). For reference, free water has a CST value of between 5 sec.

The electrocoagulation treatment was performed on two splits of a 1:1 field fresh/CLS for 3 min. at 60 A, as shown in Table 4-10. In no case was a collectible cake present.

Table 4-10 Electrocoagulation treatment effect on centrifugal separation efficiency; TS of supernatant

	Mixture	Supernatant	CST, sec
Before	5.37%	4.82% w/w	22
After 1	5.02%	4.41% w/w	25
After 2	4.91%	4.32% w/w	20

In Fig. 4-19, TS is plotted with TSS data with the error bar one standard deviation above and below the mean. The dashed arrow indicates a reduction due to centrifuging before and after centrifuging. Centrifuging the untreated sample had minimal effect on reducing TSS while the electrically treated sample was substantially effected although still quite high (+10,500 mg/L at 60 A). An abbreviated form of the previous figure (Fig. 4-20) illustrates that the reduction electrocoagulation treatment has upon the TS and TSS of a centrifuged sample. As indicated in a comparison of routinely tested mud properties, CLS fluid systems are not significantly affected by this level of current.

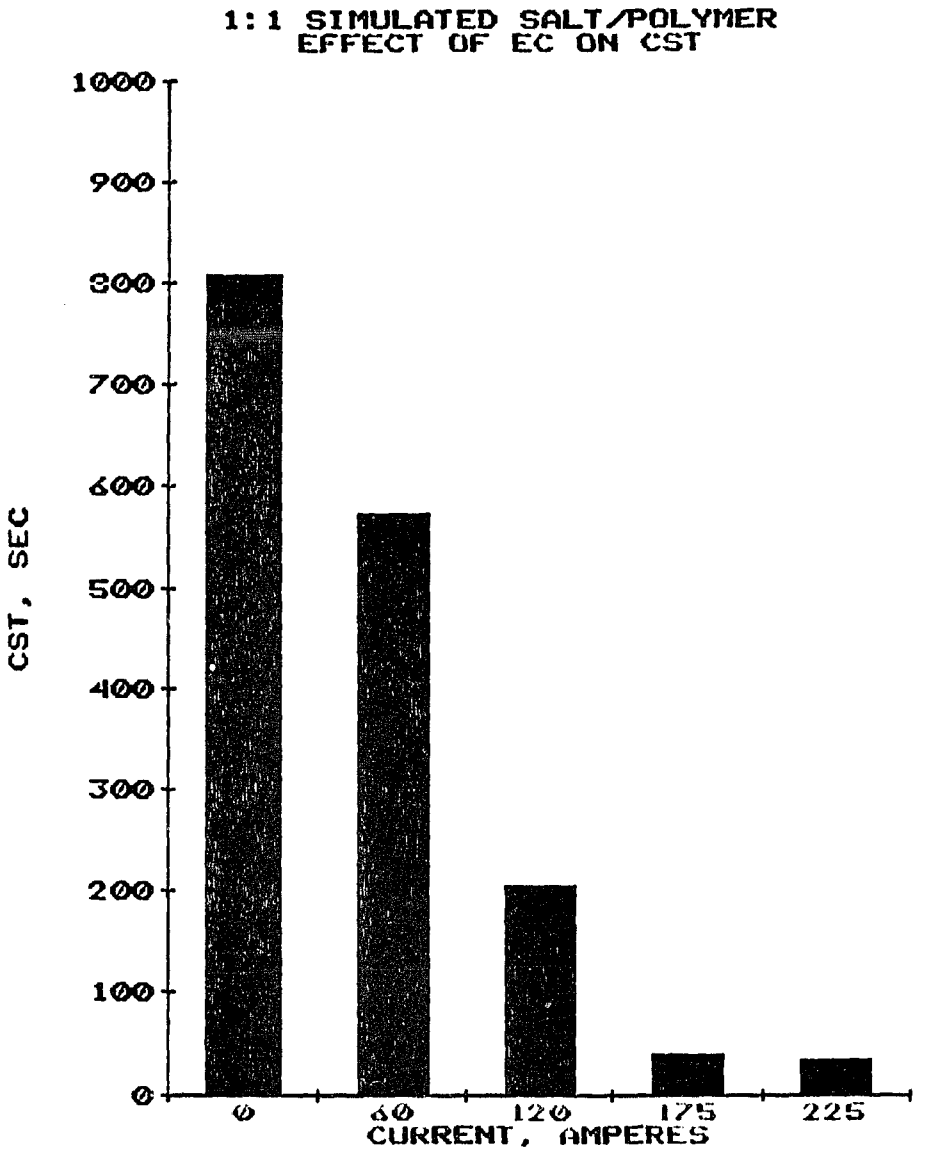

Fig. 4-18 Dependence of Capillary Suction Time to current level for EC treatment of a 1:1 simulated salt/polymer fluid

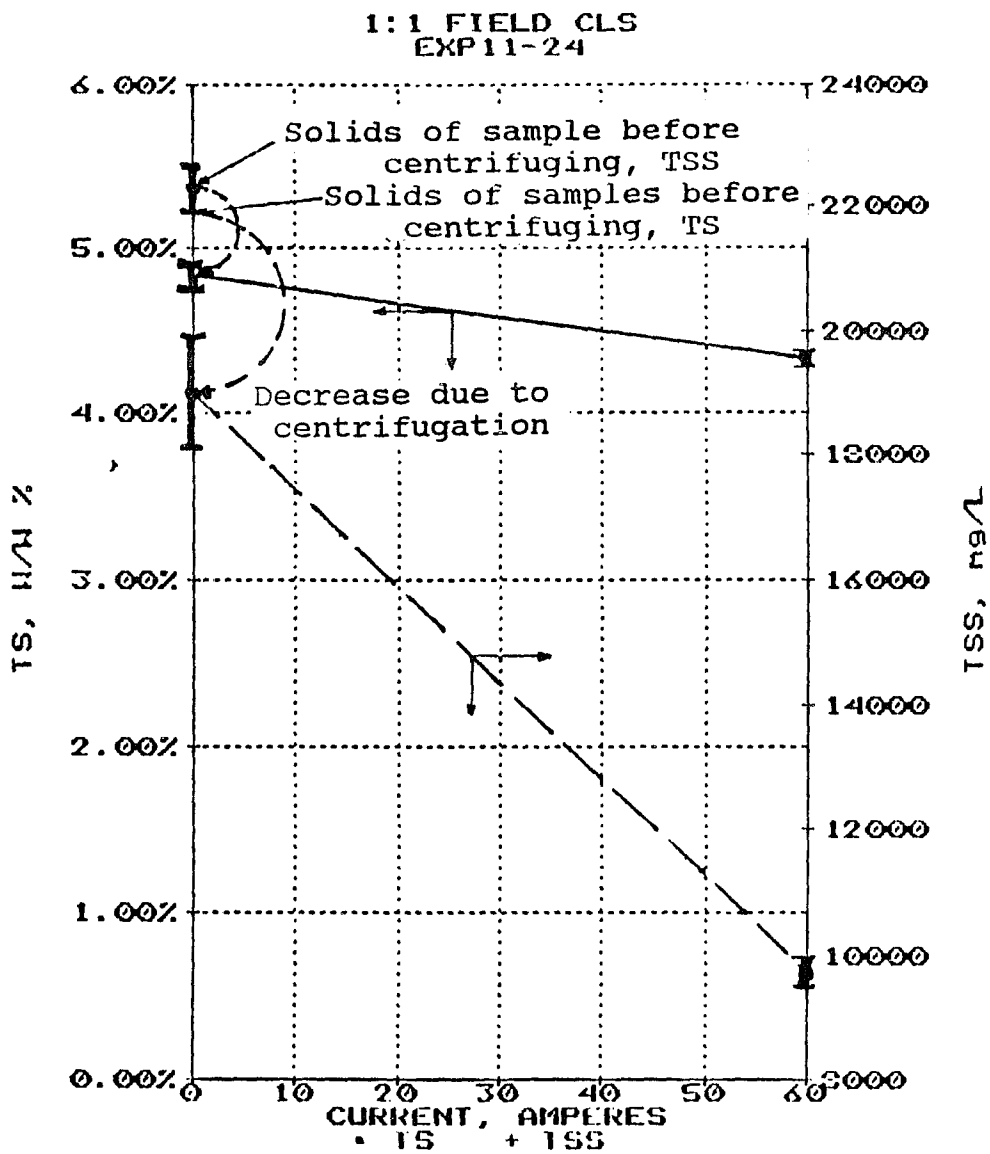

Fig. 4-19 Comparison of cake and supernatant quality of a before and after EC treatment of a 1:1 field fresh/CLS fluid

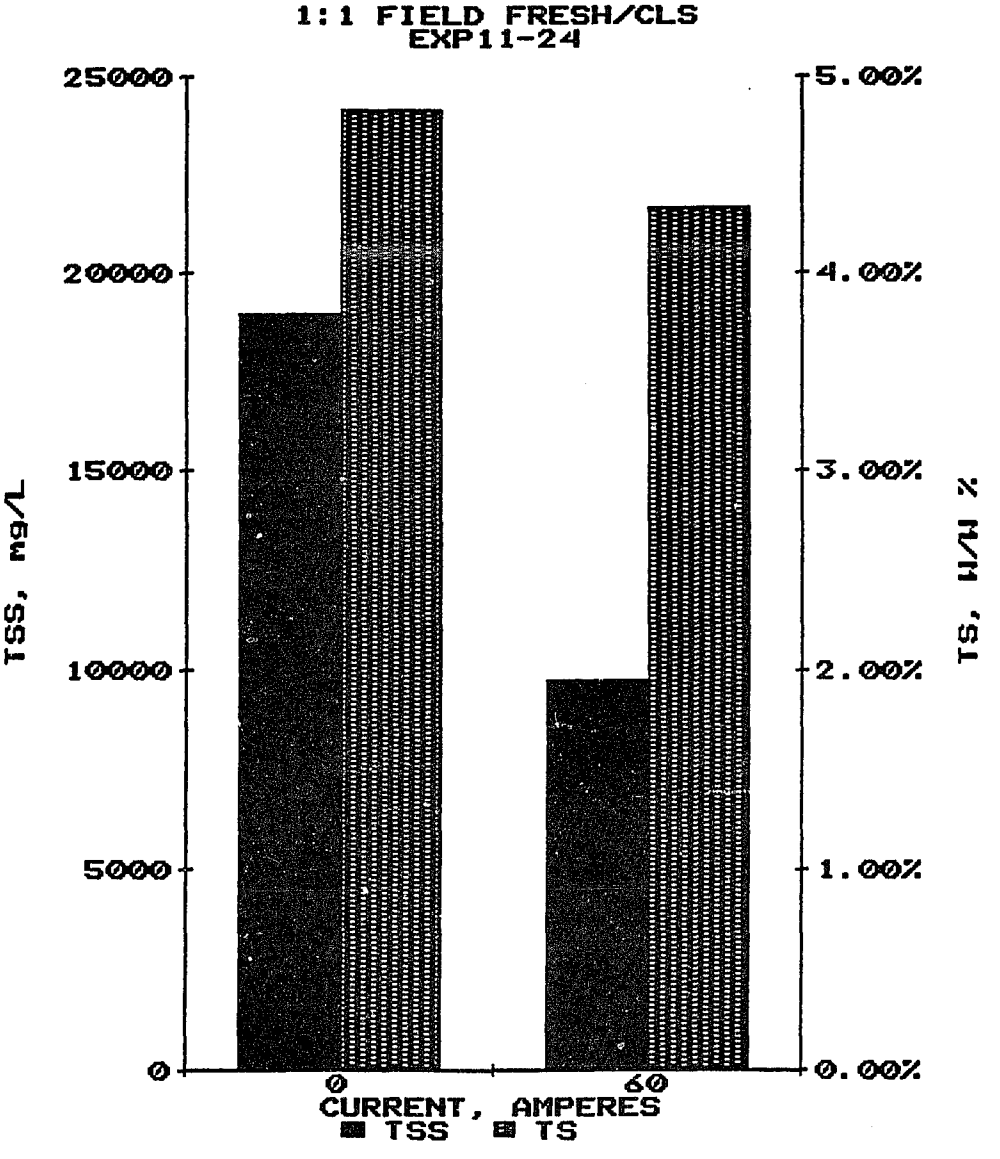

Fig. 4-20 Effect of current on supernatant quality of EC treated sample of a 1:1 field fresh/CLS fluid

The high conductivity of the 1:1 field salt/CLS meant a very large current could be applied (200 A). However, due to its high chemical stability, no significant effects were observed. The limited influence on solid/liquid separation efficiency is presented in Table 4-11. Treatment time was 2 min. CST showed a reduction with electrocoagulation treatment. TS of the fluids were evaluated at several junctures in the experimental investigation. TSS could not be meaningfully evaluated owing to the high concentration of suspended solids.

Table 4-11 Electrocoagulation treatment effect on centrifugal separation efficiency as measured by weight percent on 1:1 field salt/CLS fluid treated for 2 min.

	Mixture	Supernatant	Cake	CST
Before	19.4%	15.0%	70.4%*	1990
After	18.4%	13.6%	19.4%	1030

* The large weight percent of untreated cake of 70.4% was due to sedimentation of barite, which was present in this field sample in small quantities. This value should not be interpreted as indicative of phase segregation.

CST reflects some effect, but is not accompanied by adequate phase segregation.

The 1:1 simulated salt/polymer fluid was treated with most success as judged by supernatant quality, although cake solids content remained low (9.5% w/w). Original cake content of an untreated sample was 6.9%. Composition of the diluted mixture was previously presented in section 4.2.2.1. After electrically treating for 2 min., the samples were

centrifuged and the separation quality measured (Fig. 4-21).

The presence of electrolyte (NaCl) acted to increase conductivity so that the welding machine could output its maximum current of 225 A. Conductivity was 78,000 μmho/cm prior to dilution and 35,000 μmho/cm afterwards. The mixture was divided into five samples for treatment at 0, 60, 120, 175, and 225 A.

Above 120 A, the treatment was successful in eliminating the transition zone (Fig. 4-22). As compared with the 175 A treatment, the 225 A treatment evidenced an increase in volume percent of supernatant from 47% to 59%. From left to right, corresponding to current application increases, the transition zone decreases until it is completely absent as it becomes part of the cake. The increase of current treatment from 175 A to 225 A produces a more compactible cake. Solids content increased from 9.2% to 9.5% w/w when current was increased from 175 A to 225 A. Also of benefit is the increase in the supernatant height as current level increased. With higher current, volume of supernatant increased from 47% at 175 A to 59% at 225 A. A favorable decrease in TSS accompanies the increase in supernatant volume percent.

A relation between supernatant TSS and mixture CST (Fig. 4-23) supports the use of CST to evaluate electrocoagulation treatments. Cake dryness increased from 6.9% w/w solids for the untreated sample before centrifuging, to

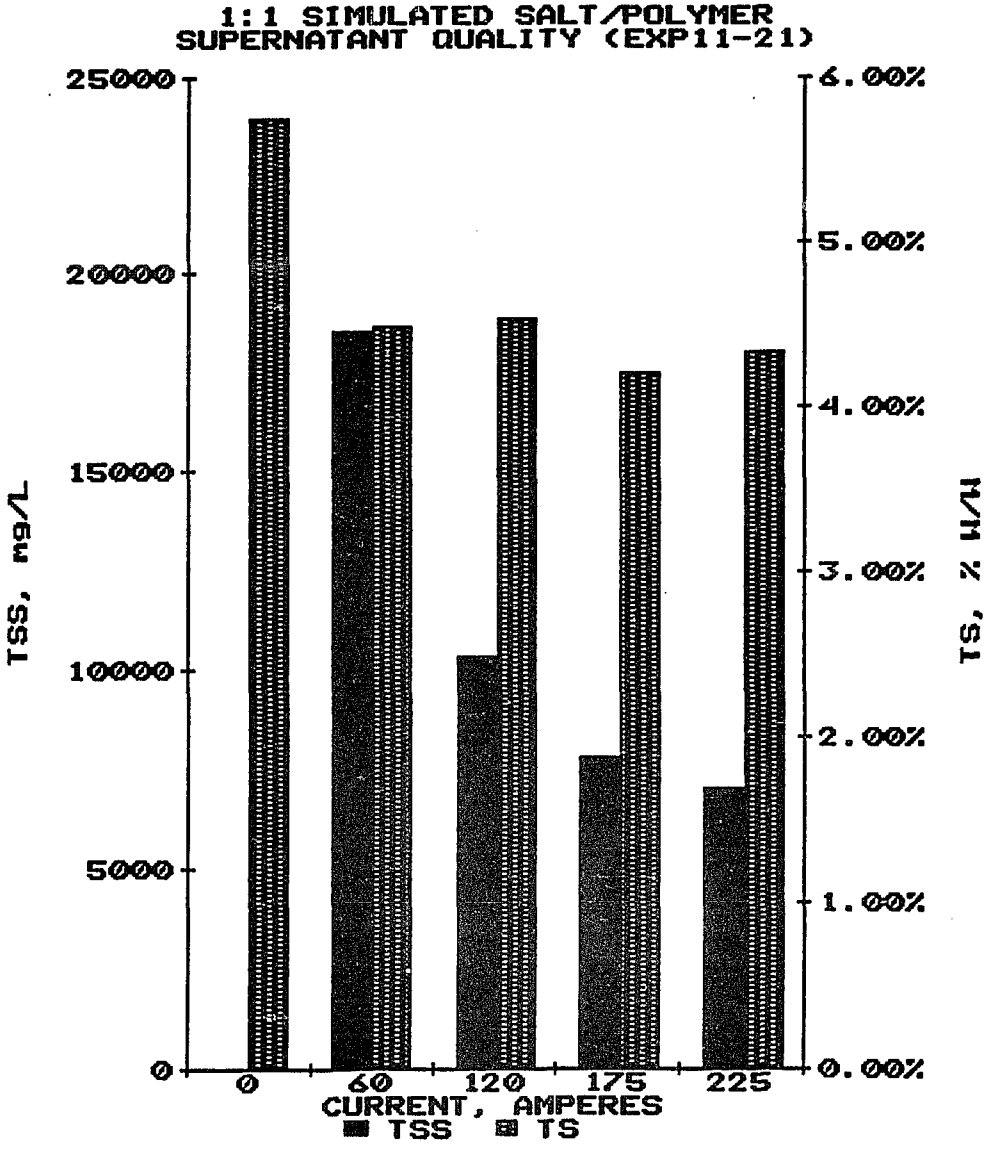

Fig. 4-21 Effect of various levels of current on the supernatant quality of a 1:1 simulated salt/polymer fluid

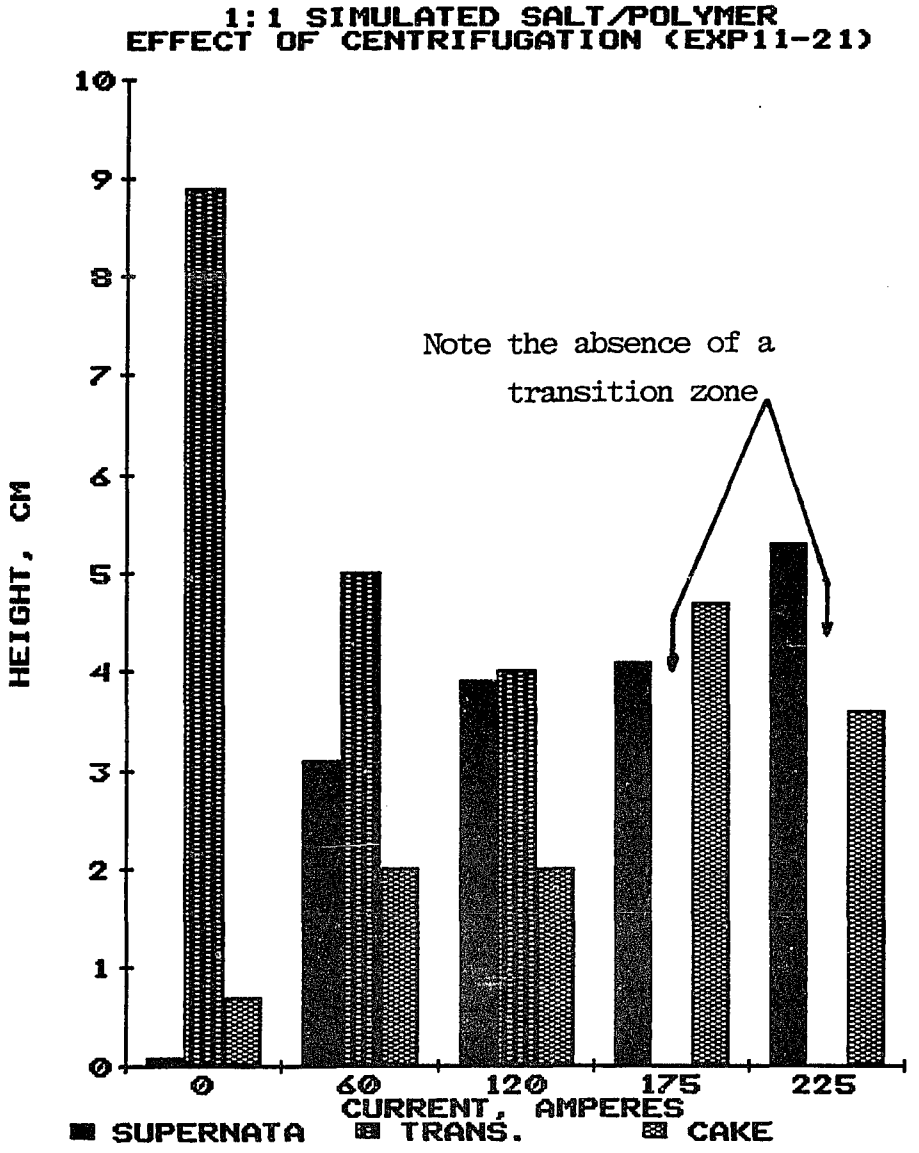

Fig. 4-22 Effect of various levels of current on the centrifuged supernatant, transition zone, and cake height of a 1:1 simulated salt/polymer fluid

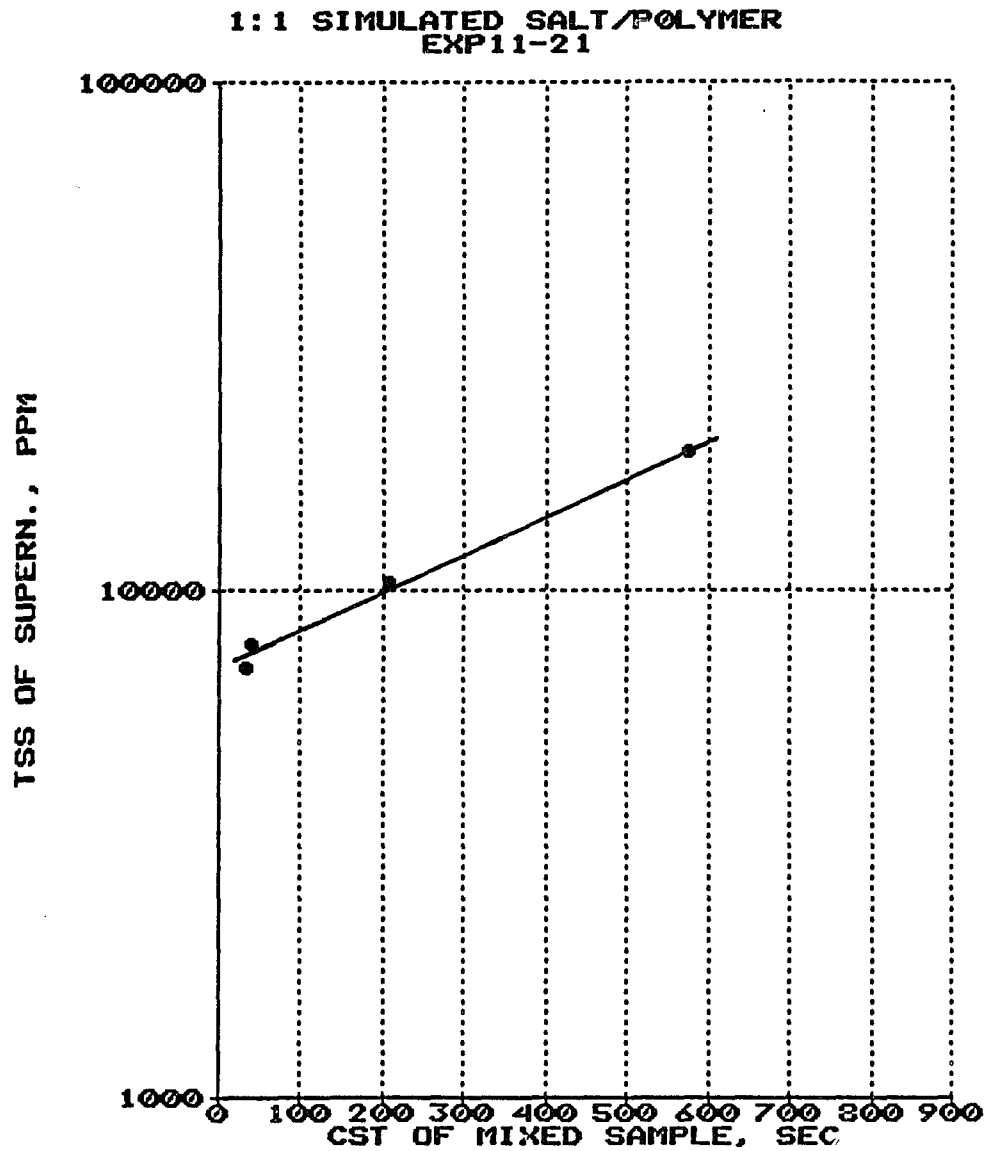

Fig. 4-23 Linear relation of log of total suspended solids to Capillary Suction Time of a 1:1 simulated salt/polymer fluid

9.5% w/w solids for the 225 A treatment. While a trend toward a drier cake is evident, it is unlikely that greater current could achieve 35% w/w solids, which was possible using chemical coagulation/flocculation in combination with centrifuging.

In summary, the most effectively treated suspension was the 1:1 simulated salt/polymer as evaluated by clarity of the supernatant. A minor hypothesis was the replacement of fraction of chemical coagulation or polymeric flocculant to reach the endpoint as a result of electrocoagulation treatment. The endpoint is a phase separation between clear water and solids.

4.3.3 Combined electrocoagulation treatment with chemical treatment

This minor objective was investigated by adding various amounts of alum coagulant to an electrically treated suspension of 4% w/w bentonite. Applied electrical energy was 880 (amps/ft^2)/(L/min) for each data point. These same levels of alum were added to an untreated suspension of the same composition. It is evident from Fig. 4-24 that electrocoagulation treatment reduced the volume of flocculant required.

The endpoint for chemical flocculation is achieved at various pH levels. Following electrocoagulation treatment, the pH was 9.1 while the untreated suspension had a pH of

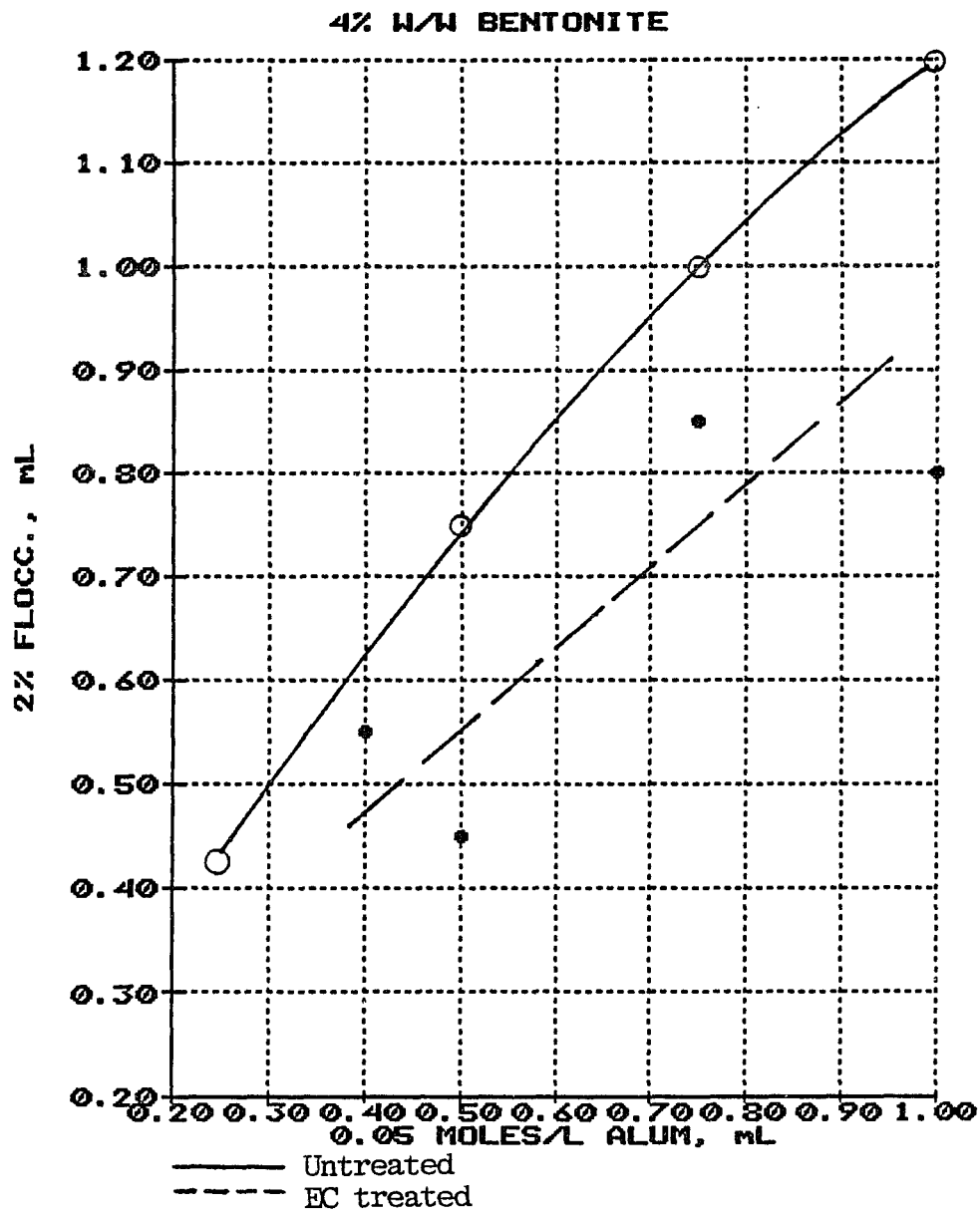

Fig. 4-24 Reduction of flocculant due to EC treatment of a 4% w/w bentonite suspension related to alum additions

8.6. In Fig. 4-25 the volume required to flocculate the suspension occurs at a lower pH for the untreated sample than is required for the electrically treated sample. This plot confirms that the pH for achieving flocculation with a polymer is relative to the particular suspension and cannot be used in an absolute sense to describe the flocculation endpoint. Therefore, electrocoagulation treatment reduces the amount of flocculant required to reach the endpoint.

Attempts at flocculating a 6% w/w bentonite suspension were unsuccessful unless first treated with a coagulant. In an alternate approach, particles adhering to the aluminum electrodes were removed and diluted 1:1. Thus, the suspension was now reduced to 3% w/w solids. The diluted suspension was treated with sufficient flocculant to reach the endpoint and was then centrifuged. The solids content of the centrifuged cake was 5.2% w/w solids, which is less than the original 6% w/w solids. Consequently, this was not thought to be a promising area of investigation.

The most readily destabilized suspension was the 1:1 simulated salt/polymer fluid. And having achieved the optimum treatment with the available equipment, the cake generated was evaluated using the methods outlined in Chapters II and III.

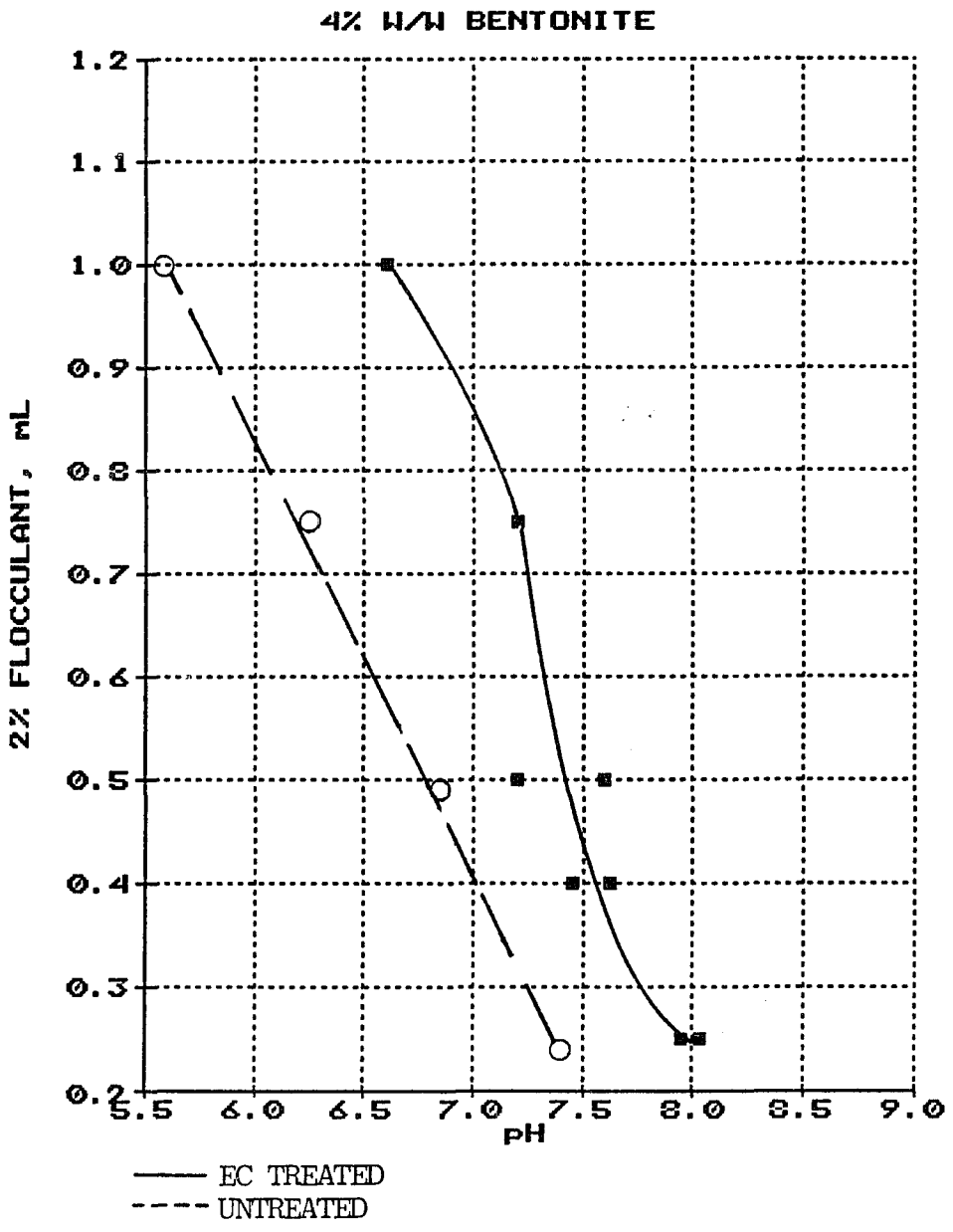

Fig. 4-25 Reduction of flocculant due to EC treatment of a 4% w/w bentonite suspension related to pH

4.3.4 Electrocoagulation effect on dewatering mechanism

This section discusses the measurement and analysis of permeability and bulk modulus which was applied to an electrically treated fluid. The selected fluid was the 1:1 simulated salt/polymer, which fluid was the one most effectively treated. As described in Chapter II, the treated suspension was placed in the centrifuge and accelerated to various rotational velocities from 300-900 rpm, noting flow rate through the compacted cake and length changes at the respective rotational velocities. The data were plotted on previously presented plots to facilitate comparisons (Fig. 4-26). In examining its permeability character against effective consolidation stress, the range of permeability matched that of the two CLS suspensions, however, much less consolidation stress was required for the change. This is due to a stronger polymer network which exists in the flocculated CLS suspensions.

An interesting similarity exits between flocculated bentonite and the electrically treated system. At the higher consolidation stress (0.4-0.9 kPa), these exhibit a similar response. However, any sensitivity which the cake exhibits is offset by the high void ratio at these same levels of consolidation stress (Fig. 4-27). High void ratio is proportional to high moisture content. Solids content was increased from 6.5% w/w to 7.5% w/w solids by centrifuging.

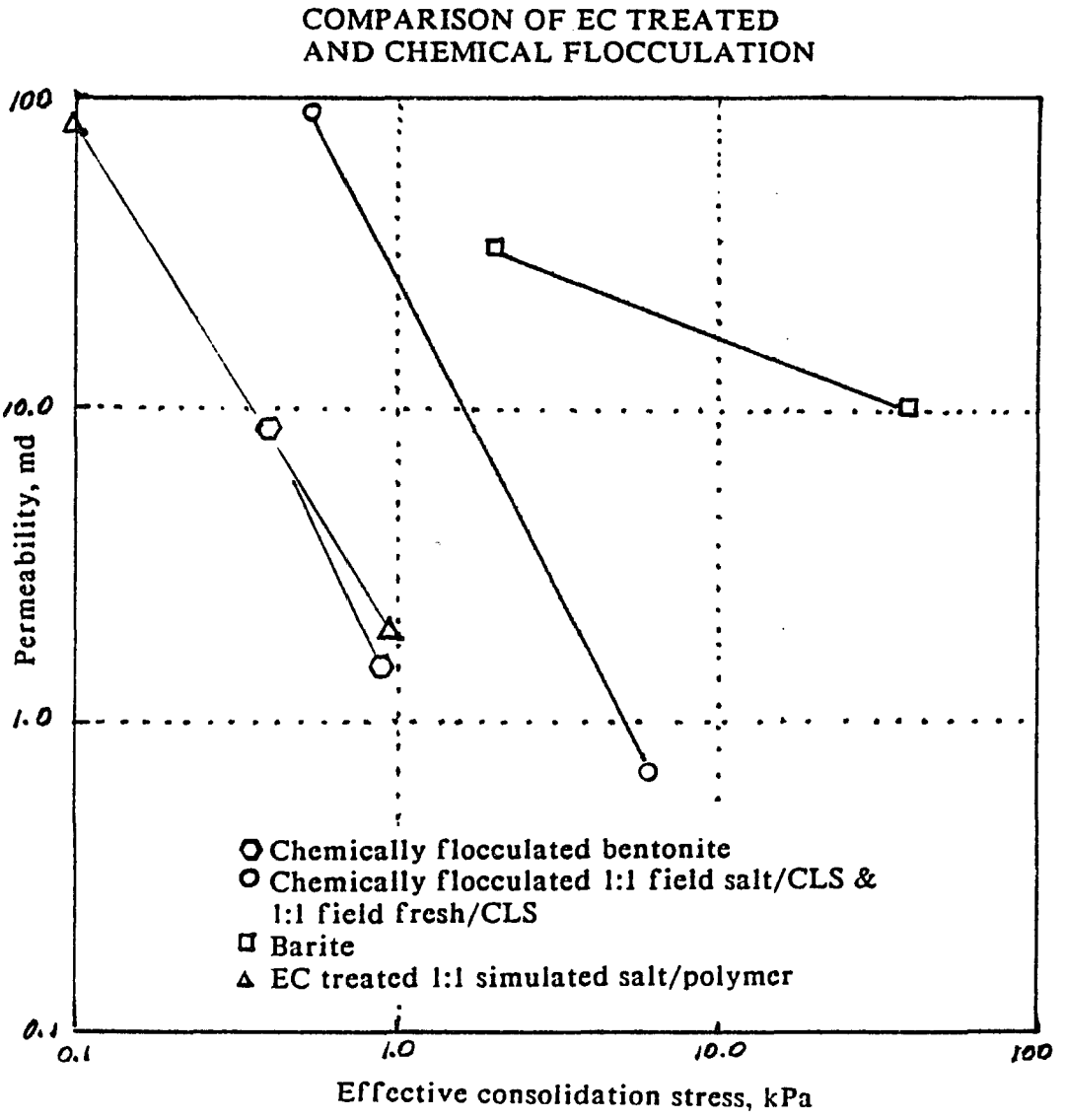

Fig. 4-26 Response of permeability vs. effective consolidation stress due to EC treatment of a 1:1 simulated salt/polymer and compared with chemical treatments

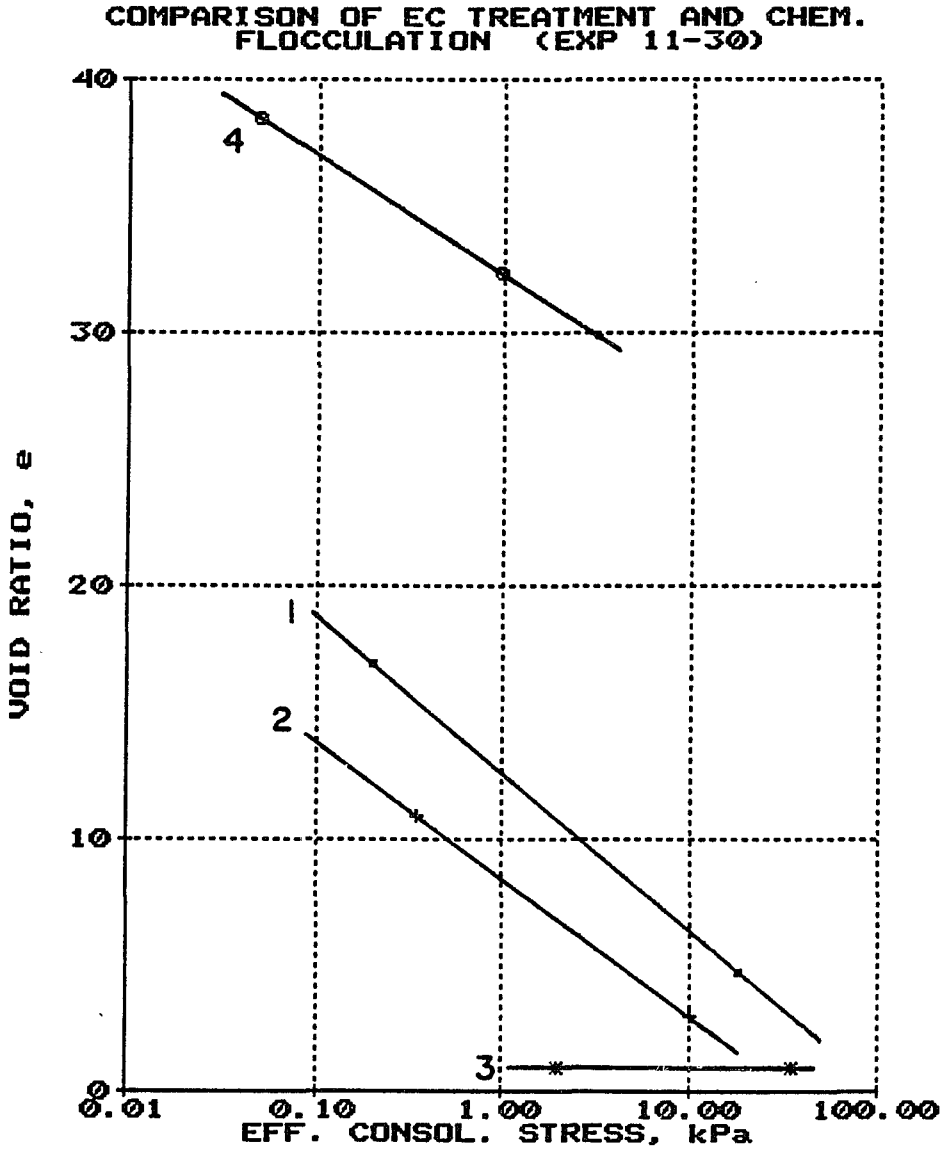

CHART LEGEND

1 CHEM. FLOCC. 1:1 FIELD FRESH/CLS
2 CHEM. FLOCC 1:1 FIELD SALT/CLS
3 BARITE
4 EC TREATED 1:1 SIMULATED SALT/POLYMER

Fig. 4-27 Response of void ratio vs. effective stress due to EC treatment of a 1:1 simulated salt/polymer and compared with chemical treatments

Therefore, it can be concluded that the content of the cake is of poor quality relative to those which are chemically flocculated. The absence of polymeric flocculants means the network is less cohesive, allowing for higher permeability, but with a cake very high in moisture.

Chapter V

Conclusions and Recommendations

In the first phase of this research, flow and mechanical properties of compressible networks were investigated. Conclusions and recommendations from this phase are:

1. The centrifuge apparatus constructed for this investigation is superior to the C-P cell in that it (a) applies centrifugal force which simulates full-scale centrifuging, (b) provides a more gentle consolidation of the delicate, sedimented network, and (c) requires that only one side be supported.

2. Two parameters are required to characterize viscoelastic networks: permeability and bulk modulus of elasticity. These two parameters can be measured simultaneously in a laboratory centrifuge.

A worthwhile extension of this study would be to combine these two properties for a specified fluid system in such a manner as to predict time to reach ultimate consolidation at a specified rotational velocity. This would enable a determination of the final, sedimented cake moisture content for a particular centrifugal force and residence time. This estimate could be used to evaluate economics associated with dewatering a particular suspension. Centrifuge speed, pre-treatment, and residence time could conceivably be optimized.

The practical application of this research would be to predict dewatering ability of a full-scale centrifuge. The procedure would be to first make permeability and modulus measurements in the laboratory. Second and using permeability data at successive speeds, a prediction could then be made for the time required to attain a specified level of compaction. This specified level would be selected based on the capability of the full-scale centrifuge. The objective would be to select both retention time and centrifuge speed in order to optimize sludge dewatering. This laboratory procedure and prediction would allow a pre-treatment and/or a particular centrifuge to be evaluated.

3. A moderate increase in centrifuge speed drastically reduces permeability of a flocculated drilling fluid.

In view of the excessive stresses applied to flocculated networks, compression-permeability data suggest that in the industrial decanting centrifuge, insufficient time is allowed for water to be expressed from the compacting cake.

A sloped inlet in the decanting centrifuge may offer some advantage by applying a gradual compression to take advantage of the high permeability initially present in a flocculated drilling fluid syspension. The sloped inlet is analogous to the sloped beach at the exit point. Greater compaction would finally be applied before the discharge point.

4. Laboratory compaction confirmed full-scale maxima

of a void ratio of four (60% w/w moisture) is the driest possible level for typical drilling fluid systems.

5. The drilling fluid system of those tested which was most difficult to dewater was the CLS fluid. One reason is due to its having a higher bulk modulus of elasticity. This property means sedimented cake moisture content will be higher.

6. A method has been presented for measuring variable cake density from top to bottom for a sedimented cake. In the one case computed, this variation was 13%.

In the second phase of the research, an alternate means for pre-treating a drilling fluid suspension was evaluated. Electrocoagulation treatment had been reported in the literature as being effective, with sufficient time, in creating a clarified water phase above the gravity sedimented cake. This treatment was attempted on drilling fluids commonly used in the petroleum industry. The objective was to replace chemical coagulation and flocculation.

Certain obstacles were encountered in applying this treatment to oilfield drilling fluids. First, drilling fluids have high solids content. Second, drilling fluid systems are chemically stable suspensions. Third, large fractions of active colloidal solids are present with relatively high surface charges. Fourth, the fluids to which electrocoagulation treatment was applied must be coagulated immediately. This is due to the limited residence time

these fluids spend in the decanting centrifuge.

If time were not a factor, electrocoagulation treatment would have merit. Two days following treatment of a 4% w/w bentonite suspension, an extremely clear supernatant was observed without centrifugation. This suggests the utility of electrically treating reserve pits. However, for the electric current levels applied here, a sufficiently rapid response was not achieved to justify replacing chemical pre-treatments with electrical treatment. Conclusions from this phase of the investigation are:

1. The CLS fluid systems, with or without salt, are unlikely candidates. Their high chemical stability was not significantly affected by electrocoagulation treatment. No improvements in separation were observed. Only slight improvement was seen in bentonite suspensions (spud mud).

2. The combination of CST, zeta potential, and centrifugal separation provided adequate means for evaluating partial success of electrocoagulation treatment of various mineral and drilling fluid suspensions.

3. The most effectively electrically treated drilling fluid was the simulated salt/polymer, which produced a clarified supernatant. However, at 225 A, its sedimented cake remained unacceptably moist.

Bibliography

Alemi, M.H., Nielsen, D.R. and Biggar, J.W. (1976):"Determining hydraulic conductivity of soil cores by centrifugation," Soil Sci. Soc. Am. J., **40**, 212.

Alexander,A.E. and Johnson, P. (1949): Colloid science, Volume I, Oxford Press, London.

Ball, R.O. (1978): Sludge dewatering, Ph.D. dissertation, Univ. of Delaware.

Baskerville, R.C. and Gale, R.S. (1968):"A simple automatic instrument for determining the filtrability of sewage sludge," Wat. Pollut. Control, **67**, 233.

Bear, J., Corapcioglu, M.Y. and Balakrishna, J. (1984):"Modeling of centrifugal filtration in unsaturated deformable porous media," Adv. Water Resources, **7**, 150.

Berry, W.F. and Justice, J.H. (1987): "Electro-Coagulation: A Process for the Future," paper presented at the 1987 Coal Preparation Meeting, Lexington, Kentucky, April 30.

Berry, W.F. (1988): Harlan Co. Mine 9-188 intercompany report, CO-AG Technology Inc., Pittsburgh.

Bingeman, J.B. and Coates, J. (1960):"Centrifugal filtration through beds of small spheres," A.I.Ch.E. Journal, **6**, 58.

Bobalek, E.G., Durst, R.E., and Yadeta, B. (1973):"A predictive model for sludge characterization useful to design and control of sludge dewatering processes in water recycle systems," Univ. of Maine - Land and Water Resources Center, Project Completion Report, U.S. DOE B-008-ME

Bockris, J. O'M. and Reddy, A.K.N. (1970): Modern Electrochemistry, Volume I -- an introduction to an interdisciplinary area, Plenum/Rosetta Ed., Plenum Pub. Corp., New York.

Bourgoyne et al., (1986): Applied Drilling Engineering, Society of Petroleum Engineers, Richardson, Texas.

Bragg, R. (1986):"The flow and filtration of non-Newtonian liquids - Part B," Filtr & Sep, **23**, No. 1, 44-47.

Branson, L. K.(1967) Introduction to electronics, Prentice-Hall, Inc., Englewood Cliffs, NJ. 594 pp.

Bray, R.P. (1989):"Amoco's aggressive compliance plan exceeds expectations in Gulf of Mexico," unpublished presentation to AADE/IADC Techn. Symposium entitled Protecting the environment through aggressive drilling fluids management, Houston, Sept. 26.

Burd, R.S. (1968):"A study of sludge handling and disposal," U.S. Dept. of Interior WP-20-4.

Buscall, R. (1982):"The elastic properties of structured dispersions: a simple centrifuge method of examination," Colloids and Surfaces, **5**, 269-283.

Carman (1937):"Fluid flow through granular beds," Trans. Inst. Chem. Engr., **15**, 150.

Chen, S.B. and Keh, H.J. (1988):"Electrophoresis in a dilute dispersion of colloidal spheres," A.I.Ch.E. Journal, **34**, 1075.

Churchwell, R.C. (1981):"Closed-loop system controls mud solids," Petroleum Engineer, Sept.

Coackley, P. and Jones, B.R.S. (1956):"Vacuum sludge filtration I," Sewage Ind. Wastes, **28**, No. 8, 963.

Coca, J., Bueno, J.L. and Sastre, H. (1982):"Electrokinetic behaviour of coal particles suspensions," J. Chemical Technology and Biotechnology, 637-642.

Coe, H.S. and Clevenger, G.H. (1916):"Methods for determining the capacities of slime-settling tanks," Trans. Am. Inst. Mining Eng., **55**, 356.

Collin, F. (1986):"Application of electrical fields to thicken and dewater sewage sludges," New Developments in Processing of Sludges and Slurries, eds. Bruce, A.M., L'Hermite, P., and Newman, P.J., Elsevier Applied Science Publishers, New York.

Comings, E.W. (1940):"Thickening calcium carbonate slurries," I&EC Funda., **32**, 663.

Corapcioglu, M.Y. and Balakrishna, M.Y. (1985):"Steady state centrifugal cake filtration," Filtr & Sep, **22**, No. 6, 381-386.

Culberton, R.L., Jr. (1986):"Test results - coagulated feed to Derrick screen at the Skyline Preparation Plant," Inter-company correspondence to J.H. Justice, CO-AG Technology, Inc., Lexington, KY, June 30.

Darcy, H.P.G.(1856): Les Fontaines Publique de La Ville De Dijon, Victor Delmont, Paris.

Davison, R.W. (1974):"Electrokinetic effects in papermaking processes," TAPPI, **57**, 85.

Dawson, R. and Annis, M.R. (1977):"Exxon tests validate total mechancial solids control," Oil & Gas J., May 30, 90-100.

Delaney, A.J. and Arcone, S.A. (1982):"Laboratory measurement of soil electric properties between 0.1 and 5 GHz," U.S. Army Corps of Engineers CRREL Report 82-10, April.

Delgado, A., Gonzalez-Caballero, F. and Bruque, J.M. (1986):"On the electrophoretic mobility and zeta potential of montmorillonite in non-aqueous media," Colloid & Polymer Sci., **264**, 435-438.

Dick, R.I. and Ewing, B.B. (1967):"The rheology of activated sludge," Journal WPCF, **39**, 543.

Dixon, D.C. (1980):"Effect of sludge funnelling in gravity thickeners," A.I.Ch.E. Journal, **26**, 471.

de Yong, J. (1974):"The treatment of flow through high porosity compressible media, in terms of a modified drag equation," paper presented at the 5th Austral. Conf. Hyd. and Fluid Mech., **2**, 210-217, Univ. of Canterbury.

Dossena, G. et al. (1988):"The AGIP experiences in treatment and disposal of wastes on deep drilling sites," paper presented at the 1988 International Conf. on Drilling Wastes, Calgary, Canada--Drilling Mud Symp., Elsevier Applied Science Publishers, New York.

Ensminger, D. (1973): Ultrasonics-the low- and high-intensity applicatins, Marcel-Dekker, Inc., New York.

Everett, D.H. (1988): Basic principles of colloid science, Royal Society of Chemistry, London, ISBN 0-85186-443-0.

Farrell, C., and Gardner-Clayson,T. (1990):"Oilfield process stream treatment by means of alternating current electrocoagulation," paper presented at the 1990 American Filtration Society National Fall Meeting, Environmental and Productivity Merits of Separation in Petroleum Engineering, Baton Rouge, Oct. 29-30.

Fitch, B. (1971):"Batch tests predict thickener performance," Chemical Engineering, **23**, 83-88.

Gaudin, A.M., Fuerstenau, M.C. and Mitchell, S.R. (1959):"Effect of pulp depth and initial pulp density in batch thickening," Trans. AIME, **11**, 613-616.

Gaudin, A.M. and Fuerstenau, M.C. (1962):"Experimental and mathematical model of thickening," Trans. Amer. Inst. Mining Eng, **223**, 122-129.

Good, P.C. and Fursman, O.C. (1968):"Centrifugal dewatering of Jamaican Red Mud," U.S. Bureau of Mines RI 7140.

Grace, H.P. (1953):"Resistance and compressibility of filter cakes," Chem. Eng. Progr., **49**, No. 6.

Gray, G.R. and Darley, H.C.H. (1980): Composition and properties of oil well Drilling Fluids, 4th ed., Gulf Pub. Co., Houston.

Gray, W.A. (1968): The packing of solid particles, Chapman & Hall, London.

Gregory, J. (1981):"Flocculation in laminar tube flow," Chem. Eng., **36**, 1789-1794.

Gregory, J. and DeMoor, A.E.L. (1983):"Filtrability of polymer-flocculated suspensions," Polymer Adsorption and Dispersion Stability, ACS Symp. Ser., **240**, 445-458.

Griffin, J.M., Hayatdavoudi, A., and Ghalambor, A. (1986): "Design of chemically balanced polymer drilling fluid leads to a reduction in clay destabilization," SPE-Drilling Engineering, Feb., 31-42.

Hanson, P.M. et al. (1986):"A review of mud and cuttings disposal for offshore and land based operations," paper presented at the Natl. Conf. on Drilling Muds , Univ. of Okla. Env. & Ground Water Research Institute, Norman, May 29-30.

Happel, J. and Brenner, H. (1973): Low Reynolds number hydrodynamics, 2nd ed., Nordhoff International, Layden, 553 pp.

Harder, B. (1988):"An investigation of alternate containment of drilling waste for Louisiana wetlands areas," unpublished report, Louisiana Geological Survey -- Energy and Mineral Resources Section, June 15.

Harris, C.C., Somasundaran, P. and Jensen, R.R. (1975):"Sedimentation of compressible materials-analysis of batch sedimentation curve," Powder Technology, **11**, 75-84.

Harvey, M.A., Bridger, K. and Tiller, F.M. (1988):"Apparatus for studying incompressible and moderately compressible cake filtration," Filtr & Sep, **25**, No. 1, 21-29.

Hatfield, W.D. (1938):"Viscosity of pseudo-plastic properties of sewage sludge," Sewage Works Journal, **10**, 3-25.

Hermia, J. (1980):"Pre- and post-treatment techniques for industrial separation," Filtr & Sep, **17**, No. 4, 362-370.

Higashitani, K., Miyafusa, S., Matsuda T. and Matsuno, Y, (1980):"Axial change of total particle concentration in Poiseuille Flow," J. Colloid Interface Sci, **77**, 21-28.

Hinds, A., Liao, A. and Lowell, J.L. (1986):"Diagnostic tests for the treatment of reserve pits," paper presented at the Natl. Conf. on Drilling Muds , Univ. of Okla. Env. & Ground Water Research Institute, Norman, May 29-30.

Hoekstra, P. and O'Brien, H. W. (1969):"The dielectric properites of clay suspensions in the frequency range from 50 Hz to 20 KHz," U.S. Corps of Engineers CRREL Report 266, August.

Hoekstra, P. and Delaney, A. (1974):"Dielectric properties of soils at UHF and microwave frequencies," J. Geophysical Research, **79**, No. 11, 1699-1708.

Holtz, R.D. and Kovacs, W.D.(1981): An introduction to geotechnical engineering, Prentice-Hall, Inc., Englewood Cliffs, New Jersey.

Horgan, J.D. and Edwards, D.L. (1961):"Forces in dielectric fluids," J. Appl. Phys., **32**, No. 9, 1784.

Hughes, M.A. (1981):"Coagulation and flocculation," Ch. 4, Part I, Svarovsky, L. (ed.), Solid-liquid separation, 2nd ed., Butterworths, Boston.

Ikeda, S. (973):"Dynamic viscoelasticity of coating films," Progress in Organic Coatings, **1**, 205-248.

Jensen, J.N. and van Benschoten, J.E. (1989): "Electrocoagulation for hazardous waste management: Fundamental aspects, applications and economic feasibility," proposal submitted to the State of New York Environmental Research Management Group., SUNY, Buffalo, NY, Department of Civil Engineering.

Jones, M., et al. (1983):"Efficiency of a single-stage cuttings washer with a mineral oil invert emulsion and its environmental significance," paper SPE 12121 presented at the 1983 Annual Meeting, San Francisco, October.

Jordan, C E, Sullivan, G.V.. Davis, B.E. and Weaver, C.P. (1980):"A Continuous Dielectric Separator for Mineral Beneficiation," U.S. Bureau of Mines, RI 8437.

Justice, J.H. (1988): In house laboratory reports, CO-AG Technolgy, Inc., Lexington, Kentucky.

Khatib, Z. and Howell, J.A. (1979):"Batch and continuous sedimentation behaviour of flocculated china clay slurries," Trans. I. Chem. Eng., **57**, 170.

Kim, Y.K. and Kingsbury, H.B. (1979):"Dynamic characterization of poroelastic materials," Exp. Mech., **19**, 252-258.

Kos, P. (1977):"Fundamentals of gravity thickening," Chem. Eng. Progr., **73**, 99.

Kynch, G.J. (1952):"A theory of sedimentation," Trans. Faraday Soc., **48**, 166.

La Mer, V.K. (1964), J. Colloid Science, **19**, 291.

Lavrov, I.S., Ponomareva, V.N. and Smirnov, O.V. (1975): "Coagulation of suspensions of refractory materials in an electric field," Trans. Zhurnal Prikladnoi Khimii, **48**, No. 8, 1740-1745, Aug., Plenum Pub. Corp., New York.

Lockyear, C.F. and White, M.J.D. (1980):"A laboratory centrifuge test for simulating gravity thickeners," paper presented at the Inst. of Chem. Eng. Conf. on Solids Sep. Processes, Dublin, April.

Lummus, J.L. and Azar, J.J. (1986): Drilling fluids optimization--a practical field approach, Pennwell Pub. Co., Tusla.

Malachosky, E., Sanders, R. and McAuley, L. (1989):"The impact of use of dewatering technology on the cost of drilling waste disposal," SPE 19528 paper presented at the 1989 Annual Meeting of the Society of Petroleum Engineers, San Antonio, Texas.

Maljian, M.V. and Howell, J.A. (1978):"Dynamic response of a continuous thickener to overloading and underloading," Trans. I. Chem. E., **56**, 56-61.

Manins, P.C. and Roberts, B.W. (1975):"Compression of an elastoporous medium", Int. J. Non-liner Mech., **13**, 75-93.

Michaels, A.S. and Bolger, J.C. (1962):"Settling rates and sediment volumes of flocculated kaolin suspensions," Ind. & Eng. Chem. Funda. **1**, No. 1, 24-33.

Moeglich, Karl (1979):"Water Purification Method and Apparatus," U.S. Patent No. 4,176,038.

Morland, L.W. (1975):"Effective stress in mixing theory," Archives of Mechanics, **27**, 883-887.

Moudgil, B.M. (1984):"Centrifuge study of use of sand and flocculants in consolidation of phosphatic clays," Reagents in the Mineral Industry, Jones and Oblatt (eds.), IMM, 95-99.

Moulik, S.P., Cooper, F.C. and Bier, M. (1967):"Forced-flow electrophoretic filtration of clay suspensions - filtration in an electric field," J. Coll. Int. Sci., **74**, 427-432.

Muralidhara, H.S. (1986): Advances in Solid-Liquid Separation, Battelle Press, Columbus.

Neidhardt, D (1985):"Rig-site system allows water reuse, cuts cleanup costs," Oil & Gas J., March 4.

Nickeson, F. H. (1982):"Electrical coagulation: a new process for prep plant water treament," Coal Mining & Processing, Sept.

NL Baroid (1975): Apparatus and Procedure for the Field Testing of Drilling Muds, Section 900, Bariod Division, Houston.

Nordquist, D.G. and Faucher, M.S. (1988):"A case history of dewatering and recycling sump drilling mud on 141 wells in the Midway Sunset Field, California," SPE 17246 paper presented at the International Association of Drilling Contractors/Society of Petroleum Engineers Drilling Conference - Proceedings, Feb. 28-March 2.

Oldshue, J.Y. (1983): Scale-up, Chemical Engineering, McGraw-Hill Publications Co., New York.

Outmans, H.D. (1963):"Mechanics of static and dynamic filtration in the borehole," Soc. of Pet. Eng. J., (Sept.) 236-244.

Pierce, E.T. (1959):"Effects of high electric fields on dielectric liquids," J. Appl. Phys. **30**, No. 3, 445-446.

Poiseuille, J.L. (1840):"Experimental researches on the movement of liquids in tubes of very small diameter," Compte Rendus, **11**, 961.

Profco (1988): Mud Lines, **2**, No. 3, Fall, PROFCO company published newsletter.

Purchas, D.B. and Wakeman, R.J. eds., (1986): Solid/liquid separation equipment scale-up, 2nd ed., Uplands Press Ltd, London.

Records, F.A. (1974):"The continuous scroll discharge decanting centrifuge," Chem. Eng., 41-47.

Richardson, J.F. and Zaki, W.W. (1954):"Sedimentation and fluidisation-Part I," Trans. Institution of Chem. Eng., **32**, 35.

Robinson, R.A. and Stokes, R.H. (1955): Electrolyte solutions - the measurement and interpretation of conductance, chemical potential and diffusion is solutions of simple electrolytes, Butterworths Scientific Publications, London.

Rosenholtz, J.L. and Smith, D.T. (1936):"The dielectric constant of mineral powders," The American Mineralogist, 115-120.

Ross, S. and Morrison, I.D. (1988): Colloidal systems and interfaces, John Wiley & Sons, New York.

Rushton, A. (1986):"Filtration of non-Newtonian fluids - Part A," Filtr & Sep, **23**, No 1, 46-43.

Ruth, B.F., Montillon, G.H. and Montonna, R.E. (1933): "Studies in filtration - II. Fundamental axiom of constant-pressure filtration," Ind. and Eng. Chem., 153.

Ruth, B.F. (1935):"Studies in filtration - III. Derivation of general filtration equations," Ind. and Eng. Chem., 708.

Ruth, B.F. (1946):"Correlating filtration theory with industrial practice," Ind. and Eng. Chem., 564.

Ryan, P. E., Stanczyk, T.F. and Parekh, B.K. (1989): "Solid/liquid separation using alternating current electrocoagulation" paper presented at the Battelle International Symposium on Solid/Liquid Separations, Columbus, OH., Dec. 5-7.

Sanders, J. (1989):"Minimized hauloff while drilling in a zero discharge area," SPE 19529 paper presented at the 1989 Annual Meeting of the Society of Petroleum Engineers, San Antonio, Texas.

Scheidegger, A.E. (1960): Physics of flow through porous media, University of Toronto, Toronto.

Scheiner, B.J., Smelley, A.G. and Brooks, D.R. (1982): "Large-scale dewatering of phosphatic clay waste from central Florida," U.S. Bureau of Mines, RI 8611.

Schlumberger (1970): Log Interpretation Charts, p. Gen-9, Schlumberger Limited, Houston.

Schumann, R. (1940): Sc.D. thesis, Department of Metallurgy, MIT.

Schwan, H.P., Schwarz, G., Maczuk, J. and Pauly,H. (1962): "On the low-frequency dielectric dispersion of colloidal particles in electrolyte solution," J. Phys. Chem., **66**, 2626-2635.

Schwarz, G. (1962):"A theory of the low-frequency dielectric dispersion of colloidal particles in electrolyte solution," J. Phys. Chem., **66**, 2636.

Scott, K.J. (1968):"Thickening of calcium carbonate slurries," Ind. & Eng. Chem. Funda., **7**, 484-583.

Scott, K.J. (1968):"Theory of thickening - factors affecting settling rate of solids in flocculated pulps," Trans. Inst. Mining Met., **77**, 85-97.

Scott, P.P. (1962): U.S. Patent 3,070,543.

Shannon, P.T., Dehaas, R.D., Stroupe, E.P. and Tory, E.M. (1964):"Batch and continuous thickening," Ind. & Eng. Chem. Funda., **3**, 250.

Shirato, M., Kato, H., Kobayashi, K., and Sakazaki, H. (1970):"Analysis of settling of thick slurries due to consolidation," J. Chem Eng (Japan), **3**, 98.

Shirato, M., Murase, T., Negawa, M. and Senda, T. (1970):"Fundamental studies of expression under variable pressure," J. Chem. Eng. (Japan), **3**, 105.

Shirato, M., Iritani, E., and Nakatsuka, S. (1987):"Filter cake dewatering by permeation of non-Newtonian fluids and by use of difficult-to-filter slurries," Filtr. and Sep., **24**, No. 2, 119-120.

Snyder, G.A. and Gregory, M.J. (1979):"Electrocoagulation of coal preparation plant waters," paper presented at the SME-AIME Fall Meeting and Exhibit, Tucson, AZ, Oct. 17-19.

Somasundaran, P., Chia, Y.H. and Gorelik, R. (1984):"Adsorption of polyacrylamides on kaolinite and its flocculation and stabilization," Polymer Adsorption and Dispersion Stability, Goddard & Vincent (eds.), ACS Symp. Series, based on 186th Meeting, Washington, D.C., August 28-September 2, 1983.

Standard Methods for the examination of water and wastewater, (1985): 16th ed., American Public Health Assoc., Washington, D.C.

Svarovsky, L. (1981): Solid-liquid separation, 2nd ed., Butterworths, Boston.

Swanick, J.D. and Davidson, M.F. (1961):"Determination of specific resistance to filtration," Wat. Waste Treat. J., **8**, 386.

Terichow, O. and May, A. (1973):"Electrophoresis and coagulation studies of some Florida phosphate slimes," U.S. Bureau of Mines, RI 7816.

Thomas, A.W. (1934): Colloid chemistry, McGraw-Hill Book Company, Inc., New York.

Thurber, N.E. (1988):"Decanting centrifuge performance study," M.S. thesis, U. of Tulsa.

Tierny, J.W. and Chiang, S. (1986):"Application of network models to filtration and dewatering," Advances in Solid-Liquid Separation, H.S. Muralidhara (ed.), Battelle Press, Columbus, pp. 141-164.

Tiller, F.M.(ed.) (1975): Theory and Practice of Solid-Liquid Separation, 2nd ed., Chemical Engineering Department, University of Houston.

Tiller, F.M. (1981):"Revision of Kynch sedimentation theory," A.I.Ch.E. Journal, **27**, 823.

Tiller, F.M. and Khatib, Z. (1984):"The theory of sediment volumes of compressible, particulate structures," J. of Coll. and Inter. Sci., **100**, No. 1, 55-67.

Tiller, F.M., Yeh, C.S., and Tsai, C.D. and Chen, W. (1987):"Generalised approach to thickening, filtration and centrifugation," Filtr. and Sep., **24**, No. 2, 121-126.

Tiller, F.M., Hsyung, N.B., and Tsai, G. (1989):"Centrifugal filtration of compressible cakes," presented at the AFS Meeting - Advances in Filtration and Separation Technology, Volume I, Filtration and Separation in Oil and Gas Drilling and Production Operations, American Filtration Society, Gulf Pub. Co., Houston.

Tory, E.M. and Shannon, P.T. (1965):"Reappraisal of the concept of settling in compression," Ind. & Eng. Chem. Funda., **49**, 194.

Turner, J.P.S., and Glasser, D. (1976):"Continuous thickening in a pilot plant," I. and EC. Funda., **15**, 23-30.

U.S. EPA (1987):"Management of wastes from the exploration, development, and production oif crude oil, natural gas, and geothermal energy--executive summaries," report to Congress, Washington, D.C. (Dec.) 27.

van Brakel, J. (1987):"Continuous pressure filtration of coal and prediction of cake permeability," Filtr. and Sep., **24**, No. 4, 268-271.

Veltkamp, A.G. and Jurg, J.W.:(1988):"Treatment of drilling wastes -- a Dutch case history," paper presented at the 1988 International Conf. on Drilling Wastes, Calgary, Canada -- Drilling Mud Symp., Elsevier Applied Science Publishers, New York.

Visilind, P.A. (1968):"The influence of stirring in the thickening of biological sludge," Ph.D. dissertaion, U. of N. Carolina.

Visilind, P.A. (1974): Treatment and Disposal of Wastewater Sludges, Ann Arbor Science, Ann Arbor, Michigan, 236 pp.

Visilind, P.A. (1977):"Characterizing sludge for centrifugal dewatering," Filtr. and Sep., **14**. No. 2, 115-117.

Wakeman, R.J. (1978):"Numerical integration of the differential equation describing the formation of and the flow in compressible filter cakes," Trans. I. Chem. Eng., **56**, 258.

Wakeman, R.J. (1982):"Effects of solids concentration and pH on electrofiltration," Filtr. and Sep., **19**, No. 4, 316-319.

Wascom, C. (1986):"Oilfield pit regulations. A first for the Louisiana Oil and Gas Industry," Proc. of a Natl. Conf. on Drilling Muds held May 29-30, Univ. of Okla. Env. & Ground Water Research Institute.

Webb, W. E. and Church, R.H. (1986):"Dielectric application of microwave frequency of minerals," U.S. Bureau of Mines, RI 9035.

Wentz, C.A., Jr. and Shiver, C.M. (1983):"Cleanup of oilfield wastes in an environmentally acceptable manner," IADC/SPE Paper No. 11402 presented at the IADC/SPE 1983 Drilling Conference held in New Orleans, Feb. 20-23.

Willus, C.A. (1977):"Problems in adapting gravity theory in predicting centrifugal sedimentation performance," Conf. on Theory, Practice, and Process Princ. for Centrifugal Separations, Engr. Found. Conf., Asilomar, CA.

Wojtanowicz, A. (1988):"Modern solids control: a centrifuge dewatering-process study," SPE - Drilling Engineering, Sept.

Wojtanowicz, A. et al. (1989):"Statistical assessment and sampling of drilling fluid reserve pits," SPE - Drilling Engineering, June.

Wojtanowicz, A. and Griffin, J.M. (1989):"Drilling fluid dewatering: economic evaluation with case history", paper SPE 20292, unpublished, Society of Petroleum Engineers, Richardson, Texas, 35 pp.

Zeitsch, K. (1978):"Theory of centrifugal drainage," presented at the Intern. Symp. on Liquid-Solid Filtration, Antwerp, Belgium, June 6-7.

Zukoski, C.F. and Saville, D.A. (1985):"An experimental test of electrokinetic theory using measurements of electrophoretic mobility and electrical conductivity," J. Coll. and Inter. Sci., **107**, No. 2, 322.

Zukoski, C.F. and Saville, D.A. (1987):"Electrokinetic properties of particles in concentrated suspensions," J. of Coll. and Inter. Sci., **115**, No. 2, 422-436.

Appendix A

Derivation of hydraulic or neutral stress as applied to a centrifugal field

From

$$P=\int \rho a\,dr \qquad \text{A-1}$$

where P = hydraulic pressure

$\rho = \rho_w$ = density of water

r = radius from axis of rotation

ω = angular velocity

$a = \omega^2 r$, neglecting gravity in the z direction

Rewriting,

$$P=\int_{R_L}^{R_b} \rho_w \omega^2 r\,dr \qquad \text{A-2}$$

The limits of integration are the top of the liquid surface (R_L) and the outer radius of the cake bottom (R_b) (Chapter II).

$$P=\int_{R_L}^{R_b} \rho_w \omega^2 r\,dr \qquad \text{A-3}$$

$$P=\frac{1}{2}\rho_w \omega^2 r^2 \Big]_{R_L}^{R_b}=\frac{1}{2}\rho_w \omega^2 (R_b^2-R_L^2) \qquad \text{A-4}$$

in consistent units. Expressed in atmospheres for use in Darcy's law, and ω = N [rpm]

$$P=5.585(10)^{-9} N^2 (R_b^2-R_L^2), atm \qquad \text{A-5}$$

Appendix B

Derivation of permeability measurement in a centrifugal field

Rearrangement of Darcy's law, linear flow case from

$$q = \frac{kA\,dP}{\mu\,dL} \qquad \text{B-1}$$

gives

$$k = \frac{q\mu\,dL}{A\,dP} \qquad \text{B-2}$$

Substituting for q, dL, dP (for $P_1 - P_2 = P_2$ when $P_1 = 0$)

$$q = \frac{dV}{dt} = \frac{A\,dR_L}{dt} \qquad \text{B-3}$$

$$-dP = P_2 = u = \frac{1}{2}\rho_w\omega^2[R_b^2 - R_L^2] \qquad \text{B-4}$$

$$dL = H_e \qquad \text{B-5}$$

Combining gives,

$$k = \frac{-A\dfrac{dR_L}{dt}}{A\dfrac{1}{2}\rho_w\omega^2[R_b^2 - R_L^2]}\,\mu H_e \qquad \text{B-6}$$

Separating variables and setting up the integration,

$$\int \frac{dR_L}{[R_b^2 - R_L^2]} = \int \frac{k\rho_w\omega^2 dt}{2\mu H_e} \qquad \text{B-7}$$

For $R_b > R_L$

$$\ln\left(\frac{R_b + R_L}{R_b - R_L}\right) = \frac{k\rho_w\omega^2 R_b t}{\mu H_e} + C_1 \qquad \text{B-8}$$

Appendix B (cont.)

Defining a function as Function R

$$R = \left(\frac{R_b + R_L}{R_b - R_L}\right) \qquad \text{B-9}$$

and converting to logarithm base 10

$$\log R = \frac{k\rho_w \omega^2 R_b}{\mu H_e} t + \frac{C_1}{2.303} \qquad \text{B-10}$$

Therefore, a plot of Function R against time will provide a slope (m) equivalent to the coefficient of t.

For a straight line slope, a unique value of k can be obtained for each set of constant conditions: ω, H_e, R_b, ρ_w, and μ with C_1 being inconsequential.

Rearranging to obtain permeability from slope (m)

$$k = \frac{2.303 \mu H_e}{R_b \rho_w \omega^2} m \qquad \text{B-11}$$

in consistent units. For millidarcies as used most commonly for data presentation and for N [rpm] replacing ω [sec^{-1}]

$$k = \frac{2.303 \mu H_e}{2 R_b 5.584 (10)^{-9} N^2} m * 1000 \, [md] \qquad \text{B-12}$$

Appendix C

Derivation of effective consolidation stress in a centrifugal field

The definition of effective consolidation stress (σ_v') is (Holtz and Kovacs, 1981, p. 213)

$$\sigma_v' = \sigma_{tot} - P \qquad \text{C-1}$$

where σ_{tot} = total normal stress

P = hydrostatic or neutral stress

Total normal stress can be expressed as

$$\sigma_{tot} = \int_0^h \rho_{sat} a \, dr \qquad \text{C-2}$$

where h = height of the saturated suspension, cm

ρ_{sat} = density of the saturated, sedimented network, g/cm^3

$a = \omega^2 r$ = acceleration experienced by the particles in the centrifugal field, $rad^2/(sec^2\text{-}cm)$

dr = the differential radial thickness normal to the height, cm

Total stress is the sum of the stress due to the liquid phase above the sedimented cake and the stress due to the saturated suspension. In a horizontal centrifugal field, gravity can be neglected due to its insignificant effect relative to the effect of the centrifugal field. Acceleration is $\omega^2 r$. The limits for the integration to compute σ_{tot} are from the air/liquid interface (R_L) to the top of the

cake (inner radius), R_c. For the sedimented cake, the limits of integration are from the radius, R_c, to the cake bottom (outer radius), R_b.

Therefore, the sum of the two terms comprising σ_{tot} can be written as

$$\sigma_{tot} = \int_{R_c}^{R_b} \rho_{sat}\, \omega^2\, r\, dr + \int_{R_L}^{R_c} \rho_w\, \omega^2\, r\, dr \qquad \text{C-3}$$

The neutral stress is due to the hydrostatic pressure of the liquid phase. It can be divided between the radii for convenience and written as two integrals,

$$P = \int_{R_L}^{R_c} \rho_w\, \omega^2\, r\, dr + \int_{R_c}^{R_b} \rho_w\, \omega^2\, r\, dr \qquad \text{C-4}$$

Subtracting u from σ_{tot} to obtain σ_v' yields

$$\sigma_v' = \int_{R_c}^{R_b} \rho_{sat}\, \omega^2\, r\, dr - \int_{R_c}^{R_b} \rho_w\, \omega^2\, r\, dr \qquad \text{C-5}$$

$$= (\rho_{sat} - \rho_w)\, \omega^2 \int_{R_c}^{R_b} r\, dr \qquad \text{C-6}$$

$$= \frac{1}{2}\, (\rho_{sat} - \rho_w)\, \omega^2\, [R_b^2 - R_c^2]\, \frac{g}{\text{sec-}cm^2} \qquad \text{C-7}$$

$$= \frac{1}{2}\, (\rho_{sat} - \rho_w)\, \omega^2\, [R_b^2 - R_c^2] * 0.0001\ kPa \qquad \text{C-8}$$

Appendix D

Routinely tested mud properties

Table D-1 Routine test of mud properties for 1:1 simulated spud mud with caustic soda

		BEFORE	AFTER
Treatment	[amperes]	0	35
Conductivity	[μmho/cm]	850	1100
Zeta Potential	[mV]	-30	-20
CST	[sec]	111	50
Centrifugal Cake Solids Content	[% w/w]	N/A	6.7
Weight	[lbm/gal]	8.5	8.5
Plastic Viscosity	[cp]	6	4
Yield Point	[lb/100 ft^2]	3	3
Gel Strength (10 sec, 10 min)	[lb/100 ft^2]	2/2	1/1
Filtrate	[cm^3/30 min]	34	21.5
Cake Thickness	[32nds of an inch]	3/	2/
Solids	[% w/w]	3.37	2.56
Methylene Blue Cap.	[cm^3/cm^3 mud]	21	22
pH		7	9.5
Alkalinity Mud (PM)	[cm^3 N/50 Acid]	N/A	N/A
Alkalinity Filtrate	[P_f/M_f cm^3 N/50 Acid]	N/A	N/A
Chlorides	[ppm]	75	75
Total Hardness	[ppm]	N/A	N/A

Appendix D (cont.)

Table D-2 Routine test of mud properties for 1:1 simulated salt/polymer

		BEFORE	AFTER
Treatment	[amperes]	0	19
Conductivity	[μmho/cm]	35000	35000
Zeta Potential	[mV]	N/A	N/A
CST	[sec]	429	243
Centrifugal Cake Solids Content	[% w/w]	N/A	7.4
Weight	[lbm/gal]	8.7	8.7
Plastic Viscosity	[cp]	9	10
Yield Point	[lb/100 ft^2]	0.5	1
Gel Strength (10 sec, 10 min)	[lb/100 ft^2]	0.5/1	1.5/2
Filtrate	[cm^3/30 min]	19	26
Cake Thickness	[32nds of an inch]	1/	1/
Solids	[% w/w]	5.51	5.44
Methylene Blue Cap.	[cm^3/cm^3mud]	10	12
pH		6.5	6.5
Alkalinity Mud (PM)	[cm^3 N/50 Acid]	0.14	.18
Alkalinity Filtrate	[P_f/M_f] cm^3 N/50 Acid]	015/.08	017/.10
Chlorides	[ppm]	13850	14440
Total Hardness	[ppm]	20.9	19.2

Appendix D (cont.)

Table D-3 Routine test of mud properties for 1:1 simulated fresh/CLS

		BEFORE	AFTER
Treatment	[amperes]	0	19
Conductivity	[μmho/cm]	4300	3900
Zeta Potential	[mV]	N/A	N/A
CST	[sec]	222	128
Centrifugal Cake Solids Content	[% w/w]	N/A	N/A
Weight	[lbm/gal]	8.55	8.55
Plastic Viscosity	[cp]	3	3
Yield Point	[lb/100 ft^2]	1	1.5
Gel Strength (10 sec, 10 min)	[lb/100 ft^2]	1/1	1/1.5
Filtrate	[cm^3/30 min]	14	16
Cake Thickness	[32nd of an inch]	2	2
Solids	[% w/w]	4.71	5.19
Methylene Blue Cap.	[cm^3/cm^3 mud]	8.5	8.5
pH		7	8.5
Alkalinity Mud (PM)	[cm^3 N/50 Acid]	1.79	1.74
Alkalinity Filtrate	[P_f/M_f cm^3 N/50 Acid]	1.15/.17	9/1.3
Chlorides	[ppm]	360	370
Total Hardness	[ppm]	565	440

Appendix D (cont.)

Table D-4 Routine test of mud properties for 1:1 field fresh/CLS

		BEFORE	AFTER
Treatment	[amperes]	0	60
Conductivity	[μmho/cm]	5500	6500
Zeta Potential	[mV]	-110	-40
CST	[sec]	22	20
Centrifugal Cake Solids Content	[% w/w]	N/A	N/A
Weight	[lbm/gal]	8.6	8.7
Plastic Viscosity	[cp]	2	1.5
Yield Point	[lb/100 ft^2]	0.5	1
Gel Strength (10 sec, 10 min)	[lb/100 ft^2]	N/A	N/A
Filtrate	[^{cm}/30 min	24.5	25
Cake Thickness	[32nds of an inch]	0/	0/
Solids	[% w/w]	5.37	5.02
Methylene Blue Cap.	[cm^3/cm^3 mud]	24	25
pH		11.5	11.5
Alkalinity Mud (PM)	[cm^3 N/50 Acid]	1.5	0.85
Alkalinity Filtrate	[P_f/M_f] cm^3 N/50 Acid]	0.8/2.2	.63/1.7
Chlorides	[ppm]	450	250
Total Hardness	[ppm]	320	300

Appendix D (cont.)

Table D-5 Routine test of mud properties for 1:1 field salt/CLS

		BEFORE	AFTER
Treatment	[amperes]	0	200
Conductivity	[μmho/cm]	933	976
Zeta Potential	[mV]	-750	-50
CST	[sec]	1989	1032
Centrifugal Cake Solids Content	[% w/w]	N/A	40.4
Weight	[lbm/gal]	9.5	9.5
Plastic Viscosity	[cp]	2.0	7.5
Yield Point	[lb/100 ft^2]	8.5	2.5
Gel Strength (10 sec, 10 min)	[lb/100 ft^2]	0.5/4	0.5/1
Filtrate	[cm^3/30 min]	12.5	11.5
Cake Thickness	[32nds of an inch]	1/32	1/32
Solids	[% w/w]	19.38	18.44
Methylene Blue Cap.	[cm^3/cm^3 mud]	12	11.5
pH		8.5	10.5
Alkalinity Mud (PM)	[cm^3 N/50 Acid]	0.85	1.21
Alkalinity Filtrate	[P_f/M_f] cm^3 N/50 Acid]	0.54/.46	031/.26
Chlorides	[ppm]	45000	50000
Total Hardness	[ppm]	900	1000

Vita

John Marvin Griffin was born in Winston-Salem, North Carolina on August 6, 1953 to Marvin A. Griffin of Pineapple, Alabama and Pearle Alice (Jane) L'Herison Griffin of New Iberia, Louisiana. He was graduated from Tuscaloosa High School in Tuscaloosa, Alabama in 1971 and obtained a B.S. in Geology from Emory University in Atlanta, Georgia in 1975. He worked in Birmingham, Alabama for a consulting engineering firm which oversaw strip mining of coal in North Alabama. He received an M.S. in Mineral Engineering in 1978 from the University of Alabama. He was employed by Amoco Production Company and Chevron USA, Inc. between 1979-1982 as a production engineer, drilling rig foreman, and drilling engineer. He taught at the University of Southwestern Louisiana in Lafayette between 1983-1987 as an Assistant Professor before returning to school for his Ph.D. Upon completion of this program, he joined the faculty of New Mexico Institute of Mining and Technology in Socorro as an Assistant Professor. He became a Registered Professional Engineer in 1990 in the state of Louisiana.

DOCTORAL EXAMINATION AND DISSERTATION REPORT

Candidate: John M. Griffin

Major Field: Petroleum Engineering

Title of Dissertation: Mechanism and Enhancement of Phase Segregation in Drilling Fluids

Approved:

A. Wojtanowicz

Major Professor and Chairman

Dean of the Graduate School

EXAMINING COMMITTEE:

Adam T Bourgoyne Jr

William J Bernard

D. Kouba

Date of Examination:

January 15, 1991